N. Kuzmanovic | 2014

Natascha Kuzmanovic
aus Hof, geb. am 16.03.1986

Studium: Chemie, Universität Regensburg,
Abschluss Master of Science
Promotion: Prof. Dr. Burkhard König, Institut für
Organische Chemie

Diese Dissertation umfasst neue Konzepte zur biologischen Anwendung von funktionalisierten photochromen Dithienylethenen, die als lichtabhängige Schalter für Enzymaktivität und Peptide agieren. Es wird die Entwicklung von Dithienylcyclopenten basierten Enzyminhibitoren berichtet, die die Aktivität des metabolischen Schlüsselenzyms mtPriA reversibel durch Licht kontrollieren können. Weiterhin ist die Anwendung photochromer Dithienylcyclopentene als Zellsignalinhibitoren für die Kaskade der extrazellulär regulierten Kinase beschrieben. Um die Wasserlöslichkeit zu verbessern, die Hydrophilie zu erhöhen und eine leichtere Derivatisierung zu erreichen, wurden Dithienylmaleimid basierte Aminosäuren synthetisiert und in Peptide eingebaut. Darüber hinaus werden neue photochrome Dithienyl-Maleinsäurehydrazide vorgestellt. Die gewonnenen Erkenntnisse besitzen besondere Relevanz im Hinblick auf die Entwicklung von neuartigen molekularen Hilfsmitteln um zelluläre Abläufe durch Licht zu kontrollieren.
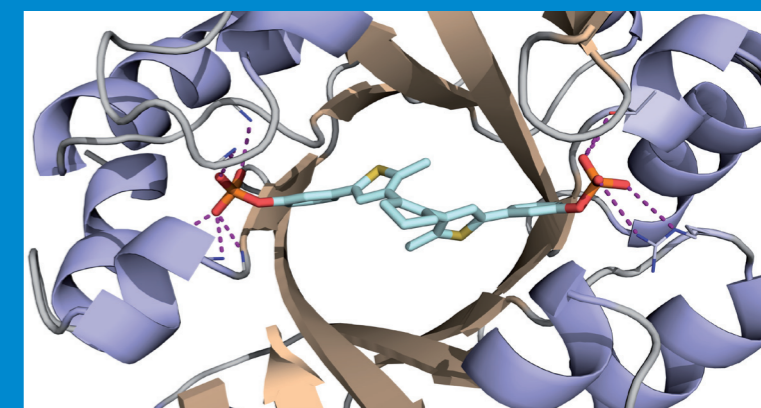
ALUMNIVEREIN CHEMIE DER UNIVERSITÄT REGENSBURG E.V.
alumniverein@chemie.uni-regensburg.de
http://www.alumnichemie-uniregensburg.de

Synthesis and Biological Activity of
Functionalized Photochromic Dithienylethens

Synthesis and Biological Activity of Functionalized Photochromic Dithienylethens

Natascha Kuzmanovic
2014

**Fakultät für
Chemie und Pharmazie**
Universität Regensburg
Universitätsstraße 31
93053 Regensburg
www.uni-regensburg.de

UR

Universität Regensburg

1

Natascha Kuzmanovic

Synthesis and Biological Activity
of Functionalized Photochromic Dithienylethens

Synthesis and Biological Activity of Functionalized Photochromic Dithienylethenes

Dissertation zur Erlangung des Doktorgrades der Naturwissenschaften (Dr. rer. nat.)
der Naturwissenschaftlichen Fakultät IV - Chemie und Pharmazie der Universität Regensburg
vorgelegt von

Natascha Kuzmanovic

Regensburg
2014

Die Arbeit wurde von Prof. Dr. Burkhard König angeleitet.
Das Promotionsgesuch wurde am 21.01.2014 eingereicht.

Prüfungsausschuss: Vorsitzender: Prof. Dr. Joachim Wegener
                    1. Gutachter: Prof. Dr. Burkhard König
                    2. Gutachter: Prof. Dr. Kirsten Zeitler
                    weiterer Prüfer: Prof. Dr. Reinhard Sterner

Dissertationsreihe der Fakultät für Chemie und Pharmazie der Universität Regensburg, Band 1

Synthesis and Biological Activity of Funcionalized Photochromic Dithienylethens

Natascha Kuzmanovic

Now can come what want.

Uschi Disl, Biathletin

TABLE OF CONTENTS

1 SUMMARY

This thesis focuses on the design, synthesis and evaluation of novel functionalized photochromic dithienylethenes (DTEs) for applications in biology.

Chapter 1 deals with the creation of dithienylcyclopentene based enzyme inhibitors to reversibly control the activity of the metabolic branch-point enzyme PriA from *Mycobacterium tuberculosis* (*mt*PriA) by light. The enzyme's natural rotational symmetry encouraged us to design two-pronged DTEs with terminal phosphate or phosphonate functional groups. Switching from the flexible, ring-open to the rigid, ring-closed isomer reduces inhibition activity by one order of magnitude, whereby *mt*PriA's performance can even be remote-controlled by light during catalysis. Molecular Dynamics simulations support our experiments showing that the open form is energetically more favorable while bound in the active site. Thus the concept of utilizing the enzyme structure for the inhibitor design has been proven.

In **chapter 2** the development of photochromic dithienylcyclopentenes as cell signal inhibitors for the extracellular-regulated kinase (ERK) pathway is reported. Through Molecular Docking we identified promising DTE based ERK inhibitors, which were subsequently synthesized and photochemically evaluated. The mediocre thermal stability of their ring-closed photoisomers requires that the test solutions are irradiated directly before use. Incubation of cells with the title compounds caused significant inhibition by the ring-open isomers, whereas the ring-closed forms' activity seems reduced and cytotoxicity was observed. Further experiments with isolated ERK could not sufficiently substantiate these results though. This already gives a hint on the complexity of this topic as any other tier of the entire signal cascade might be affected. Nevertheless, interesting trends were found and new compounds could be identified, which allow for the light-dependent regulation of the ERK signal.

Aiming for better water-solubility, increased hydrophilicity and easier derivatization, dithienylmaleimide based amino acids were synthesized and incorporated in peptides, as described in **chapter 3**. We combined independently prepared N- and C-terminal thienyl components by Perkin condensation to form the maleimide core. Subsequent derivatization of the photoswitchable amino acid is easily achieved by standard solid phase peptide coupling. The resulting compounds show excellent photochromic performance in polar solvents and are thus suitable candidates for biological applications.

Moreover, novel photochromic dithienyl maleic hydrazides are introduced in **chapter 4**. The reaction of dithienylmaleimides with hydrazine generates DTEs bearing maleic hydrazide as ethene unit. Initial NMR measurements indicate that it might occur predominantly as the monolactim tautomer. Concurrently, we observed photoswitchable solvatochromism of the obtained compound, but its repeated application is restricted by rapid photodegradation. Further investigations are necessary to thoroughly characterize the compounds and their behavior. These interesting pioneering observations could contribute to establish a new generation of DTE photoswitches.

In conclusion, this thesis presents new concepts for the biological application of functionalized photochromic dithienylethenes, which act as light-dependent switches for enzyme activity and peptides. The implications of this work are especially relevant for the development of novel molecular tools to remote-control cellular processes by light.

2 ZUSAMMENFASSUNG

Diese Arbeit befasst sich mit der Gestaltung, der Synthese und der Untersuchung von neuen funktionalisierten photochromen Dithienylethenen (DTEs) für biologische Anwendungen.

Kapitel 1 handelt von der Entwicklung von Dithienylcyclopenten basierten Enzyminhibitoren, die die Aktivität des metabolischen Schlüsselenzyms PriA aus *Mycobacterium tuberculosis* (*mt*PriA) reversibel durch Licht kontrollieren können. Die natürliche Rotationssymmetrie des Enzyms hat uns dazu bewogen, symmetrische Inhibitoren mit terminalen Phosphat- oder Phosphonat-Ankern zu entwerfen. Durch das Schalten vom flexiblen, offenen Isomer zur starren, geschlossenen Form verringert sich die Inhibitionsaktivität um eine Größenordnung, wobei die Enzymsteuerung durch Licht auch während der Katalyse funktioniert. Moleküldynamik-Simulationen stützen die experimentellen Daten und zeigen, dass die Bindung der offenen Form im aktiven Zentrum energetisch bevorzugt ist. Damit wurde bewiesen, dass man abgeleitet von der Enzymstruktur Inhibitoren konstruieren kann.

In **Kapitel 2** wird die Anwendung photochromer Dithienylcyclopentene als Zellsignalinhibitoren für die Kaskade der extrazellulär regulierten Kinase (ERK) berichtet. Mittels molekularen Dockings wurden potentielle, vom DTE-Gerüst abgeleitete, ERK-Inhibitorstrukturen bestimmt, welche anschließend synthetisiert und photochemisch untersucht wurden. Die mittelmäßige thermische Stabilität der geschlossenen Photoisomere erfordert, dass die Proben direkt vor ihrem Einsatz belichtet werden. Bei der Inkubation von Zellen mit den Zielsubstanzen können deren offene Isomere das ERK-Signal hemmen, wohingegen die Wirkung der geschlossenen Formen geringer erscheint und Zellschädigung festgestellt wurde. Weitere Experimente mit isolierter ERK konnten diese Ergebnisse jedoch nicht ausreichend untermauern und deuten auf die Komplexität dieser Thematik hin, da jede weitere Stelle der gesamten Signalkaskade betroffen sein könnte. Dennoch wurden interessante Tendenzen entdeckt und neue Substanzen gefunden, die das ERK-Signal abhängig von der Beleuchtung regulieren können.

Um die Wasserlöslichkeit zu verbessern, die Hydrophilie zu erhöhen und eine leichtere Derivatisierung zu erreichen, wurden Dithienylmaleimid basierte Aminosäuren synthetisiert und in Peptide eingebaut, was in **Kapitel 3** beschrieben ist. Dabei verknüpften wir die separat hergestellten N- und C-terminalen Thienylkomponenten durch eine Perkin-Kondensation, wobei der Maleimidkern entstand. Eine anschließende Derivatisierung der photoschaltbaren Aminosäure kann durch gewöhnliche Festphasenpeptidsynthese per Standardprotokoll erfolgen. Die hergestellten Substanzen zeigen hervorragende photochrome Eigenschaften in polaren Lösungsmitteln und eignen sich daher für biologische Anwendungen.

Darüber hinaus werden neue photochrome Dithienyl-Maleinsäurehydrazide in **Kapitel 4** vorgestellt. Die Reaktion von Dithienylmaleimiden mit Hydrazin erzeugt DTEs, die mit einem Maleinsäurehydrazid als Etheneinheit ausgestattet sind. Erste NMR-Messungen deuten darauf hin, dass es vermutlich als Monolactimtautomer vorliegt. Gleichzeitig beobachteten wir eine photoschaltbare Solvatochromie der hergestellten Substanz, jedoch ist eine wiederholte Anwendung durch den raschen Zerfall bei Beleuchtung eingeschränkt. Es sind weitere Untersuchungen nötig um eine fundierte Charakterisierung vorzunehmen. Diese interessanten wegbereitenden Beobachtungen können dazu beitragen eine neue Generation von DTE-Photoschaltern zu entwickeln.

Zusammenfassend zeigt diese Arbeit neue Konzepte zur biologischen Anwendung von funktionalisierten photochromen Dithienylethenen auf, welche als lichtabhängige Schalter für Enzymaktivität und Peptide agieren. Die gewonnenen Erkenntnisse besitzen besondere Relevanz im Hinblick auf die Entwicklung von neuartigen molekularen Hilfsmitteln um zelluläre Abläufe durch Licht zu kontrollieren.

CHAPTER 1

3 EXPLOITING PROTEIN SYMMETRY TO DESIGN LIGHT-CONTROLLABLE ENZYME INHIBITORS*

3.1 Introduction

The artificial control of biological processes by light is a rapidly emerging area of protein design.[1] Three basic strategies for the light-regulation of biomolecules have been reported: Besides caging of key positions with photolabile protecting groups[2] and reprogramming of naturally occurring photoreceptors,[3-5] designed molecules that can be reversibly switched by light (photoswitches) have been used to direct protein or cellular function.[6] Recently, substantial progress has been made in the regulation of neuronal activity by designing light-inducible ligands for ion channels and receptors.[7-8] As the molecular recognition of specific ligand parts leads to a nonlinear signal response in neural systems, even small changes in the binding efficacy upon light irradiation significantly influence the cellular output.[9] However, when aiming to reversibly control enzymatic activities, switching of a photoresponsive group must substantially affect the enzyme's active site. Covalent incorporation of a molecular photoswitch near the catalytic center is able to fulfill this task.[6, 10] The required coupling step between protein and photoswitch can be circumvented by designing a light-controlled inhibitor.[6, 11-13]
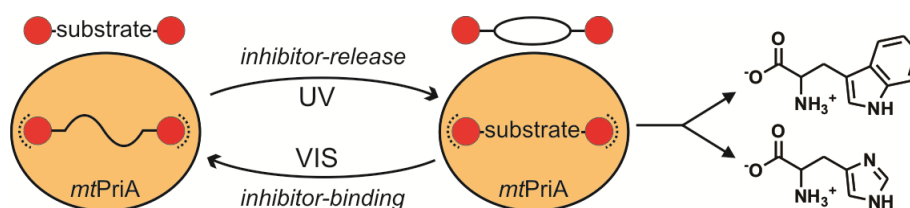
Figure 1. Reversible light-dependent control of *mt*PriA activity.

We aimed to design a light-controllable inhibitor for phosphoribosyl-isomerase A from *Mycobacterium tuberculosis* (*mt*PriA, Figure 1). *mt*PriA is a branch-point enzyme in amino acid biosynthesis as it catalyzes two chemically equivalent sugar isomerization reactions in tryptophan and histidine biosynthesis.[14] In the latter, the aminoaldose N′-[(5′-phosphoribosyl)-formimino]-5-aminoimidazole-4-carboxamide ribonucleotide (ProFAR) is converted to the corresponding aminoketose N′-[(5′-phosphoribulosyl)-formimino]-5-aminoimidazole-4-carboxamide-ribonucleotide (PRFAR) (Figure 2a). Since humans can neither synthesize histidine nor tryptophan, *mt*PriA is a potential target for anti-tuberculosis drugs.[15-16] Structurally, *mt*PriA belongs to the class of $(\beta\alpha)_8$-barrels, which is a frequently encountered and highly versatile fold among enzymes.[17-18] *mt*PriA exhibits a clear twofold symmetry (Figure 2b),[19-20] which indicates its evolution from a $(\beta\alpha)_4$-half-barrel precursor.[21] Consequently, two phosphate binding sites are found opposite each other to fix the substrate ProFAR and the product PRFAR (Figure 2b). We thus reasoned that

a C2-symmetric photoswitch with terminal phosphate-anchors would be an excellent foundation for building a light-controllable inhibitor of *mt*PriA.
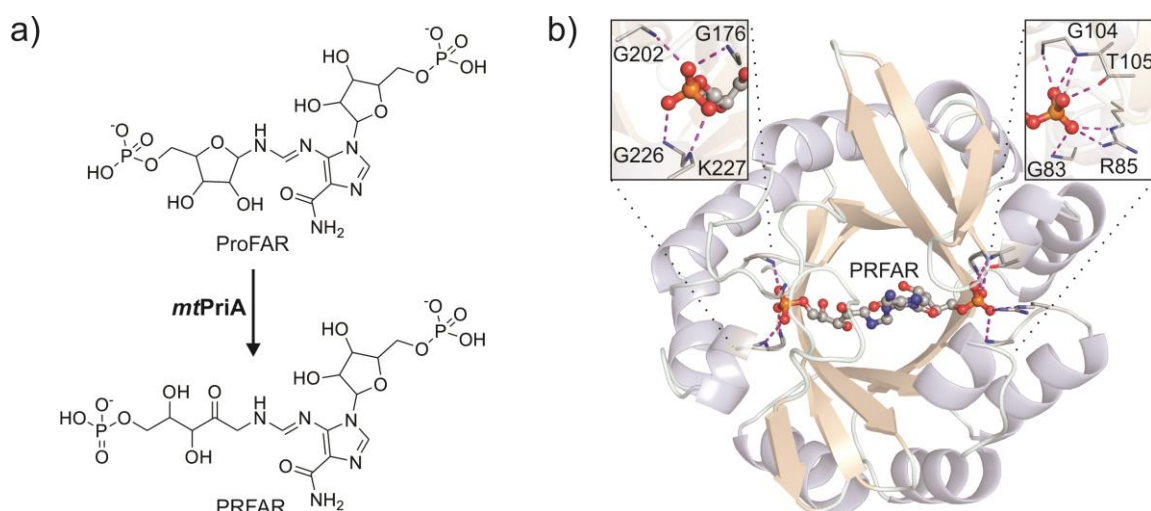
Figure 2. Reaction and structure of *mt*PriA. a) *mt*PriA catalyzes the conversion of ProFAR to PRFAR within histidine biosynthesis. b) Ribbon diagram of the (βa)₈-barrel structure of *mt*PriA with bound product PRFAR (PDB ID 3ZS4[19]). The view is along the two-fold symmetry axis of the protein. PRFAR is anchored by two opposite phosphate binding sites, which are enlarged in the insets. Formed hydrogen bonds are indicated by dashed lines (structure is slightly rotated for clarity in either case).

Two types of organic photochromic systems possess the desired twofold rotational symmetry: stilbene[22] or azobenzene switches[23] and the diarylethene scaffold.[24] Although azobenzene derivatives have been widely used in biological systems, they suffer from incomplete photoconversion and thermal reversibility.[1] In contrast, photoresponsive compounds based on 1,2-dithienylethene (DTE) generally feature switching rates of over 90% conversion with both photoisomers being thermally stable.[12, 24] Hence, we opted for DTE as core and provided it with different phosphate and phosphonate anchors (Scheme 1).

3.2 Results and Discussion

3.2.1 Synthesis

Starting with the bischlorodithienylethene **1**, Suzuki coupling yielded either the aromatic hydroxides **2-4** or the aromatic bromides **8-9**. The former were subsequently converted to ortho-, meta- and para-phosphates **5-7**, while the latter were used to synthesize the phosphonic acid esters **10-11**, which were finally hydrolyzed to afford meta- and para-phosphonates **12-13**.
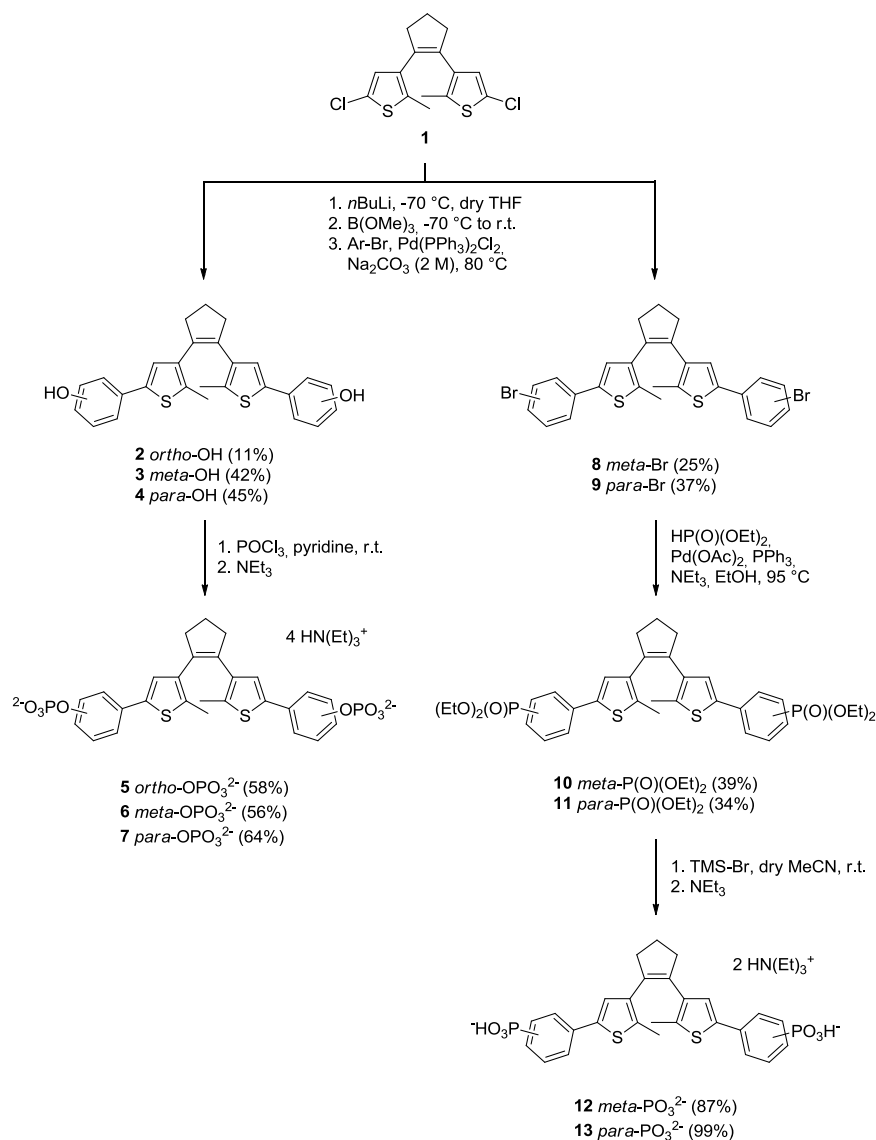
Scheme 1. Synthesis of DTE-phosphates and DTE-phosphonates.

3.2.2 Photochromism

The DTE molecular structure can reversibly be toggled between a ring-open and ring-closed photoisomer (Scheme 2), which significantly alters its overall conformational flexibility.[12] Energy minimizations of the open and closed forms of all potential inhibitors confirmed for the phosphorous atoms distances between 15.8 and 19.6 Å (Scheme 2), which is in good accordance with the 16.9 Å observed for the corresponding atoms in the *mt*PriA structure with co-crystallized PRFAR (PDB ID 3ZS4[19]) (see Experimental Material and Methods for details). Only the open and closed isomers of ortho-phosphate **5** exhibit rather short P-P distances of 12.3 Å and 11.3 Å, respectively, in their energetically most favorable geometries; in addition, less populated, more extended conformers can be observed.

d (P-P) / Å:		
compound	open	closed
5	12.3	11.3
6	16.7	16.2
7	19.6	18.4
12	16.9	15.8
13	18.9	18.1
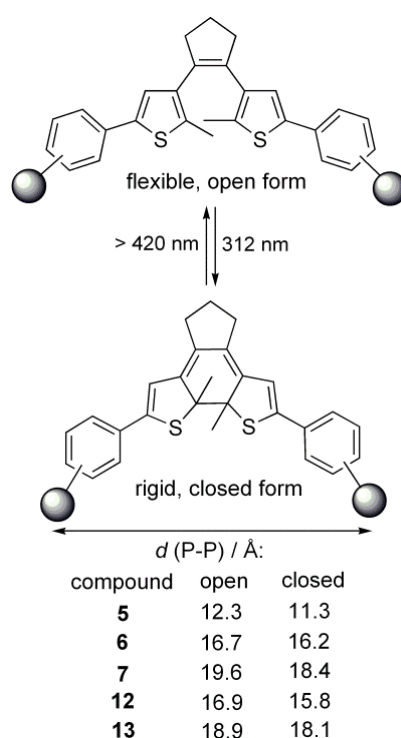
Scheme 2. Photochemical switching and corresponding calculated P-P distances in DTE-phosphates and DTE-phosphonates.

When ring-open forms of compounds **5-7**, **12** and **13** are irradiated with 312 nm light, the absorption band at 280 nm immediately decreases. Simultaneously, new absorption maxima at 350 nm and 525 nm are formed turning the initially colorless solutions pink (see Figure 5). In each case, the spectral changes are completed after 30 s of irradiation and the corresponding photostationary states contain between 93% and 97% of the closed isomers, as judged by HPLC analyses (see Figure 6). The open forms can be recovered by irradiation with visible light (> 420 nm) and all switches are robust over several ring-closing/ring-opening cycles (see Figure 7).

3.2.3 Biological Test Results

The *mt*PriA activity can be monitored spectrophotometrically at 300 nm in a coupled enzyme assay (Scheme 3).[25] As all synthesized compounds were stable under assay conditions, their inhibitory effect could be investigated in steady-state enzyme kinetics. For this purpose, substrate saturation curves were measured in presence of different concentrations of compounds **5-7**, **12** and **13** in their open and closed forms (curves are shown for compound **6** in Figure 8). Indeed, all investigated DTE-phosphates and DTE-phosphonates have the ability to inhibit the *mt*PriA reaction in both isomeric forms, thus proving the viability of the design concept. As expected for competitive inhibition, the turnover numbers k_{cat} were identical in presence and absence of inhibitor (see experimental section, Table 2). The observed increase of the Michaelis constants caused by the inhibitors (Table 2) was used to calculate the inhibition constants K_i (Formula 1), which are given in Table 1.

Table 1. Inhibition constants K_i of compounds **5**-**7**, **12** and **13** in their ring-open and ring-closed forms.

Inhibitor	K_i / μM[a]	
	ring-open	ring-closed
5	8.1 ± 2.1	7.0 ± 1.2
6	0.55 ± 0.12	4.4 ± 0.3
7	3.5 ± 0.3	3.7 ± 0.4
12	1.6 ± 0.1	4.9 ± 0.3
13	6.8 ± 0.6	22.7 ± 4.7

[a] The values of K_i were obtained from the data shown in Table 2 using Formula 1.

The determined inhibition constants are in the low micromolar range (Table 1) and therefore comparable or even better than the enzyme's K_M value for the natural substrate ProFAR (K_M^{ProFAR} = 8.6 μM; see Table 2). In agreement with the well-suited distance of its phosphorous atoms (Scheme 2), the open isomer of phosphate **6** exhibits the highest binding affinity (K_i = 0.55 μM). However, when switched to its rigid, closed form, the inhibition activity is lowered by roughly one order of magnitude (K_i = 4.4 μM). A similar trend is observed for the respective phosphonate **12**, whose binding affinity in the open form (K_i = 1.6 μM) is decreased about 3-fold upon ring-closure (K_i = 4.9 μM). In contrast, the inhibitory effects of phosphates **5** and **7** are nearly identical in their ring-open and ring-closed forms (Table 1). Interestingly, the introduction of a phosphonate moiety in para-position (compound **13**) causes a 3-fold difference in the inhibition activity of the open (K_i = 6.8 μM) and closed photoisomer (K_i = 22.7 μM). The removal of the oxygen bridge between

the terminal anchor and the switchable core further reduces the overall flexibility, which seems to predominantly affect the already rigid, closed isomer.

The performance of *mt*PriA can also be remote-controlled by light during catalysis. Starting up with compound **6** in its strongly inhibiting, open form, the reaction velocity is enhanced about 3-fold, when switching to the less active, ring-closed isomer (Figure 3).
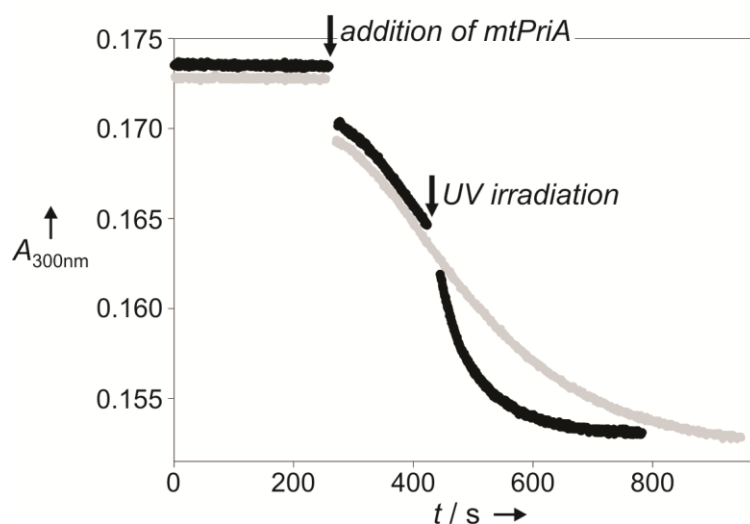
Figure 3. Change in *mt*PriA activity upon ring-closure of compound **6**. The turnover of 5 μM ProFAR was followed photometrically at 300 nm in the presence of 4 μM **6** in its open form under typical assay conditions (25 °C, 50 mM Tris/acetate pH 8.5, 100 mM ammonium acetate, 0.18 μM HisF and 0.15 μM *mt*PriA). After having reached its maximal velocity, the reaction mixture was either left in the photometer (grey) or removed to irradiate it with 312 nm light for 10 s (black). A reference solution without enzymes was used to correct the baseline shift resulting from different absorption values of the open and closed isomer at 300 nm.

3.2.4 Molecular Modeling

As pointed out before, the mechanistic principle, which induces the different binding affinities of the photoisomers, is based on a change in conformational flexibility.[12] Due to free rotation around the C-C bonds joining the thiophene heterocycles with the central cyclopentene ring and the terminal phenyl groups, DTE-phosphate **6** is able to adopt various geometries in its ring-open form. On the other hand, the closed isomer is completely conjugated and thus far more restricted in its motility. In order to get insights into the binding modes of the inhibitors, Molecular Dynamics (MD) simulations of the open and closed isomer of compound **6** bound to *mt*PriA were performed. Although both forms are clearly fixed at the phosphate binding sites (Figure 4a and 4c), obvious differences can be observed in their structural cores. While the open isomer converges to similar,

C2-symmetric conformers in three independent calculations (Figure 4b), more diverse binding modes are found for the ring-closed isomer (Figure 4d). Here, one terminal phenyl ring is twisted and adopts various geometries to facilitate proper coordination of the terminal phosphate group. The measured difference in inhibition activity is also reflected in the binding energies determined during the simulations, which consistently show that interaction with the open form is energetically more favorable (see Table 3). Taken together, the higher flexibility of the open isomer allows for better adaptation to the enzyme's active site and apparently overcompensates the loss in entropy upon binding.
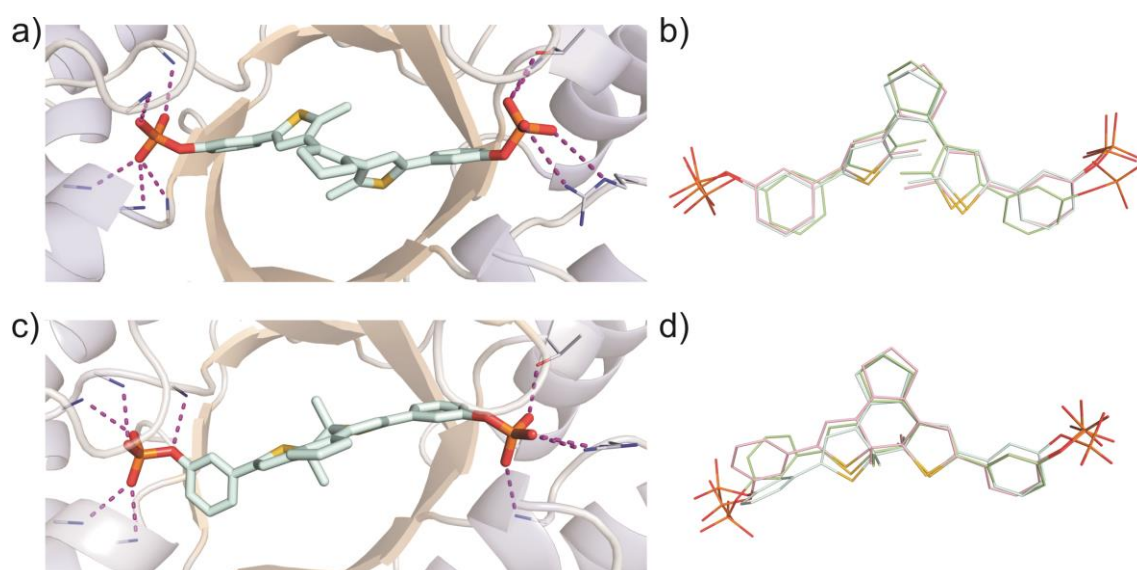
Figure 4. MD simulations of *mt*PriA and bound meta-phosphate **6**. For each isomer, three independent calculations were performed and representative enzyme structures for the open (a) and closed (c) form are shown. A superposition of the energetically most favorable conformer of each simulation is depicted in the open conformation (b) and the closed conformation (d).

3.3 Conclusion

In summary, we have demonstrated that natural protein symmetry can be advantageously utilized to design light-controllable enzyme inhibitors. The two-pronged DTE switches can reversibly be toggled between a high- and low-affinity form, where both photoisomers are nearly quantitatively formed and thermally stable. Hence, the enzyme's performance can alternately be enhanced and reduced by irradiation with UV and visible light, respectively. The viability of a dual-anchored DTE inhibitor has been shown before[12] and the design concept can in principle be transferred to functionally quite different enzyme systems. Phosphate is a frequently encountered element of metabolic substrates, and various other $(\beta\alpha)_8$-barrel enzymes such as pyridoxine 5'-phosphate synthase[26] or aldolases[27-28] possess two phosphate binding sites. For these enzymes, inhibitors may be designed with a similar approach, which would allow for an independent photocontrol of several metabolic processes in a spatiotemporal fashion.

3.4 Supporting Information

3.4.1 Synthesis and Characterization of New Compounds

General. Commercial reagents and starting materials were purchased from Acros Organics, Alpha-Aesar or Sigma Aldrich and used without further purification. Solvents were used in p.a. quality and dried according to common procedures, if necessary. Flash column chromatography was performed on a Biotage Isolera One automated flash purification system with UV/Vis detector using Sigma Aldrich MN silica gel 60 M (40-63 μm, 230-400 grain diameter) for normal phase or pre-packed Biotage SNAP cartridges (KP-C18-HS) for reversed phase chromatography. Reaction monitoring via TLC was performed on alumina plates coated with silica gel (Merck silica gel 60 F_{254}, 0.2 mm). NMR spectra were recorded on a Bruker Avance 400 ([1]H 400.13 MHz, [13]C 100.61 MHz, [31]P 161.96 MHz, T = 300 K) instrument. The spectra are referenced against the NMR-solvent, chemical shifts δ are reported in ppm and coupling constants J are given in Hz. Resonance multiplicity is abbreviated as: s (singlet), d (doublet), t (triplet), m (multiplet) and b (broad). Carbon NMR signals are reported using DEPT 135 spectra with (+) for primary/tertiary, (−) for secondary and (q) for quaternary carbons. Mass spectra were recorded on Finnigan MAT95 (EI-MS), Agilent Q-TOF 6540 UHD (ESI-MS, APCI-MS), Finnigan MAT SSQ 710 A (EI-MS, CI-MS) or ThermoQuest Finnigan TSQ 7000 (ES-MS, APCI-MS) spectrometer. UV/Vis absorption spectroscopy was performed using a Varian Cary BIO 50 UV/Vis/NIR spectrometer.

Photochemistry. Standard hand-held lamps (Herolab, 312 nm, 6 W) were used for visualizing TLC plates and to carry out the ring-closure reactions at 312 nm. The ring-opening reactions were performed with the light of a 200 W tungsten light bulb which was passed through a 420 nm cut-off filter to eliminate higher energy light. The power of the light is given based on the specifications supplied by the company when the lamps were purchased. A light detector was not used to measure the intensity during the irradiation experiments.

General procedure A for Suzuki coupling. 1,2-Bis(5-chloro-2-methylthiophen-3-yl)cyclopent-1-ene **1**[29] (1.0 eq.) was dissolved in dry THF under nitrogen atmosphere. After cooling to -78 °C, *n*-butyl lithium (2.2 eq.) was added dropwise via syringe and the resulting purple solution was stirred in the cold for 45 min. The reaction mixture was treated with trimethyl borate (4.0 eq.) and the yellow solution was stirred at -78 °C for 30 min. Subsequently, the cold bath was removed and the reaction was stirred at r.t. for further 60 min to form the boronic ester intermediate. After quenching with aqueous sodium

carbonate (2 M) the two phase system was degassed for 15 min by nitrogen purge. Then the appropriate aryl bromide (2.2 or 4.0 eq.) and Pd(PPh$_3$)$_2$Cl$_2$ (10 mol%) were added and the reaction mixture was heated to reflux overnight. After cooling to r.t., it was diluted with EtOAc and water and the phases were separated. The aqueous phase was extracted with EtOAc twice, the combined organic phases were dried over sodium sulfate and the solvents removed under reduced pressure. Purification of the crude product was performed by automated flash column chromatography.

General procedure B for phosphate ester formation. A crimp top vial was equipped with the desired bisphenol DTE (1.0 eq.) and a stirring bar and capped. It was set under nitrogen atmosphere and pyridine (20 eq.) in dry CH$_2$Cl$_2$ (1 mL) was added by syringe. After cooling to 0 °C a solution of phosphorous oxychloride (10 eq.) in dry THF (1 mL) was added dropwise via syringe over 5 min. The purple reaction mixture was stirred for 2 h at r.t. under nitrogen atmosphere and subsequently quenched with acetone/water (1:1, 2 mL). Volatiles were removed *in vacuo* and the crude product was purified by automated reversed phase flash column chromatography.
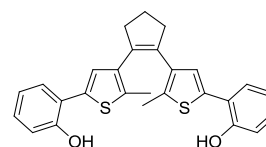
Synthesis of 2,2'-(4,4'-(cyclopent-1-ene-1,2-diyl)bis(5-methylthiophene-4,2-diyl)) diphenol (2). Compound **2** was prepared from 1,2-bis(5-chloro-2-methylthiophen-3-yl)cyclopent-1-ene **1** (1.50 g, 4.55 mmol), *n*-butyl lithium (1.3 M in hexane, 7.68 mL, 10.0 mmol), trimethyl borate (2.03 mL, 18.2 mmol), 2-bromophenol (1.16 mL, 10.0 mmol) and Pd(PPh$_3$)$_2$Cl$_2$ (320 mg, 0.46 mmol) following the general procedure **A** for Suzuki coupling with 50 mL dry THF and 20 mL aq. Na$_2$CO$_3$ (2 M). Automated flash column chromatography (PE/EtOAc, 15-25% EtOAc) and subsequent reversed phase automated flash column chromatography (MeOH/water with 0.05% TFA, 3-100% MeOH) afforded 223 mg (0.50 mmol, 11%) of **2** as purple oil. **^{1}H-NMR: δ_H(400 MHz, CDCl$_3$):** 2.10 (2H, dt, *J* = 7.4, 7.5 Hz, cyclopentene-C*H*$_2$), 2.16 (6H, s, 2 C*H*$_3$), 2.84 (4H, t, *J* = 7.4 Hz, 2 cyclopentene-C*H*$_2$), 6.85 (2H, s, 2 thiophene-*H*), 6.89 – 6.97 (4H, m, 4 phenyl-*H*), 7.15 – 7.22 (2H, m, phenyl-*H*), 7.30 (2H, dd, *J* = 7.6, 1.6 Hz, phenyl-*H*); **^{13}C-NMR: δ_C(101 MHz, CDCl$_3$):** 14.1 (+), 23.2 (−), 37.8 (−), 116.3 (+), 120.8 (+), 121.1 (q), 127.6 (+), 129.2 (+), 129.8 (+), 134.5 (q), 135.4 (q), 135.6 (q), 136.6 (q), 152.4 (q); **ESI-MS:** m/z (%): 443.1 (100) [M-H]$^-$; calcd. for C$_{27}$H$_{24}$O$_2$S$_2$ 443.1145; found 443.1147.
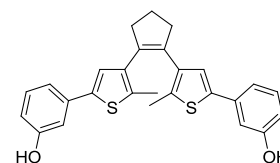
Synthesis of 3,3'-(4,4'-(cyclopent-1-ene-1,2-diyl)bis(5-methylthiophene-4,2-diyl)) diphenol (3). Compound **3** was prepared from 1,2-bis(5-chloro-2-methylthiophen-3-yl)cyclopent-1-ene **1** (1.84 g, 5.59 mmol), *n*-butyl lithium (1.6 M in hexane, 7.68 mL, 12.3 mmol), trimethyl borate (2.49 mL, 22.4 mmol), 3-bromophenol (2.13 g, 12.3 mmol) and Pd(PPh$_3$)$_2$Cl$_2$ (393 mg, 0.56 mmol) following the general procedure **A** for Suzuki coupling with 100 mL dry THF and 20 mL aq. Na$_2$CO$_3$ (2 M). Automated flash column chromatography (PE/EtOAc, 15-30% EtOAc) and subsequent reversed phase automated flash column chromatography (MeOH/water with 0.05% TFA, 30-100% MeOH) afforded 1.04 g (2.35 mmol, 42%) of **3** as red oil. **¹H-NMR: δ$_H$(400 MHz, CDCl$_3$):** 2.00 (6H, s, 2 C*H*$_3$), 2.08 (2H, dt, *J* = 7.4 Hz, cyclopentene-C*H*$_2$), 2.83 (4H, t, *J* = 7.4 Hz, 2 cyclopentene-C*H*$_2$), 3.51 (2H, bs, 2 phenyl-O*H*), 6.71 (2H, dd, *J* = 1.9 Hz, 8.0 Hz, 2 phenyl-*H*), 6.95 – 6.99 (2H, m, 2 phenyl-*H*), 7.00 (2H, s, 2 thiophene-*H*), 7.07 (2H, *J* = 7.9 Hz, 2 phenyl-*H*), 7.19 (2H, t, *J* = 7.9 Hz, 2 phenyl-*H*); **¹³C-NMR: δ$_C$(101 MHz, CDCl$_3$):** 14.4 (+), 23.0 (−), 38.4 (−), 112.2 (+), 114.1 (+), 117.9 (+), 124.4 (+), 130.1 (+), 134.7 (q), 134.8 (q), 136.1 (q), 136.7 (q), 139.2 (q), 156.0 (q); **EI-MS:** m/z (%) 444.1 (100) [M]⁺, 429.0 (35) [M-CH$_3$]⁺; calcd. for C$_{27}$H$_{24}$O$_2$S$_2$ 443.1145; found 443.1156.
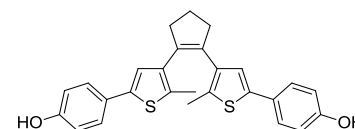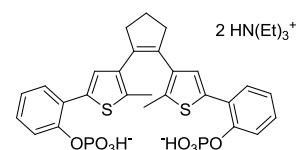

Synthesis of 4,4'-(4,4'-(cyclopent-1-ene-1,2-diyl)bis(5-methylthiophene-4,2-diyl)) diphenol (4). Compound **4** was prepared from 1,2-bis(5-chloro-2-methylthiophen-3-yl)cyclopent-1-ene **1** (209 mg, 0.64 mmol), *n*-butyl lithium (1.6 M in hexane, 0.88 mL, 1.41 mmol), trimethyl borate (0.29 mL, 2.56 mmol), 4-bromophenol (439 mg, 2.54 mmol) and Pd(PPh$_3$)$_2$Cl$_2$ (42 mg, 0.06 mmol) following the general procedure **A** for Suzuki coupling with 50 mL dry THF and 10 mL aq. Na$_2$CO$_3$ (2 M). Automated flash column chromatography (PE/EtOAc, 15-25% EtOAc), subsequent reversed phase automated flash column chromatography (MeOH/water with 0.05% TFA, 30-100% MeOH) and lyophilization afforded 127 mg (0.29 mmol, 45%) of **4** as red oil. **¹H-NMR: δ$_H$(400 MHz, CDCl$_3$):** 1.98 (6H, s, 2 C*H*$_3$), 2.10 (2H, p, *J* = 7.7 Hz, cyclopentene-C*H*$_2$), 2.83 (4H, t, *J* = 7.5 Hz, 2 cyclopentene-C*H*$_2$), 4.88 (2H, bs, 2 phenyl-O*H*), 6.80 (4H, d, *J* = 8.7 Hz, 4 phenyl-*H*), 6.90 (2H, s, 2 thiophene-*H*), 7.37 (4H, d, *J* = 8.7 Hz, 4 phenyl-*H*); **¹³C-NMR: δ$_C$(101 MHz, CDCl$_3$):**

14.4 (+), 23.0 (−), 38.5 (−), 115.7 (+), 123.1 (+), 126.8 (+), 127.7 (q), 133.5 (q), 134.6 (q), 136.6 (q), 139.4 (q), 154.8 (q); **EI-MS:** m/z (%) 444.0 (100) [M]$^+$, 429.0 (35) [M-CH$_3$]$^+$; calcd. for C$_{27}$H$_{24}$O$_2$S$_2$ 443.1145; found 443.1148.

Synthesis of (4,4'-(cyclopent-1-ene-1,2-diyl)bis(5-methylthiophene-4,2-diyl))bis(2,1-phenylene) bis(phosphate) (5). Compound **5** was prepared from **2** (65 mg, 0.15 mmol), pyridine (0.24 mL, 2.92 mmol) and phosphorous oxychloride (0.13 mL, 1.46 mmol) following the general procedure **B** for phosphate ester formation. Automated reversed phase flash column chromatography (MeOH/water with 0.5% NEt$_3$, 20-100% MeOH) and subsequent lyophilization afforded 66 mg (0.09 mmol, 58%) of **5** as purple foam. **^{1}H-NMR: δ$_H$(400 MHz, MeOD):** 1.21 (18H, t, J = 7.3 Hz, 2 H$^+$N(CH$_2$CH_3)$_3$), 1.99 (6H, s, 2 thiophene-CH_3), 2.04 – 2.13 (2H, m, cyclopentene-CH_2), 2.87 (4H, t, J = 7.5 Hz, 2 cyclopentene-CH_2), 3.03 (12H, q, J = 7.3 Hz, 2 H$^+$N(CH_2CH$_3$)$_3$), 6.99 (2H, t, J = 7.6 Hz, 2 phenyl-H), 7.10 – 7.18 (2H, m, 2 phenyl-H), 7.40 (2H, s, thiophene-H), 7.51 (2H, d, J = 7.8 Hz, 2 phenyl-H), 7.63 (2H, d, J = 8.3 Hz, 2 phenyl-H); **^{13}C-NMR: δ$_C$(101 MHz, MeOD):** 9.1 (+), 14.4 (+), 24.0 (−), 39.6 (−), 47.5 (−), 121.4 (+), 123.8 (+), 126.6 (q), 128.2 (+), 128.4 (+), 128.7 (+), 135.8 (q), 136.1 (q), 136.5 (q), 137.4 (q), 150.8 (q); **^{31}P-NMR: δ$_P$(162 MHz, MeOD):** -3.40 (s); **ESI-MS:** m/z (%) 806.0 (100) [(M^{4-}+3H)+2(N(Et)$_3$)]$^-$, 603.0 (44) [M^{4-}+3H]$^-$; calcd. for C$_{27}$H$_{25}$O$_8$P$_2$S$_2$ 603.0472; found 603.0477.
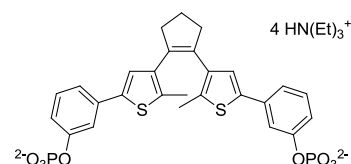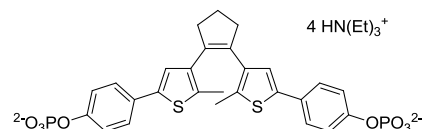

Synthesis of (4,4'-(cyclopent-1-ene-1,2-diyl)bis(5-methylthiophene-4,2-diyl))bis(3,1-phenylene) bis(phosphate) (6). Compound **6** was prepared from **3** (26 mg, 0.06 mmol), pyridine (100 μL, 1.18 mmol) and phosphorous oxychloride (50 μL, 0.56 mmol) following the general procedure **B** for phosphate ester formation. Automated reversed phase flash column chromatography (MeOH/water with 0.5% NEt$_3$, 20-100% MeOH) and subsequent lyophilization afforded 33 mg (0.03 mmol, 56%) of **6** as purple foam. **^{1}H-NMR: δ$_H$(400 MHz, MeOD):** 1.21 (36H, t, J = 7.3 Hz, 4 H$^+$N(CH$_2$CH_3)$_3$), 1.96 (6H, s, 2 thiophene-CH_3), 2.11 (2H, dt, J = 7.5, 7.6 Hz, cyclopentene-CH_2), 2.86 (4H, t, J = 7.4 Hz, 2 cyclopentene-CH_2), 2.97 (24H, q, J = 7.3 Hz, 4 H$^+$N(CH_2CH$_3$)$_3$), 7.11 – 7.13 (4H, m, 4 phenyl-H), 7.15 (2H, s, 2 thiophene-H), 7.17 – 7.23 (2H, m, 2 phenyl-H), 7.50 (2H, s, 2 phenyl-H); **^{13}C-NMR: δ$_C$(101 MHz, MeOD):**

9.5 (+), 14.5 (+), 24.1 (−), 39.5 (−), 47.1 (−), 118.1 (+), 120.0 (+), 120.3 (+), 125.3 (+), 130.5 (+), 135.3 (q), 136.1 (q), 136.7 (q), 138.2 (q), 141.1 (q), 156.4 (q); **31P-NMR: δP(162 MHz, MeOD):** -0.78 (s); **ESI-MS:** m/z (%) 806.0 (100) [(M4−+3H)+2(N(Et)3)]−, 603.0 (21) [M4−+3H]−; calcd. for $C_{27}H_{25}O_8P_2S_2$ 603.0472; found 603.0478.
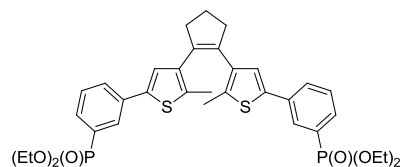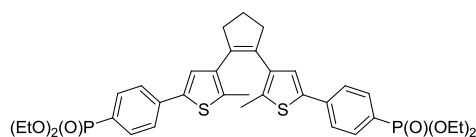

Synthesis of (4,4'-(cyclopent-1-ene-1,2-diyl)bis(5-methylthiophene-4,2-diyl))bis(4,1-phenylene) bis(phosphate) (7). Compound **7** was prepared from **4** (50 mg, 0.11 mmol), pyridine (191 μL, 2.36 mmol) and phosphorous oxychloride (103 μL, 1.12 mmol) following the general procedure **B** for phosphate ester formation. Automated reversed phase flash column chromatography (MeOH/water with 0.5% NEt3, 20-100% MeOH) and subsequent lyophilization afforded 73 mg (0.07 mmol, 64%) of **7** as purple oil. **1H-NMR: δH(400 MHz, MeOD):** 1.26 (36H, t, *J* = 7.3 Hz, 4 H+N(CH2C*H*3)3), 1.99 (6H, s, 2 thiophene-C*H*3), 2.08 (2H, dt, *J* = 7.5, 7.6 Hz, cyclopentene-C*H*2), 2.84 (4H, t, *J* = 7.4 Hz, 2 cyclopentene-C*H*2), 3.09 (24H, q, *J* = 7.3 Hz, 4 H+N(C*H*2CH3)3), 6.97 (2H, s, 2 thiophene-*H*), 7.20 (4H, d, *J* = 8.7 Hz, 4 phenyl-*H*), 7.40 (4H, d, *J* = 8.6 Hz, 4 phenyl-*H*); **13C-NMR: δC(101 MHz, MeOD):** 9.2 (+), 14.5 (+), 24.1 (−), 39.3 (−), 47.4 (−), 121.8 (+), 124.6 (+), 127.1 (+), 130.6 (q), 134.8 (q), 136.2 (q), 138.1 (q), 140.9 (q), 154.5 (q); **31P-NMR: δP(162 MHz, MeOD):** -2.26 (s); **ESI-MS:** m/z (%) 806.0 (100) [(M4−+3H)+2(N(Et)3)]−, 603.0 (15) [M4−+3H]−; calcd. for $C_{27}H_{25}O_8P_2S_2$ 603.0472; found 603.0465.

Synthesis of tetraethyl((4,4'-(cyclopent-1-ene-1,2-diyl)bis(5-methylthiophene-4,2-diyl))bis(3,1-phenylene)) bis(phosphonate) (10). A crimp top vial was loaded with compound **8**[30] (277 mg, 0.49 mmol), palladium acetate (11 mg, 0.05 mmol), triphenylphosphine (39 mg, 0.15 mmol) and a stirring bar and capped. It was set under nitrogen atmosphere at which point diethyl phosphite (0.15 mL, 1.18 mmol), triethylamine (0.20 mL, 1.47 mmol) and ethanol (4 mL) were added via syringes and the purple solution was refluxed for 48 h. After cooling to r.t. the reaction mixture was diluted with ethanol (5 mL), transferred to a round bottom flask and the volatiles were removed at the rotary evaporator. The brown residue was purified by automated flash column chromatography (PE/EtOAc, 40-95% EtOAc) yielding **10** (128 mg, 0.19 mmol, 39%) as purple oil. **1H-NMR:**

δ_H(**400 MHz, CDCl$_3$**): 1.29 (12H, t, J = 7.1 Hz, 2 P(O)(OCH$_2$CH_3)$_2$), 1.96 (6H, s, 2 thiophene-CH_3), 1.99 – 2.13 (2H, m, cyclopentene-CH_2), 2.82 (4H, t, J = 7.4 Hz, 2 cyclopentene-CH_2), 3.91 – 4.24 (8H, m, 2 P(O)(OCH_2CH$_3$)$_2$), 7.10 (2H, s, 2 thiophene-H), 7.39 (4H, td, J = 7.7, 4.4 Hz, 2 phenyl-H), 7.54 – 7.71 (4H, m, 4 phenyl-H), 7.93 (2H, dt, J = 14.1, 1.4 Hz, 2 phenyl-H); **^{13}C-NMR**: δ_C(**101 MHz, CDCl$_3$**): 14.5 (+), 16.3 (+), 23.0 (−), 38.6 (−), 62.2 (−), 124.8 (+), 128.2 (+), 128.3 (q), 129.0 (+), 129.1 (+), 130.0 (+), 134.7 (q), 134.9 (q), 135.4 (q), 136.9 (q), 138.4 (q); **^{31}P-NMR**: δ_C(**162 MHz, CDCl$_3$**): 19.0 (s); **ESI-MS**: m/z (%) 685.2 (100) [M+H]$^+$, 1391.4 (65) [2M+Na]$^+$; calcd. for C$_{35}$H$_{42}$O$_6$P$_2$S$_2$ 685.1971; found 685.1976.
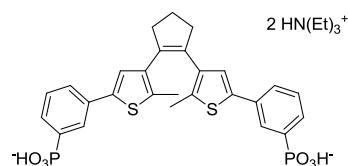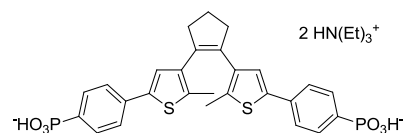

Synthesis of tetraethyl ((4,4'-(cyclopent-1-ene-1,2-diyl)bis(5-methylthiophene-4,2-diyl))bis(4,1-phenylene)) bis(phosphonate) (11). A crimp top vial was loaded with compound **9**[31] (248 mg, 0.44 mmol), palladium acetate (10 mg, 0.04 mmol), triphenylphosphine (34 mg, 0.14 mmol) and a stirring bar and capped. It was set under nitrogen atmosphere at which point diethyl phosphite (0.13 mL, 1.04 mmol), triethylamine (0.18 mL, 1.31 mmol) and ethanol (4 mL) were added via syringes and the purple solution was refluxed for 48 h. After cooling to r.t. the reaction mixture was diluted with ethanol (5 mL), transferred to a round bottom flask and the volatiles were removed at the rotary evaporator. The brown residue was purified by automated flash column chromatography (PE/EtOAc, 95% EtOAc) yielding **11** (102 mg, 0.15 mmol, 34%) as purple oil. **^{1}H-NMR**: δ_H(**400 MHz, CDCl$_3$**): 1.31 (12H, t, J = 7.1 Hz, 2 P(O)(OCH$_2$CH_3)$_2$), 1.99 (6H, s, 2 thiophene-CH_3), 2.02 – 2.14 (2H, m, cyclopentene-CH_2), 2.83 (4H, t, J = 7.4 Hz, 2 cyclopentene-CH_2), 3.92 – 4.29 (8H, m, 2 P(O)(OCH_2CH$_3$)$_2$), 7.11 (2H, s, 2 thiophene-H), 7.55 (4H, dd, J = 8.3, 3.7 Hz, 4 phenyl-H), 7.75 (4H, dd, J = 12.9, 8.3 Hz, 4 phenyl-H); **^{13}C-NMR**: δ_C(**101 MHz, CDCl$_3$**): 14.5 (+), 16.3 (+), 16.4 (+), 23.0 (−), 38.5 (−), 62.1 (−), 124.9 (+), 125.1 (+), 125.4 (+), 127.2 (q), 132.4 (+), 132.5 (+), 134.8 (q), 136.2 (q), 137.0 (q), 138.2 (q), 138.4 (q); **^{31}P-NMR**: δ_C(**162 MHz, CDCl$_3$**): 19.3 (s); **ESI-MS**: m/z (%) 685.2 (100) [M+H]$^+$, 1391.4 (44) [2M+Na]$^+$; calcd. for C$_{35}$H$_{42}$O$_6$P$_2$S$_2$ 685.1971; found 685.1977.

Synthesis of ((4,4'-(cyclopent-1-ene-1,2-diyl)bis(5-methylthiophene-4,2-diyl))bis(3,1-phenylene))diphosphonic acid (12). Compound **10** (118 mg, 0.17 mmol) was dissolved in

dry acetonitrile (15 mL) and treated with trimethylsilyl bromide (1.14 mL, 8.62 mmol). The reaction mixture was stirred at r.t. overnight. Volatiles were removed at the rotary evaporator. After purification by automated reversed phase flash column chromatography (MeOH/water with 0.5% NEt$_3$, 3-100% MeOH) and lyophilization compound **12** (114 mg, 0.15 mmol, 87%) was obtained as dark purple oil. **^{1}H-NMR: δ_H(400 MHz, MeOD):** 1.23 (18H, t, *J* = 7.3 Hz, 2 H$^+$N(CH$_2$C*H*$_3$)$_3$), 1.98 (6H, s, 2 thiophene-C*H*$_3$), 2.05 – 2.16 (2H, m, cyclopentene-C*H*$_2$), 2.86 (4H, t, *J* = 7.4 Hz, 2 cyclopentene-C*H*$_2$), 3.07 (12H, q, *J* = 7.3 Hz, 2 H$^+$N(C*H*$_2$CH$_3$)$_3$), 7.16 (2H, s, thiophene-*H*), 7.33 (2H, td, *J* = 7.7, 3.5 Hz, 2 phenyl-*H*), 7.44 – 7.59 (2H, m, 2 phenyl-*H*), 7.67 (2H, dd, *J* = 12.1, 7.5 Hz, 2 phenyl-*H*), 8.01 (2H, d, *J* = 13.1 Hz, 2 phenyl-*H*); **^{13}C-NMR: δ_C(101 MHz, MeOD):** 9.2 (+), 14.6 (+), 24.1 (−), 39.5 (−), 47.4 (−), 125.4 (+), 127.4 (+), 128.7 (+), 129.5 (+), 130.6 (+), 135.2 (q), 135.7 (q), 136.2 (q), 138.3 (q), 139.2 (q), 141.0 (q); **^{31}P-NMR: δ_P(162 MHz, MeOD):** 12.5 (s); **ESI-MS:** m/z (%) 571.1 (100) [M^{4-}+3H]$^-$; calcd. for C$_{27}$H$_{25}$O$_6$P$_2$S$_2$ 571.0573; found 571.0570.

Synthesis of ((4,4'-(cyclopent-1-ene-1,2-diyl)bis(5-methylthiophene-4,2-diyl))bis(4,1-phenylene))diphosphonic acid (13). Compound **11** (82 mg, 0.12 mmol) was dissolved in dry acetonitrile (5 mL) and treated with trimethylsilyl bromide (0.79 mL, 6.00 mmol). The reaction mixture was stirred at r.t. overnight. Volatiles were removed at the rotary evaporator. After purification by automated reversed phase flash column chromatography (MeOH/water with 0.5% NEt$_3$, 3-100% MeOH) and lyophilization compound **13** (76 mg, 0.10 mmol, 82%) was obtained as dark purple oil. **^{1}H-NMR: δ_H(400 MHz, MeOD):** 1.25 (18H, t, *J* = 7.3 Hz, 2 H$^+$N(CH$_2$C*H*$_3$)$_3$), 1.99 (6H, s, 2 thiophene-C*H*$_3$), 2.09 (2H, dt, *J* = 7.5, 7.6 Hz, cyclopentene-C*H*$_2$), 2.85 (4H, t, *J* = 7.4 Hz, 2 cyclopentene-C*H*$_2$), 3.09 (12H, q, *J* = 7.3 Hz, 2 H$^+$N(C*H*$_2$CH$_3$)$_3$), 7.17 (2H, s, thiophene-*H*), 7.50 (4H, dd, *J* = 8.4, 2.8 Hz, 4 phenyl-*H*), 7.73 (4H, dd, *J* = 12.1, 8.3 Hz, 4 phenyl-*H*); **^{13}C-NMR: δ_C(101 MHz, MeOD):** 9.2 (+), 14.7 (+), 24.1 (−), 39.4 (−), 47.4 (−), 125.4 (+), 125.8 (q), 132.6 (+), 136.2 (q), 136.7 (q), 136.9 (q), 138.4 (q), 138.5 (q), 140.7 (q); **^{31}P-NMR: δ_P(162 MHz, MeOD):** 12.9 (s); **ESI-MS:** m/z (%) 571.1 (100) [M^{4-}+3H]$^-$; calcd. for C$_{27}$H$_{25}$O$_6$P$_2$S$_2$ 571.0573; found 571.0579.

3.4.2 Photochromism of DTE-phosphates and DTE-phosphonates

Photochemical syntheses of ring-closed isomers. Solutions of compounds **5-7**, **12** and **13** (12.5 μM) in 50 mM Tris/acetate pH 8.5 were irradiated for 30 s with a 312 nm lamp yielding pink solutions containing the ring-closed isomers. The changes in the UV/Vis absorption spectra are representatively shown for compound **6** in Figure 5. The photostationary states contain between 93 and 97% of the ring-closed isomers according to HPLC analyses. The respective HPLC chromatograms of compound **6** in its open and closed form are depicted in Figure 6.
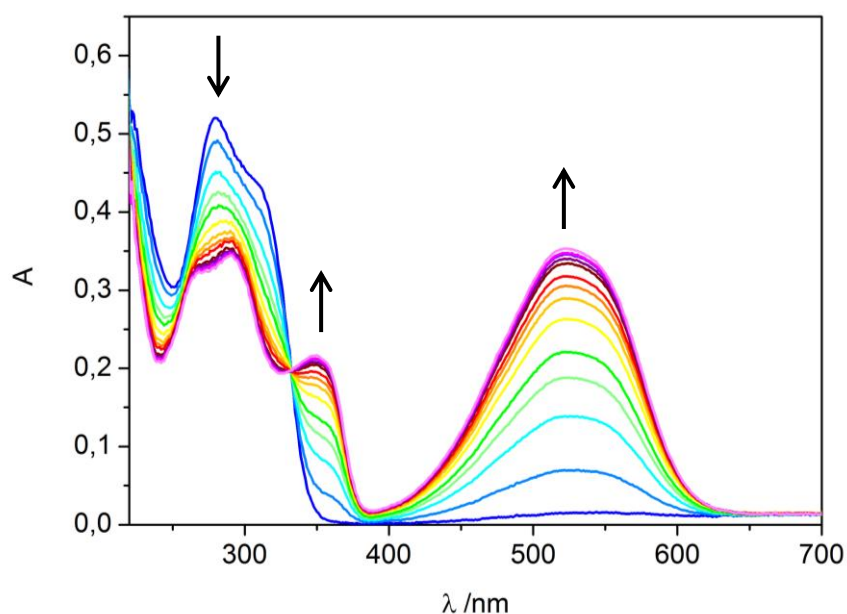
Figure 5. UV/Vis absorption spectra evolution of compound **6** upon irradiation with 312 nm light. Arrows indicate the changes of the absorption maxima of 12.5 μM **6** in 50 mM Tris/acetate pH 8.5 with irradiation intervals of 2 s from 0 to 30 s, which is illustrated by the color change from blue (open isomer) to purple (closed isomer).

Photochemical cycling studies. In order to test the robustness of the photochromic systems, photochemical cycling studies were recorded for all switches (Figure 7). In each case, a solution of 12.5 μM inhibitor in 50 mM Tris/acetate pH 8.5 was alternately irradiated with 312 nm light for 30 s and with visible light for 15 min over various cycles and the absorption change at 525 nm was monitored.
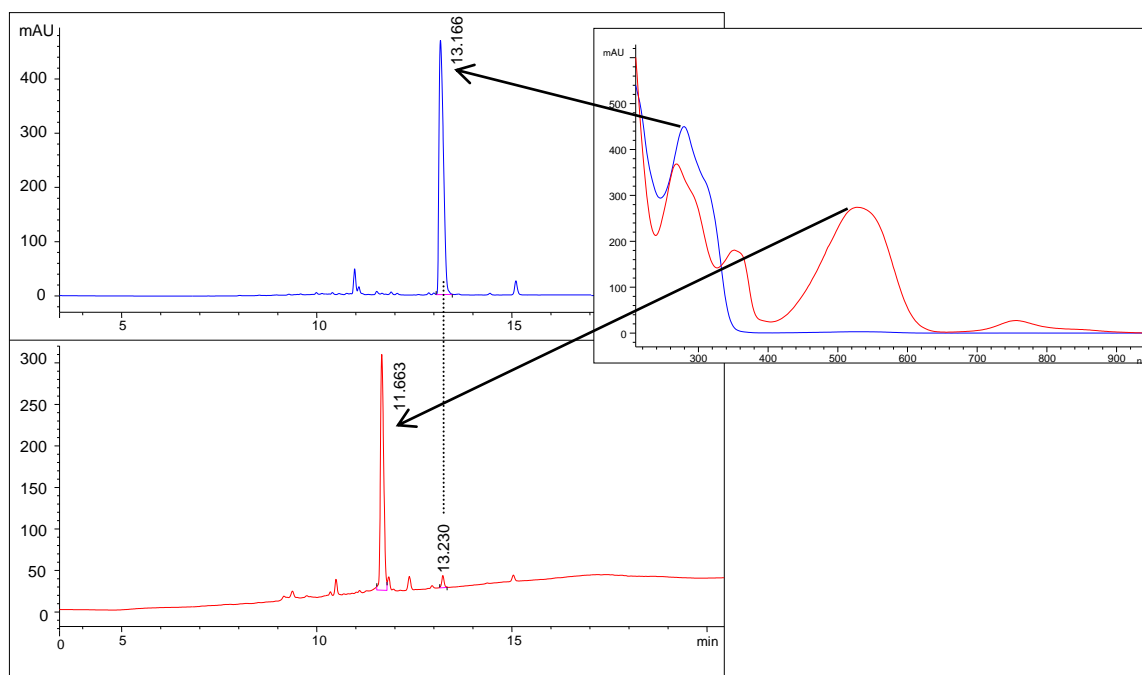
Figure 6. Representative HPLC chromatograms for the determination of the photostationary state of compound **6** (100 µM in 50 mM Tris/acetate pH 8.5). The UV/Vis signal was detected at 288 nm. The chromatograms before (upper) and after (lower) irradiation with 312 nm light for 30 s indicate that 97% of the open isomer (blue curve) were converted to the closed isomer (red curve). The absorption spectra of both forms are shown in the right panel.
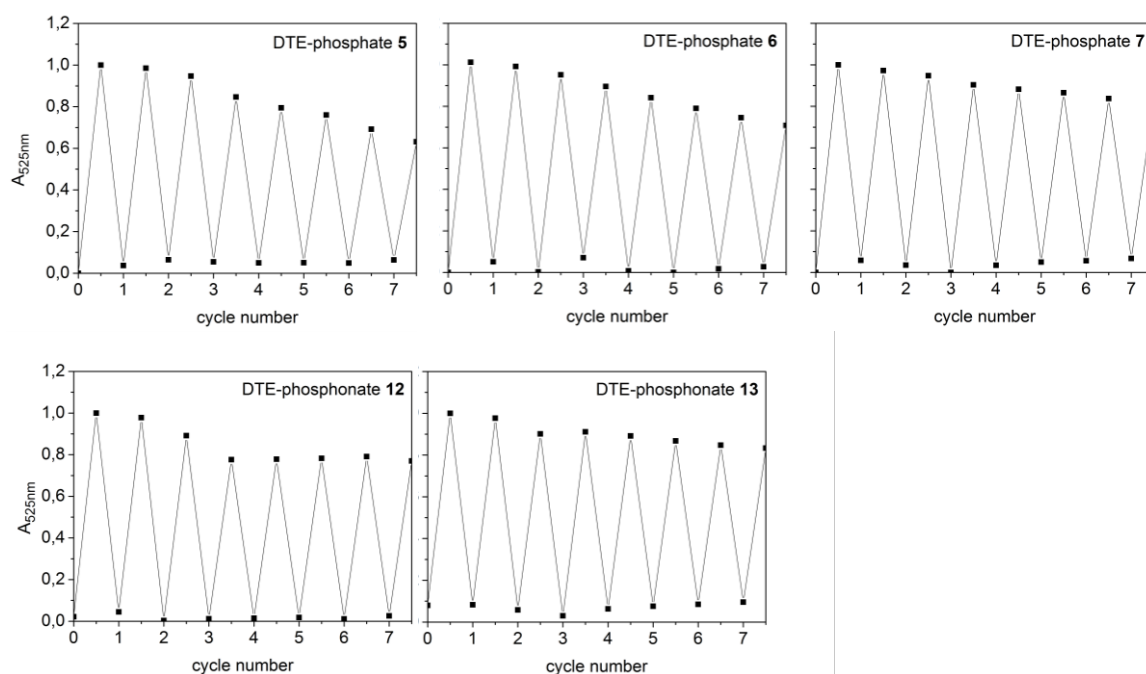
Figure 7. Cycle performance of compounds **5**-**7**, **12** and **13**. Changes in absorption at 525 nm were measured during an alternated irradiation of each inhibitor solution (12.5 µM in 50 mM Tris/acetate pH 8.5) with 312 nm light for 30 s and greater than 420 nm light for 15 min.

3.4.3   Cloning, Heterologous Expression in *E. coli*, and Purification of *mt*PriA

The gene coding for *mt*PriA was amplified by PCR using pETM-11-*mt*PriA[19] as a template and cloned into the vector pET24a(+) (Stratagene) via the terminal restriction sites for *Nde*I and *Xho*I. *mt*PriA was heterologously expressed in *E. coli* BL21-Gold cells (Stratagene) transformed with pET(24a)(+)-mt*pri*A. To this end, five liters of Luria Broth (LB) medium supplemented with 75 μg/mL kanamycin were inoculated with a pre-culture and incubated at 37 °C. After an OD_{600} of 0.6 was reached, the temperature was lowered to 20 °C. Expression was induced by adding 0.5 mM IPTG, and growth was continued overnight. Cells were harvested by centrifugation (Sorvall/RC5B, GS3, 15 min, 4000 rpm, 4 °C) and suspended in 50 mM Tris/HCl pH 8.0, 300 mM NaCl, 10 mM imidazole. After lysing by sonication (Branson Sonifier W-250D, 2 x 2 min in 15 sec intervals, 45% pulse, 0 °C), cells were centrifuged again (Sorvall/RC5B, SS34, 30 min, 13.000 rpm, 4 °C) to separate the soluble from the insoluble fraction of the cell extract. As a first purification step, *mt*PriA was subjected to a Ni^{2+} affinity chromatography using its C-terminal hexa-histidine tag. To this end, the soluble supernatant was loaded onto a HisTrapFF crude column (5 mL; GE Healthcare), which had been equilibrated with 50 mM Tris/HCl pH 8.0, 300 mM NaCl, 10 mM imidazole. After washing the column with the equilibration buffer, a linear gradient of 10-500 mM imidazole was applied and *mt*PriA eluted between 40 and 100 mM imidazole. Main fractions were pooled and further purified via size exclusion chromatography. For this purpose, a Superdex200 column (HiLoad 26/60, 320 mL, GE Healthcare) was equilibrated and operated with 50 mM Tris/HCl pH 8.0, 200 mM sodium chloride, 2 mM dithiothreitol at 4 °C. Fractions with pure protein were pooled and dialyzed twice against 50 mM Tris/HCl pH 8.0. According to SDS-PAGE (12.5% acrylamide), *mt*PriA was more than 95% pure. About 1 mg of protein was obtained per liter of culture.

3.4.4   Steady-state Enzyme Kinetics of *mt*PriA

Steady-state enzyme kinetics of the *mt*PriA reaction were measured spectrophotometrically at 300 nm as described.[25] In a coupled enzyme assay the substrate ProFAR was initially converted to PRFAR, which was further processed by the enzyme HisF from *Thermotoga maritima* (*tm*HisF) to yield imidazole glycerol phosphate (ImGP) and aminoimidazole carboxamide ribonucleotide (AICAR) (Scheme 3). As ProFAR and PRFAR exhibit identical absorption spectra, the second step is indispensible in order to monitor the reaction progress at 300 nm ($\Delta\varepsilon_{300}$(ProFAR-AICAR) = 5.637 mM^{-1}cm^{-1}). It furthermore prevents product inhibition of the *mt*PriA reaction.[32]
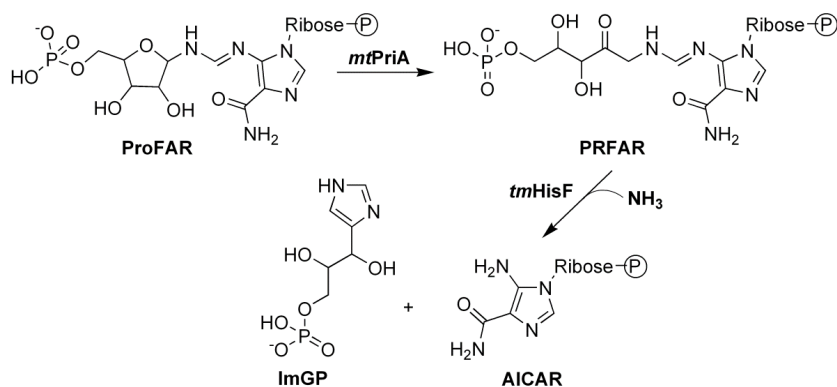
Scheme 3. Coupled enzyme assay for photometric determination of *mt*PriA activity.

The steady-state catalytic parameters of *mt*PriA in the absence of inhibitor were determined in triplicate at 25 °C in 50 mM Tris/acetate pH 8.5 in the presence of 100 mM ammonium acetate, 2-73 µM ProFAR, and 0.2 µM *tm*HisF (Table 2). Reactions were initiated with 0.2 µM *mt*PriA, when the baseline signal was constant. To determine the inhibition constants of compounds **5-7**, **12** and **13** in their open and closed forms, three saturation curves were measured in presence of different inhibitor concentrations in each case. Reaction mixtures contained 100 mM ammonium acetate, 3-190 µM ProFAR, 0.4-20 µM inhibitor (closed inhibitor forms were synthesized photochemically prior to addition to the reaction mixture), and 0.04-0.2 µM *tm*HisF in 50 mM Tris/acetate pH 8.5. Substrate turnover was initiated with 0.04-0.2 µM *mt*PriA. The molar concentration of *mt*PriA and *tm*HisF did not exceed a tenth of the respective inhibitor concentration. Additionally, to rule out artifacts, the photostability of inhibitor **6** was representatively investigated under assay conditions: 15 µM of **6** in both isomeric forms were irradiated for 30 minutes at 300 nm in the spectrophotometer and no change in the absorption spectra was observed. Moreover, it was assured that the performance of *mt*PriA is rate-limiting in each kinetic setup, as doubling of its concentration resulted in a doubled initial velocity. Finally, the inhibition constant K_i of each DTE compound could be calculated from Formula 1, where K_m is the Michaelis constant of *mt*PriA and K_m^{app} is the apparent K_m value determined in the presence of a distinct inhibitor concentration $c(I)$. All kinetic parameters are given in Table 2 and steady-state enzyme kinetics of **6** in its open and closed form are illustrated in Figure 8.

$$K_i = \frac{K_m \cdot c(I)}{K_m^{app} - K_m}$$

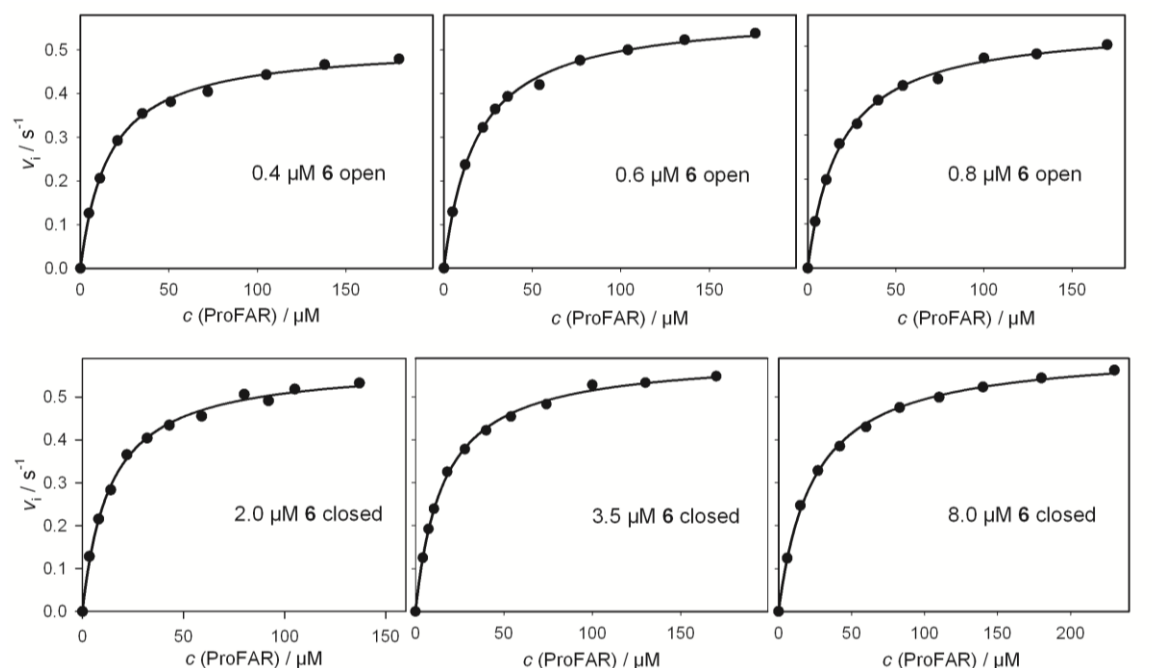**Formula 1.** Determination of inhibition constant K_i.

Figure 8. Substrate saturation curves of *mt*PriA in the presence of inhibitor **6** in its open (upper curves) and closed (lower curves) form. See Table 2 for deduced steady-state kinetic parameters.

Table 2. Steady-state kinetic constants for the ProFAR isomerization activity of *mt*PriA in absence and presence of compounds **5**-**7**, **12** and **13** in their ring-open and ring-closed forms.

Inhibitor	$c(I)$ / µM open / closed	k_{cat} / s^{-1}	K_m / µM	K_i / µM
-		0.49	8.6	
		0.49	9.2	
		0.57	8.1	
5	5.0 / 5.0	0.47 / 0.58	12.7 / 13.9	10.5 / 8.1
	10.5 / 10.5	0.59 / 0.55	20.9 / 21.5	7.3 / 7.0
	18.0 / 18.0	0.55 / 0.60	32.5 / 35.2	6.5 / 5.8
6	0.4 / 2.0	0.52 / 0.56	16.2 / 12.4	0.45 / 4.5
	0.6 / 3.5	0.59 / 0.60	18.7 / 15.9	0.51 / 4.1
	0.8 / 8.0	0.55 / 0.61	18.5 / 23.7	0.69 / 4.6
7	2.0 / 3.5	0.47 / 0.58	13.1 / 16.2	3.8 / 4.0
	3.5 / 7.0	0.47 / 0.55	17.7 / 24.8	3.3 / 3.7
	5.0 / 10.5	0.47 / 0.53	21.7 / 35.6	3.3 / 3.3
12	1.5 / 4.0	0.57 / 0.55	16.3 / 15.2	1.7 / 5.2
	2.5 / 10.0	0.58 / 0.57	22.3 / 27.1	1.6 / 4.6
	4.0 / 15.0	0.60 / 0.55	29.4 / 34.9	1.7 / 4.9
13	5.0 / 15.0	0.60 / 0.58	15.7 / 15.1	6.1 / 19.8
	10.0 / 15.0	0.60 / 0.57	20.7 / 15.0	7.1 / 20.2
	15.0 / 20.0	0.59 / 0.57	26.6 / 14.7	7.2 / 28.2

Three substrate saturation curves were recorded at different inhibitor concentrations $c(\text{I})$ for each form (open/closed). The deduced k_{cat} and K_m values are shown. The shown K_i values were calculated with Formula 1 from the increase of the apparent K_m value with respect to the K_m value in absence of inhibitor. The mean values and standard deviations of K_i for each inhibitor are given in Table 1.

3.4.5 Molecular Modeling

Energy minimization of the open and closed isomers of compounds 5-7, 12 and 13.
The conformer distribution of compounds **5**, **6**, **7**, **12** and **13** in their open and closed isomers was calculated by Wavefunction Spartan'10[33] using molecular mechanics in water (MMFFaq) in the ground state with 20.000 conformers examined, a total charge of -2 for phosphonates or -4 for phosphates, singlet multiplicity, subject to symmetry and global calculations. Sorted by energy minimum the five best results for each calculation were averaged and are shown in Scheme 2.

Molecular Dynamics (MD) simulations of *mt*PriA with compound 6 bound in its open and closed form. Modeling and MD simulations were performed with YASARA Structure Version 13.4.21 employing the YAMBER3 force field.[34] Simulations were run at 298 K under periodic boundary conditions and with explicit water, using a multiple time step of 1 fs for intramolecular and 2 fs for intermolecular forces. Lennard-Jones forces and long-range electrostatic interactions were treated with a 7.86 Å cutoff, the latter were calculated using the Particle Mesh Ewald method.[35] Temperature was adjusted using a Berendsen thermostat based on the time-averaged temperature and simulations were carried out at constant pressure. The parameterization of the open and closed forms of compound **6** was performed using the AM1BCC protocol[36], that assigns atomic charges by applying additive bond charge corrections (BCCs) to semi-empirical AM1 atomic charge calculations. Based on the crystal structure of *mt*PriA (PDB ID 3ZS4), the original ligand PRFAR was removed and manually replaced by compound **6** in the open and closed form in order to fit the phosphate binding pockets. The simulation cell was defined as 5 Å larger than the protein along each axis (cell dimensions 52 × 47 × 44 Å³), filled with water to a density of 0.997 g/mL, and counterions were added to a final concentration of 0.9% NaCl. The protonation states of protein side chains were assigned according to Krieger *et al.*[37] In order to remove conformational stress, two phases of equilibration were conducted: After a 100 ps equilibration with frozen protein coordinates, the whole system was equilibrated for 1 ns. The two equilibrated models of the open and closed form were subsequently used for the six

following (three for each conformer) production MD simulations. To reassign initial atom velocities and thus seed independent calculations, the temperature was slightly changed (+/-0.0001 K) for the respective second and third simulation runs of the open/closed form. Trajectories were sampled at intervals of 100 ps for a total of 10 ns for each model. Each snapshot was energy minimized as follows: After removing conformational stress by a steepest descent minimization, the procedure continued by simulated annealing (time step 2 fs, atom velocities scaled down by 0.9 every 10th step) until convergence was reached, i.e. the energy improved by less than 0.05 kJ/mol per atom during 200 steps. Binding energies were obtained for each energy minimized snapshot using YASARA's integrated binding energy function that computes the energetic difference of the ligand at bound state and at infinite distance from its binding site. Representative enzyme models (shown in Figure 4) for each simulation are based on the energy minimized snapshots with the best binding energy. The ligand binding energies and standard deviations (see Table 3) were calculated by using the full production trajectory.

Table 3. Ligand binding energies derived from MD simulations of *mt*PriA and compound **6** in its open and closed form.[a]

	Ligand binding energy (open) [kJ/mol]	Ligand binding energy (closed) [kJ/mol]
run 1	-2171 ± 55	-2062 ± 64
run 2	-2162 ± 59	-1919 ± 71
run 3	-2122 ± 77	-2049 ± 60

[a] Three independent simulations were performed in each case; see Experimental Methods for details.

3.5 References

[1]   C. Brieke, F. Rohrbach, A. Gottschalk, G. Mayer, A. Heckel, *Angew. Chem. Int. Ed. Engl.* **2012**, *51*, 8446-8476.

[2]   A. Deiters, *ChemBioChem* **2010**, *11*, 47-53.

[3]   U. Krauss, T. Drepper, K. E. Jaeger, *Chem.-Eur. J.* **2011**, *17*, 2552-2560.

[4]   O. Yizhar, L. E. Fenno, T. J. Davidson, M. Mogri, K. Deisseroth, *Neuron* **2011**, *71*, 9-34.

[5]   F. Zhang, J. Vierock, O. Yizhar, L. E. Fenno, S. Tsunoda, A. Kianianmomeni, M. Prigge, A. Berndt, J. Cushman, J. Polle, J. Magnuson, P. Hegemann, K. Deisseroth, *Cell* **2011**, *147*, 1446-1457.

[6]   W. Szymanski, J. M. Beierle, H. A. Kistemaker, W. A. Velema, B. L. Feringa, *Chem. Rev.* **2013**.

[7]   T. Fehrentz, M. Schönberger, D. Trauner, *Angew. Chem. Int. Ed. Engl.* **2011**, *50*, 12156-12182.

[8]   I. Tochitsky, M. R. Banghart, A. Mourot, J. Z. Yao, B. Gaub, R. H. Kramer, D. Trauner, *Nat. Chem.* **2012**, *4*, 105-111.

[9]   M. R. Banghart, A. Mourot, D. L. Fortin, J. Z. Yao, R. H. Kramer, D. Trauner, *Angew. Chem. Int. Ed. Engl.* **2009**, *48*, 9097-9101.

[10] S. Muramatsu, K. Kinbara, H. Taguchi, N. Ishii, T. Aida, *J. Am. Chem. Soc.* **2006**, *128*, 3764-3769.

[11] S. Herre, T. Schadendorf, I. Ivanov, C. Herrberger, W. Steinle, K. Rück-Braun, R. Preissner, H. Kuhn, *ChemBioChem* **2006**, *7*, 1089-1095.

[12] D. Vomasta, C. Högner, N. R. Branda, B. König, *Angew. Chem. Int. Ed. Engl.* **2008**, *47*, 7644-7647.

[13] D. Vomasta, A. Innocenti, B. König, C. T. Supuran, *Bioorg. Med. Chem. Lett.* **2009**, *19*, 1283-1286.

[14] F. Barona-Gomez, D. A. Hodgson, *EMBO Rep.* **2003**, *4*, 296-300.

[15] K. Mdluli, M. Spigelman, *Curr. Opin. Pharmacol.* **2006**, *6*, 459-467.

[16]   H. Shen, F. Wang, Y. Zhang, Q. Huang, S. Xu, H. Hu, J. Yue, H. Wang, *FEBS J.* **2009**, *276*, 144-154.

[17]   B. Höcker, C. Jürgens, M. Wilmanns, R. Sterner, *Curr. Opin. Biotechnol.* **2001**, *12*, 376-381.

[18]   R. K. Wierenga, *FEBS Lett.* **2001**, *492*, 193-198.

[19]   A. V. Due, J. Kuper, A. Geerlof, J. P. von Kries, M. Wilmanns, *Proc. Natl. Acad. Sci. U. S. A.* **2011**, *108*, 3554-3559.

[20]   J. Kuper, C. Doenges, M. Wilmanns, *EMBO Rep.* **2005**, *6*, 134-139.

[21]   F. List, R. Sterner, M. Wilmanns, *ChemBioChem* **2011**, *12*, 1487-1494.

[22]   D. H. Waldeck, *Chem. Rev.* **1991**, *91*, 415-436.

[23]   A. A. Beharry, G. A. Woolley, *Chem. Soc. Rev.* **2011**, *40*, 4422-4437.

[24]   M. Irie, *Chem. Rev.* **2000**, *100*, 1685-1716.

[25]   T. J. Klem, V. J. Davisson, *Biochemistry* **1993**, *32*, 5177-5186.

[26]   M. G. Franco, B. Laber, R. Huber, T. Clausen, *Structure* **2001**, *9*, 245-253.

[27]   E. Lorentzen, E. Pohl, P. Zwart, A. Stark, R. B. Russell, T. Knura, R. Hensel, B. Siebers, *J. Biol. Chem.* **2003**, *278*, 47253-47260.

[28]   T. Wagner, I. A. Shumilin, R. Bauerle, R. H. Kretsinger, *J. Mol. Biol.* **2000**, *301*, 389-399.

[29]   L. N. Lucas, J. J. D. de Jong, J. H. van Esch, R. M. Kellogg, B. L. Feringa, *Eur. J. Org. Chem.* **2003**, 155-166.

[30]   T. Kudernac, J. J. De Jong, J. Van Esch, B. L. Feringa, D. Dulic, S. J. Van Der Molen, B. J. Van Wees, *Mol. Cryst. Liq. Cryst.* **2005**, *430*, 205-210.

[31]   M. Akazawa, K. Uchida, J. J. D. de Jong, J. Areephong, M. Stuart, G. Caroli, W. R. Browneb, B. L. Feringa, *Org. Biomol. Chem.* **2008**, *6*, 1544-1547.

[32]   C. Jürgens, A. Strom, D. Wegener, S. Hettwer, M. Wilmanns, R. Sterner, *Proc. Natl. Acad. Sci. U. S. A.* **2000**, *97*, 9925-9930.

[33]   Spartan '10 v.11.11.10, *Wavefunction Inc.*, 18401 Von Karman Ave., Suite 18370, Irvine, CA 92612.

[34]   E. Krieger, T. Darden, S. B. Nabuurs, A. Finkelstein, G. Vriend, *Proteins* **2004**, *57*, 678-683.

[35]   U. Essmann, L. Perera, M. L. Berkowitz, T. Darden, H. Lee, L. G. Pedersen, *J. Chem. Phys.* **1995**, *103*, 8577-8593.

[36]   A. Jakalian, D. B. Jack, C. I. Bayly, *J. Comput. Chem.* **2002**, *23*, 1623-1641.

[37]   E. Krieger, J. E. Nielsen, C. A. Spronk, G. Vriend, *J. Mol. Graphics Modell.* **2006**, *25*, 481-486.

CHAPTER 2

4 TOWARDS PHOTOSWITCHABLE KINASE INHIBITORS[†]

4.1 Introduction

The detailed understanding how molecular mechanisms proceed during cell signal transduction remains an important topic of cell biology. Phosphorylation by protein kinases is one of the most frequent modes to regulate vital processes in the human body like gene expression, protein translation, cell cycle progression and apoptosis.[1] More than 500 different protein kinases are encoded in the human genome.[2] As components of cellular cascade systems they mediate each other sequentially (cf. Figure 9), usually by transferring the γ-phosphate of adenosine triphosphate (ATP) covalently to serine, threonine or tyrosine hydroxides of their specific substrates. It has been assessed that malfunction of the kinases contributes to human diseases including obesity, diabetes, rheumatoid arthritis, neurodegenerative disorders and cancer.[2-4] Kinases are therefore one of the most important targets in drug discovery but the information on the exact mechanisms of molecular control is still limited.[3, 5]

The extracellular-regulated kinase (ERK) pathway (Figure 9) plays a central role in cancer research as it controls the growth and survival of a broad spectrum of human tumors.[6] When growth factors bind extracellularly to a specific transmembrane receptor they launch signal transduction through the protein kinase cascade Ras-Raf-MEK-ERK. ERK occurs either as ERK1 or ERK2, which are closely related to each other (84% sequence identity) and share many if not all functions; they are therefore usually referred to as ERK1/2.[7] As pivot of this cascade, ERK1/2 activates transcription factors in the cell nucleus to initiate protein expression, cell proliferation, or apoptosis.[7] Inhibiting ERK1/2 thus allows for new anti-tumor treatments and several inhibitors are currently subjected to clinical trials.[8] However, deciphering the mechanisms of the ERK pathway continues to be an important and challenging task.[4, 7]
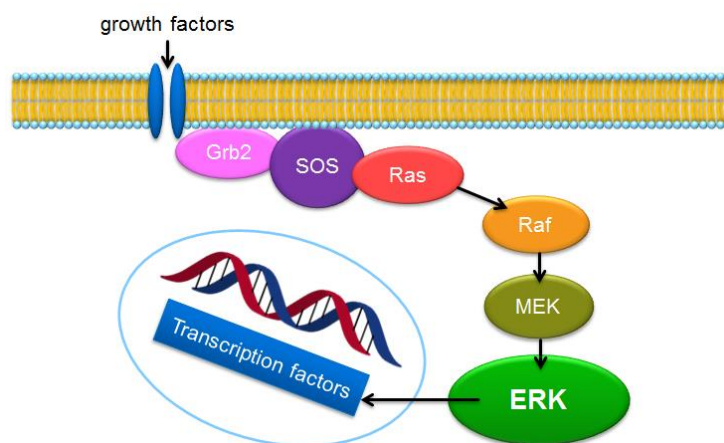

Figure 9. The extracellular-regulated kinase (ERK) pathway.

The development of remote-controllable, fast-acting and selective ERK1/2 inhibitors may provide a convenient tool to further investigate the dynamic operation and time-dependent parameters for signaling output. As outlined in Chapter 1, the regulation of biomolecules by light has gained a rapidly growing interest in science.[9-11] Most examples include azobenzene units due to easy synthetic access, high photostability and ultrafast kinetics. Exploiting their quick response nature, photoswitchable ion channel or receptor ligands were developed to reversibly control neuronal activity.[12-15] However, their performance is limited because they do not allow a complete photoconversion and the thermal *cis* to *trans* reisomerization is fast.[12] In contrast, photoswitchable molecular tools based on the 1,2-dithienylethene (DTE) scaffold exhibit high photostationary states and thermal stability of both photoisomers in the dark,[16] which makes them ideal candidates for the light-dependent control of rather slow biological processes such as enzymatic reactions or DNA hybridization.[17-24]
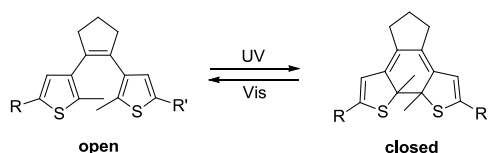
Scheme 4. Light-induced switching of a DTE between its open isomer and closed isomer.

Irradiation with UV or visible light, respectively, toggles DTEs between the open and the closed photoisomer (Scheme 4). Selective ATP competitive ERK1/2 inhibitors (Figure 10) and the open isomer share similar shapes which correlate in size and electronics.[25-26] Equipped with suitable hydrogen bonding motifs the DTE may join the ATP binding site of the kinase and thereby inhibit enzyme activity. As the conformation of the respective closed isomer is far more rigid (Scheme 4), its affinity to the catalytic center is expected to be reduced, which in turn enhances kinase activity. Hence we aimed to develop DTE based ERK1/2 inhibitors, which toggle kinase activity upon irradiation with light. Our desired photoswitchable kinase inhibitors should allow for the non-invasive, reversible remote-control of cellular kinase function in real time and thereby provide a convenient tool to deepen the understanding of cellular signal mechanisms. Based on these studies new methods of anticancer therapy could be established.
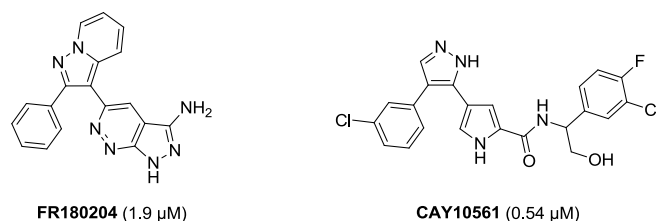

FR180204 (1.9 µM)   **CAY10561** (0.54 µM)

Figure 10. Selective ERK2 inhibitors with IC_{50} values in brackets.[25-26]

4.2   Results and Discussion

4.2.1   Molecular Docking

In order to design photoswitchable kinase inhibitors, suitable DTE based structures were virtually screened. The binding mode and affinity between small-molecule ligands and the kinase receptor were calculated by Molecular Docking.[27] ERK2 (PDB ID 1TVO) was used as receptor grid and the library of ligands consisted of open and closed isomer dithienylcyclopentene derivatives with different short hydrogen bonding motifs at their thiophene moieties. Hits were identified by scoring function and chosen manually, whereby the binding mode and affinity of the respective open/-closed photoisomer pairs must differ significantly. The compounds drawn in Figure 11 adopted similar positions as the co-crystallized ligand **FR180204** in the catalytic site (Figure 12). Concurrently, their particular ring-closed counterparts were randomly distributed as result of weak interactions with the designed grid area of the enzyme.
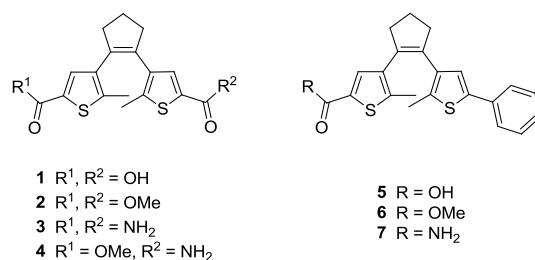

1 R^1, R^2 = OH
2 R^1, R^2 = OMe
3 R^1, R^2 = NH_2
4 R^1 = OMe, R^2 = NH_2

5 R = OH
6 R = OMe
7 R = NH_2

Figure 11. DTEs **1**-**7** were identified as hits after virtual screening with ERK2 receptor (PDB ID 1TVO). Their respective ring-closed isomers afforded significantly lower docking scores.
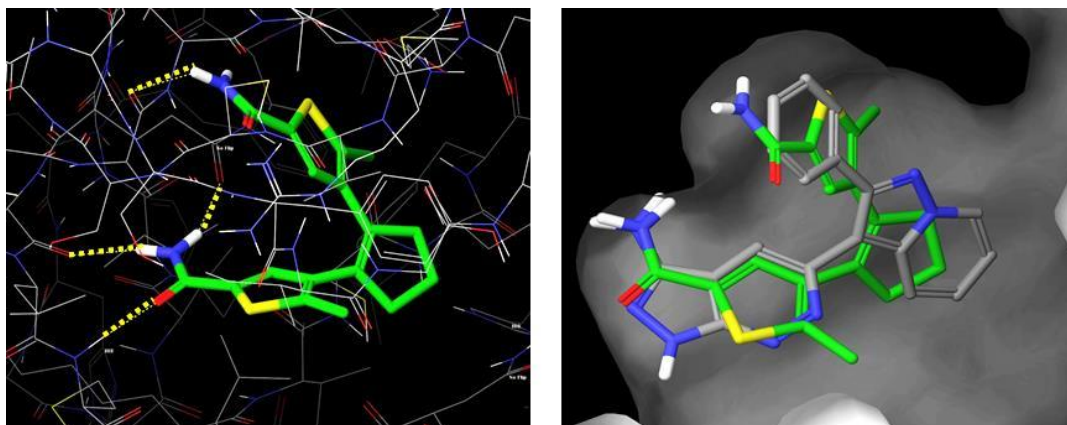

Figure 12. Binding mode of the ring-open DTE **3** (green) in the ATP binding pocket of the target kinase ERK2. Left: four hydrogen bonds to the protein are indicated in yellow. Right: superposition of **3** with reference ligand **FR180204** (grey), the protein surface is shown as grey shadows.

4.2.2   Synthesis

The desired photoswitchable kinase inhibitors were prepared via bischloro-DTE **11** and chloro-phenyl-DTE **12** according to literature known procedures (Scheme 5).[28-29] Starting with chlorination of 2-methyl-thiophene **8**, subsequent Friedel-Crafts acylation followed by McMurry coupling led to compound **11** in moderate to good yields (58-79%). Further modification to obtain compound **12** was accomplished by Suzuki coupling (64% yield).
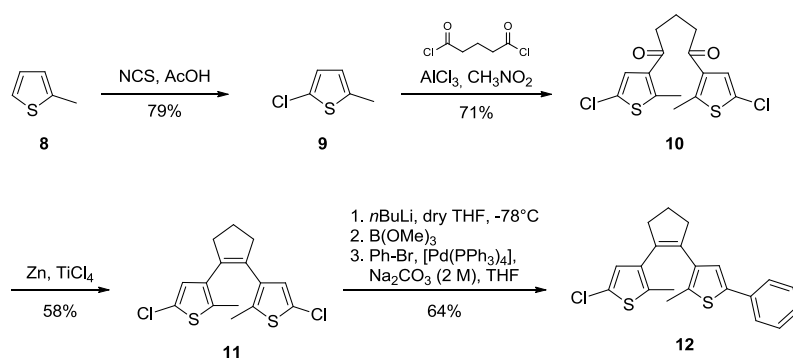
Scheme 5. Synthesis of the bischloro-DTE **11** and chloro-phenyl-DTE **12** as precursors for further derivatization.

In order to afford carboxy-DTEs **1** and **5**, the chlorine atoms of compounds **11** and **12** were transformed into carboxylic acids via lithium halide exchange with *n*-butyl lithium, followed by treating with gaseous carbon dioxide and acidic work-up (Scheme 6). Reactions achieved very good yields of 98 to 99%. Acidic esterification of **1** and **5** in methanol led to methyl ester-DTEs **2** and **6** in excellent yields of 94 to 96%. DTEs **1** and **5** were treated with thionyl chloride and subsequently converted into either amide or methyl ester residues using gaseous ammonia in anhydrous THF to yield DTEs **3** and **7** (61-71%) or a solution of ammonia in methanol to access DTE **4** (35%).
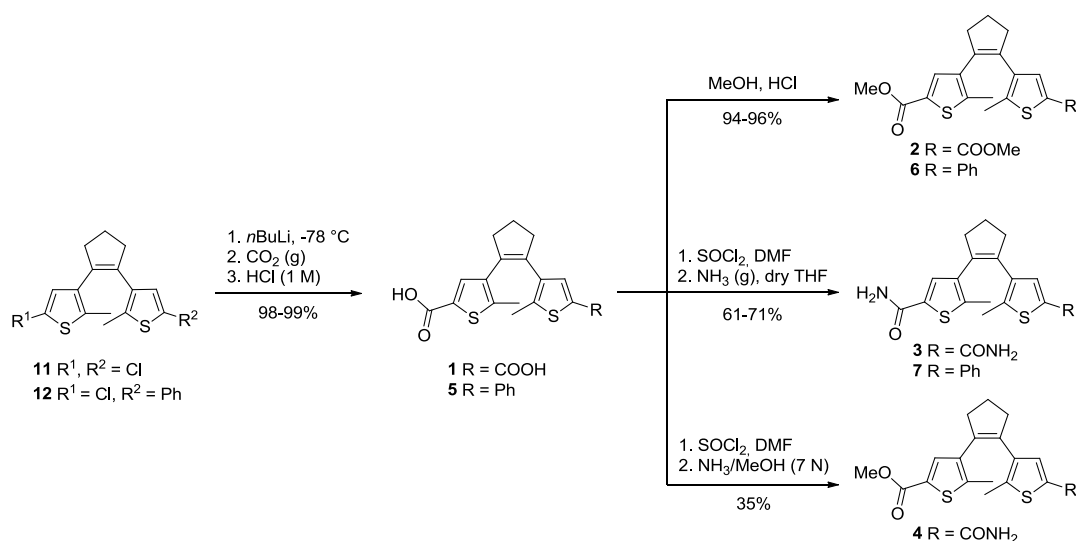
Scheme 6. Synthetic pathway to access the target DTEs **1**-**7**.

4.2.3 Photochromism

The photochemical properties of the target DTEs **1-7** were spectrophotometrically studied. All title compounds exhibited excellent photochromic behavior in methanol solutions. Figure 13 shows exemplarily the UV/Vis absorption spectra evolution of compound **4** upon irradiation with 312 nm light in periods of 6 s. The absorption band at 260 nm decreases and two new maxima arise at around 355 and 525 nm, which results from the ring-closed isomer formation, and turns the initially colorless solution pink (Figure 13). The photostationary states (PS) are reached after 36 to 72 s of UV irradiation (Table 4, appendix Figure A1). Exposure to visible light (> 420 nm) induces the reopening, which is usually complete after 15 min and can be observed by decoloration and return to the original spectrum.
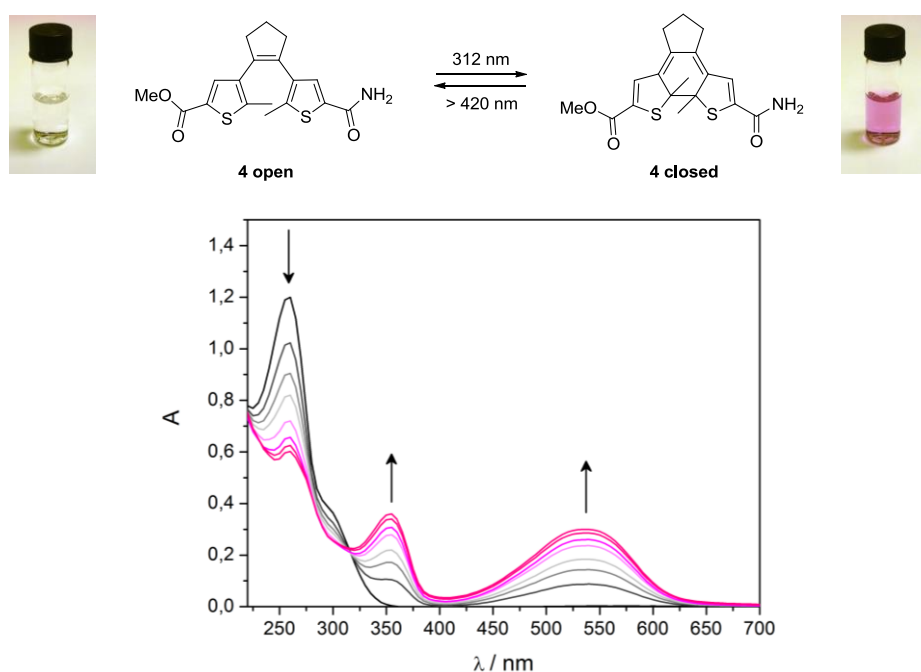

Figure 13. Light-induced interconversion of compound **4** between its open and closed isomer and its UV/Vis absorption spectra evolution (50 µM in MeOH) upon irradiation with 312 nm light; arrows indicate the changes of the absorption maxima with irradiation periods of 6 s; the colors of the respective solutions are depicted.

The cycle performance of the title compounds **1-7** was studied by alternately irradiation with 312 nm and greater than 420 nm light. Figure 14 depicts the photostability of DTE **4** with a high fatigue resistance of 91% after eight ring-closing/-opening cycles. The spectra for DTEs **1-3** and **5-7** are included in the appendix in Figure A2 with moderate to good fatigue resistance rates ranging from 62 to 83% (Table 4).
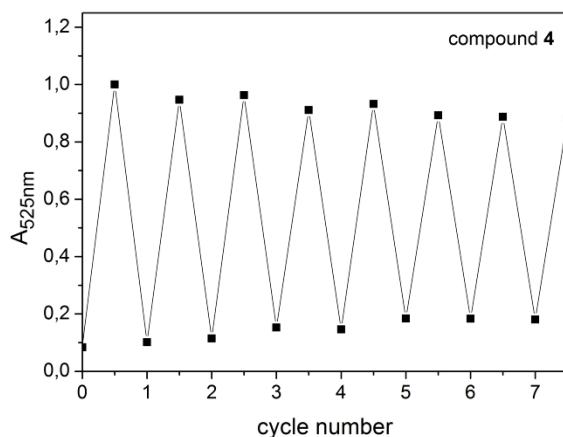
Figure 14. Cycle performance of compound **4**. Changes in absorption at 525 nm were measured during an alternated irradiation of the inhibitor solution (50 µM in MeOH) with 312 nm light for 60 s and greater than 420 nm light for 15 min.

Table 4 summarizes the photochemical properties of the target DTEs **1**-**7** including the time of UV irradiation to reach the PS (t_{PS}), the fatigue resistance after recording eight ring-closing/-opening cycles, and the thermal stability of the closed photoisomers. We could not observe any consistent correlation between substitution pattern and the examined parameters.

Table 4. Photochemical properties of the target DTEs **1**-**7**.

Compound	t_{PS} [s]	Fatigue resistance[a] [%]	Thermal stability[b] [%]
1	54	75	37
2	66	83	46
3	72	80	31
4	42	91	36
5	54	79	52
6	60	66	77
7	36	62	48

[a] after 8 cycles, [b] after storage in 10 mM DMSO solutions for 6 months at -20 °C in the dark.

4.2.4 Biological Test Results

Whole-cell dose response experiments.

To study the inhibitory activity of the photoswitchable kinase inhibitors **1-7** a whole-cell reporter gene assay was performed.[30] Thereby, the ERK1/2 activity of HEK cells was detected at distinct amounts of inhibitor to generate dose response curves. Initially, neurotensin stimulates the neurotensin receptor 1 to launch the phosphorylation cascade, which activates ERK1/2 further downstream. Activated ERK1/2 in turn phosphorylates the transcription factor Elk1, which leads to accumulation of luciferase in the cell. The luminescence signal is thus proportional to ERK1/2 activation and a reduced luminescence indicates the inhibition of ERK1/2. The inhibitory activity of DTEs **1-7** against ERK1/2 was examined as open and closed isomers separately. We irradiated the photoswitches prior to incubation of the cells. The experiments were performed in the dark and the ERK2 inhibitor **FR180204** was used as reference.
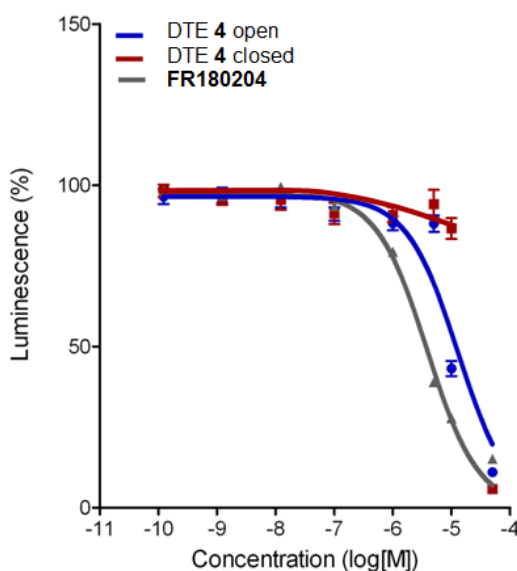

Figure 15. Inhibition curves of **4** in its open (blue) and closed (red) isomer. The reference inhibitor **FR180204** is marked in grey.

We observed that all compounds were sufficiently transported into the cells as determined by UV/Vis absorption measurements of the cell lysate after centrifugation. Figure 15 shows exemplarily the inhibition curves of DTE **4** in its open (IC_{50} 13 μM) and closed isomer (IC_{50} n.a.). Indeed, the design concept seems viable regarding the distinct performances of the two isoforms. Table 5 summarizes the test results for all inhibitors **1-7** and the particular dose response curves for DTEs **1-3** and **5-7** are included in the appendix in Figure A3. The open isomer compounds of DTEs **1-4** and **7** achieved inhibition constants in the micromolar range, while only DTE **2, 4** and **7** reached the efficacy of the reference inhibitor. Their respective closed isomers were solely active at the highest concentration, which may

indicate cytotoxicity. However, we could not observe any toxic effects of the ring-open isomers. DTEs **5** and **6** exhibited not enough activity at the concentrations applied. Taken together, these results confirm efficient photoswitchable activities of the designed molecules **2, 4** and **7** within the ERK cascade in HEK cells. Nevertheless, cells contain a complex machinery of various factors, which could response to interaction with the DTEs and generate the observed signal. We hence performed further *in vitro* investigations to support the observed findings.

Table 5. Test results of whole-cell dose response experiments. The open-isomers of **1-7** were tested three times in triplicate, and their respective closed isomers two times in triplicate for each concentration.

Compound	open IC_{50} [µM]	$pIC_{50} \pm$ SE	Efficacy [%]	closed IC_{50} [µM]	$pIC_{50} \pm$ SE	Efficacy [%]
FR180204	3.8	5.42 ± 0.02	100	-	-	-
1	4.9	5.31 ± 0.33	17 ± 4	2.3	5.64 ± 0.46	16 ± 3
2	20	4.69 ± 0.06	99 ± 2	41	4.39 ± 0.07	94 ± 2
3	5.9	5.23 ± 0.43	14 ± 4	> 50	< 4.30	60 (@ 50 µM)
4	13	4.89 ± 0.05	96 ± 2	n.a.	n.a.	n.a.
5	> 50	< 4.30	45 (@ 50 µM)	n.a.	n.a.	n.a.
6	> 50	< 4.30	45 (@ 50 µM)	n.a.	n.a.	n.a.
7	16	4.79 ± 0.07	100 ± 2	37	4.43 ± 0.10	98 ± 2

Radiometric kinase activity assay

To approve the photoswitchable kinase inhibition, a radiometric *in vitro* ERK2 activity assay was employed at Millipore UK Ltd.[31] DTE **4** was exemplarily prepared as ring-open or ring-closed forms, which were incubated with isolated ERK2, radioactive γ-^{33}P-ATP and a peptidic substrate in the dark. The signal is detected by scintillation counting of the resulting radioactive peptide and correlates positively with kinase activity. Indeed, the test results confirmed inhibitory activity against ERK2 (Figure 16). Surprisingly, no significant difference in the behavior of the two isoforms could be observed (Figure 16). Insufficient

geometric diversity of the photoisomers could either be the reason or the two curves could be caused by the same molecule as result of reisomerization. The latter is presumably the case since the observed IC_{50} of 28 µM for both isoforms matches to the open isomer data of the whole-cell approach. At a first glance, the thermal reopening outlined in Table 4 may be responsible, but considering the interactions in the enzyme's active site, enzymatic reisomerization is also imaginable.
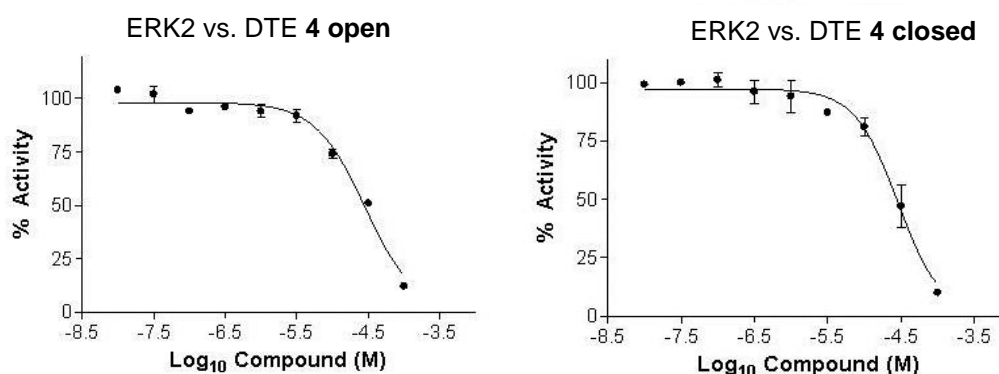

Figure 16. Inhibition curves of DTE **4** in its open (left) and closed (right) photoisomer against ERK2.

Enzymatic reisomerization studies

In order to exclude the influence of the enzyme on the ring-opening reaction, ERK2 (0.12 µM, 0.5 µg/mL in HEPES buffer, pH 7.50) was incubated with the closed photoisomers of compound **4** (50 µM) and the changes were followed photometrically over 16 h. To quantify unspecific protein interactions the inhibitor's behavior was additionally studied in presence of BSA (75 nM, 0.5 µg/mL), a serum albumin which usually acts as standard.
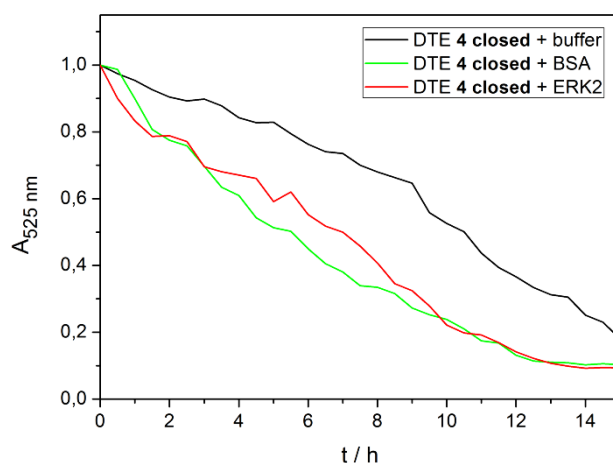

Figure 17. The influence of the proteins ERK2 and BSA on the ring-closing/-opening reaction of DTE **4** was photometrically recorded over 16 h.

In comparison with buffer environment, the absorbance of the ERK2 inhibitor **4** decreased slightly faster in presence of a protein. We could not observe any proof for specific interaction with ERK2 since incubation of BSA resulted in comparable curves (Figure 17). The influence of proteins on the equilibrium of the photoisomers is negligibly slow compared to kinase activity under assay conditions. Thus we could not assess any correlation between the enzyme activity test results and enzymatic reisomerization. Consequently, the thermal reopening (Table 4) of the closed forms is considered to be responsible for the observed trend. To generate reliable results, the photoswitch probes require fresh preparation by illumination with the respective light source.

Luminescent kinase activity assay

To circumvent the storage and transport duration of the externally employed radiometric assay, a commercially available luminescent kinase activity assay was analogously performed using freshly prepared photoswitch solutions.[32] Isolated ERK2 was incubated with the open and closed forms of the DTEs **1**-**7** straight after irradiation. The assay measures the amount of ADP formed by the kinase reaction. ADP is subsequently converted to ATP, which in turn generates light using the luciferase/luciferin reaction. Thus, the luminescent signal correlates positively with the ADP amount and kinase activity. The resulting curves exhibit a sigmoidal shape, but surprisingly with increasing output signal (Figure 18), which could not be explained so far. Based on these studies the inhibitory effects of the whole-cell approach could not be confirmed against isolated ERK2. Given the vast numbers of enzymes, receptors and other participants involved in the ERK pathway, it remains challenging to identify the anchor point, where and how the designed DTEs interfere in cell signaling.
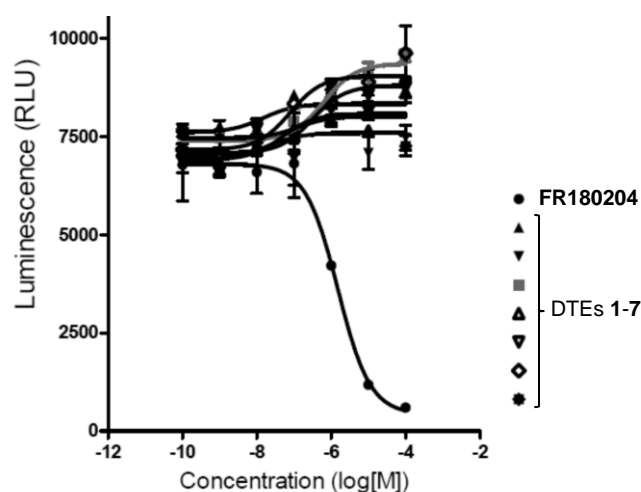

Figure 18. Test results of the *in vitro* luminescent ERK2 kinase activity assay.

4.3   Conclusion

In summary, we have developed a series of photochromic dithienylcyclopentenes which showed light-dependent cell signaling inhibition addressing the extracellular-regulated kinase pathway. The structural design of the envisaged ATP competitive kinase inhibitors was derived from Molecular Docking calculations using ERK2 as target protein. Several suitable inhibitors were synthesized and photochemically studied exhibiting fast photoconversion, moderate to high fatigue resistance rates, but only moderate thermal stability. To generate reliable results, it was thus absolutely essential to irradiate the photoswitch probes straight before testing. Their inhibitory activity was investigated by different enzyme activity assays. A commercially available whole-cell assay provided inhibition constants in the micromolar range for the ring-open photoisomers of several DTEs. After photoisomerization by UV light, their inhibitory activity dropped and cytotoxic effects were observed. Unfavorably, we could not confirm these findings by incubation of isolated ERK2. The affected site, where our inhibitors interfere in the cellular ERK pathway, was not identified yet. In order to gain further insight, their activity needs to be investigated separately towards all tiers of the ERK cascade. As ERK1/2 plays the key role in the ERK pathway, it remains a pivotal element of cancer research to identify the enzyme's exact functioning in the complex cellular phosphorylation networks.

4.4 Experimental Materials and Methods

4.4.1 Synthesis and Characterization of New Compounds

General. Commercial reagents and starting materials were purchased from Acros Organics, Alpha-Aesar, Fluka, Sigma Aldrich or VWR and used without further purification. Solvents were used in p.a. quality and dried according to common procedures, if necessary. Compounds **1**, **2**, **5**, **11** and **12** were prepared according to previously reported procedures.[28-29] Flash column chromatography was performed on a Biotage Isolera One automated flash purification system with UV/Vis detector using Sigma Aldrich MN silica gel 60 M (40-63 μm, 230-400 grain diameter) for normal phase or pre-packed Biotage SNAP cartridges (KP-C18-HS) for reversed phase chromatography. Reaction monitoring via TLC was performed on alumina plates coated with silica gel (Merck silica gel 60 F_{254}, 0.2 mm). Melting points were determined using a Stanford Research Systems OptiMelt MPA 100. NMR spectra were recorded on Bruker Avance 300 (^{1}H 300.13 MHz, ^{13}C 75.48 MHz) and Bruker Avance 400 (^{1}H 400.13 MHz, ^{13}C 100.61 MHz) instruments. The spectra are referenced against the NMR-solvent, chemical shifts δ are reported in ppm and coupling constants J are given in Hz. Resonance multiplicity is abbreviated as: s (singlet), d (doublet), t (triplet), m (multiplet) and b (broad). Carbon NMR signals are reported using DEPT 135 spectra with (+) for primary/tertiary, (−) for secondary and (q) for quaternary carbons. Mass spectra were recorded on Finnigan MAT95 (EI-MS), Agilent Q-TOF 6540 UHD (ESI-MS, APCI-MS), Finnigan MAT SSQ 710 A (EI-MS, CI-MS) or ThermoQuest Finnigan TSQ 7000 (ES-MS, APCI-MS) spectrometer. UV/Vis absorption spectroscopy was performed using a Varian Cary BIO 50 UV/Vis/NIR spectrometer. IR-spectra were recorded with a Specac Golden Gate Diamond Single Reflection ATR System in a Bio-Rad FT-IR-Spectrometer Excalibur FTS 3000. Signal intensity is abbreviated with s = strong, m = medium and w = weak.

Photochemistry. Standard hand-held lamps (Herolab, 312 nm, 6 W) were used for visualizing TLC plates and to carry out the ring-closure reactions at 312 nm. The ring-opening reactions were performed with the light of a 200 W tungsten light bulb which was passed through a 420 nm cut-off filter to eliminate higher energy light. The power of the light is given based on the specifications supplied by the company when the lamps were purchased. A light detector was not used to measure the intensity during the irradiation experiments.
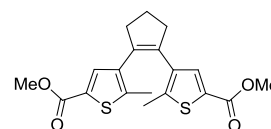
4,4'-(Cyclopent-1-ene-1,2-diyl)bis(5-methylthiophene-2-methyl ester) (2). Biscarboxy dithienylcyclopentene **1** (500 mg, 1.43 mmol) was dissolved in methanol (150 mL) and eight drops of HCl (conc.) were added. The brown solution was heated to 85 °C for 4 days. After evaporating the solvent *in vacuo* the crude product was purified by flash column chromatography (PE/EtOAc 1:2) yielding 505 mg (1.34 mmol, 94%) of compound **2** as brown oil; **¹H-NMR (400 MHz, CDCl₃):** δ = 1.90 (6H, s, 2 thiophene-CH_3), 2.05 (2H, q, J = 7.5 Hz, cyclopentene-CH_2), 2.77 (4H, t, J = 7.5 Hz, 2 cyclopentene-CH_2), 3.84 (6H, s, 2 COOCH_3), 7.50 (2H, s, thiophene-H); **¹³C-NMR (100 MHz, CDCl₃):** δ = 14.8 (+), 22.8 (−), 38.6 (−), 52.0 (+), 129.2 (q), 134.4 (+), 134.7 (q), 136.6 (q), 142.8 (q), 162.6 (q); **UV/Vis:** open isomer: λ_{max} = 260 nm, closed isomer: λ_{max} = 355, 540 nm; **MS (EI):** m/z (%) = 84.0 (100), 376.1 (26, M⁺·); **HR-MS (ESI):** calcd. for $C_{19}H_{20}O_4S_2$ 377.0876; found 377.0870.
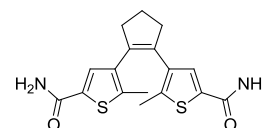

4,4'-(Cyclopent-1-ene-1,2-diyl)bis(5-methylthiophene-2-carboxamide) (3). Biscarboxy dithienylcyclopentene **1** (250 mg, 0.72 mmol) was dissolved in dry THF (50 mL) under nitrogen atmosphere and treated with thionyl chloride (0.21 mL, 2.87 mmol) and 4 drops of DMF. After stirring the reaction mixture for 20 h at room temperature under nitrogen atmosphere the solvent and thionyl chloride were removed *in vacuo*. The brown residue was dissolved in dry THF (50 mL) and gaseous ammonia was bubbled through for 15 min by precipitation of NH₄Cl which was removed by filtration. After removing the solvent under reduced pressure the crude product was intensively washed with chloroform and water over a filter until the filtrate turned colorless. Dissolving the filtration residue in acetone and removing the solvent under high vacuum yielded 51 mg (0.15 mmol, 21%) of compound **3** as colorless solid; **m.p.:** 223 °C; **¹H-NMR (400 MHz, acetone-d6):** δ = 1.94 (6H, s, 2 CH_3), 2.10 – 2.03 (2H, m, cyclopentene-CH_2), 2.81 (4H, t, J = 7.5 Hz, 2 cyclopentene-CH_2), 7.50 (2H, s, 2 thiophene-H); **¹³C-NMR (100 MHz, acetone-d6):** δ = 14.7 (+), 23.5 (−), 39.1 (−), 130.4 (+), 135.6 (q), 136.8 (q), 137.3 (q), 140.8 (q), 163.7 (q); **UV/Vis:** open isomer: λ_{max} = 260 nm, closed isomer: λ_{max} = 350, 525 nm; **MS (EI):** m/z (%) = 693.1 (100) [2MH⁺], 346.9 (60) [MH⁺], 363.9 (50) [MNH₄⁺]; **HR-MS (ESI):** calcd. for $C_{17}H_{18}N_2O_2S_2$ 347.0882; found 347.0877.
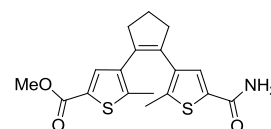
Methyl 4-(2-(5-carbamoyl-2-methylthiophen-3-yl)cyclopent-1-enyl)-5-methyl-thio-phene-2-carboxylate (4). Bismethylester dithienylcyclopentene **2** (100 mg, 0.27 mmol) was dissolved in a solution of ammonia in methanol (7 N, 40 mL) in an autoclave vessel. After sealing in an autoclave, the brown solution was heated to 110 °C for 17 h generating pressure of 5 bar. The solvent and the ammonia were removed by nitrogen stream. The crude product was purified by flash column chromatography (PE/EtOAc 1:2) yielding 38 mg (0.11 mmol, 39%) of compound **4** as brown foam; **^{1}H-NMR (300 MHz, CDCl$_3$):** δ = 1.91 (3H, s, thiophene-CH_3), 1.94 (3H, s, thiophene-CH_3), 2.05 (2H, p, J = 7.5 Hz, cyclopentene-CH_2), 2.77 (4H, t, J = 7.5 Hz, 2 cyclopentene-CH_2), 3.83 (3H, s COOCH_3), 5.93 (2H, bs, CONH_2), 7.22 (1H, s, thiophene-H), 7.50 (1H, s, thiophene-H); **^{13}C-NMR (75 MHz, CDCl$_3$):** δ = 14.8 (+), 22.9 (−), 38.5 (−), 52.0 (+), 129.2 (q), 130.6 (+), 133.2 (q), 134.5 (+), 134.8 (q), 136.5 (q), 141.2 (q), 142.9 (q), 162.6 (q), 162.8 (q); **UV/Vis:** open isomer: λ_{max} = 260 nm, closed isomer: λ_{max} = 355, 540 nm; **MS (EI):** m/z (%) = 361.1 (100, M$^{+\cdot}$), 301.1 (97, M$^{+\cdot}$-COOMe); **HR-MS (ESI):** calcd. for $C_{18}H_{19}NO_3S_2$ 362.0879; found 362.0875.
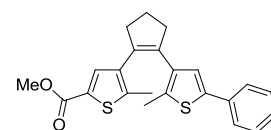
Methyl 5-methyl-4-(2-(2-methyl-5-phenylthiophen-3-yl)cyclopent-1-en-1-yl)thio-phene-2-carboxylate (6). Monocarboxy-DTE **5** (100 mg, 0.26 mmol) was dissolved in methanol (25 mL) and treated with 3 drops of HCl (conc.). It was heated to reflux for 72 h. The solvent was removed at the rotary evaporator and the crude mixture was purified by flash column chromatography (PE/EtOAc 19:1) yielding 98 mg (0.25 mmol, 96%) of compound **6** as red oil; **^{1}H-NMR (400 MHz, CDCl$_3$):** δ = 1.94 (3H, s, CH_3), 1.95 (3H, s, CH_3), 2.13 – 2.03 (2H, m, cyclopentene-CH_2), 2.89-2.75 (4H, m, 2 cyclopentene-CH_2), 3.85 (3H, s, C(O)OCH_3), 6.97 (1H, s, thiophene-H), 7.23 (1H, t, J = 7.4 Hz, phenyl-H), 7.33 (2H, t, J = 7.6 Hz, 2 phenyl-H), 7.48 (2H, d, J = 8.2 Hz, 2 phenyl-H), 7.58 (1H, s, thiophene-H); **^{13}C-NMR: (100 MHz, CDCl$_3$):** δ = 14.4 (+), 14.8 (+), 22.9 (−), 38.6 (−), 52.0 (+), 123.7 (+), 125.3 (+), 127.1 (+), 128.8 (+), 128.9 (q), 133.6 (q), 134.3 (q), 134.4 (q), 134.7 (+), 135.8 (q), 136.3 (q), 137.0 (q), 140.0 (q), 143.0 (q), 162.7 (q); **UV/Vis:** open isomer: λ_{max} = 265, 295 nm, closed isomer: λ_{max} = 255, 295, 355, 540 nm; **MS (ESI):** m/z (%) = 395.1 (100, MH$^{+\cdot}$); **HR-MS (ESI):** calcd. for $C_{23}H_{22}O_2S_2$ 395.1134; found 395.1133.
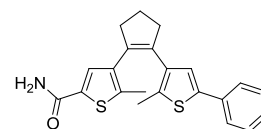
5-Methyl-4-(2-(2-methyl-5-phenylthiophen-3-yl)cyclopent-1-en-1-yl)thiophene-2-carboxamide (7). Monocarboxy-DTE **5** (100 mg, 0.26 mmol) was dissolved in dry THF (25 mL) under nitrogen atmosphere and treated with thionyl chloride (38 μL, 0.53 mmol) and 2 drops of DMF. After stirring the reaction mixture for 17 h at room temperature under nitrogen atmosphere the solvent and thionyl chloride were removed *in vacuo*. The residual blue oil was dissolved in dry THF (25 mL) and gaseous ammonia was bubbled through for 15 min by precipitation of NH_4Cl and a color change of the solution from blue to purple. It was diluted with diethyl ether (10 mL), washed with water (15 mL) and the phases separated. The aqueous phase was extracted twice with diethyl ether (10 mL) and the combined organic phases dried over $MgSO_4$ and the solvent removed at the rotary evaporator. Purification was performed by flash column chromatography (PE/acetone 4:1) yielding 66 mg (0.17 mmol, 67%) of compound **7** as purple foam; **^{1}H-NMR: (400 MHz, CDCl$_3$):** δ = 1.95 (3H, s, C*H*$_3$), 2.02 (3H, s, C*H*$_3$), 2.14 – 2.04 (2H, m, cyclopentene-C*H*$_2$), 2.87 – 2.73 (4H, m, cyclopentene-C*H*$_2$), 5.68 (2H, bs, C(O)N*H*$_2$), 6.98 (1H, s, thiophene-*H*), 7.25 – 7.20 (1H, m, phenyl-*H*), 7.25 (1H, s, thiophene-*H*), 7.34 (2H, t, *J* = 7.6 Hz, 2 phenyl-*H*), 7.48 (2H, d, *J* = 8.2 Hz, 2 phenyl-*H*); **^{13}C-NMR: (100 MHz, CDCl$_3$):** δ = 14.4 (+), 14.9 (+), 23.0 (–), 38.4 (–), 38.5 (–), 123.7 (+), 125.3 (+), 127.1 (+), 128.9 (+), 130.8 (+), 132.8 (q), 133.7 (q), 134.3 (q), 134.5 (q), 135.9 (q), 136.3 (q), 136.9 (q), 140.1 (q), 142.3 (q), 163.7 (q); **UV/Vis:** open isomer: λ_{max} = 265, 290 nm, closed isomer: λ_{max} = 255, 295, 355, 525 nm; **MS (ESI):** m/z (%) = 380.1 (100, MH$^{+\cdot}$), 759.2 (67, 2 MH$^{+\cdot}$); **HR-MS (ESI):** calcd. for $C_{22}H_{21}NOS_2$ 380.1137; found 380.1138.

4.4.2 Molecular Docking

The crystal structure of ERK2 (PDB code 1TVO) with a co-crystallized receptor was retrieved from RCSB protein data bank and used as target structure for docking studies. The Protein Preparation Wizard of MacroModel (Maestro v. 9.0) was applied to prepare the enzyme for Glide calculations, which were performed by Glide XP (Maestro v. 9.0) to generate the receptor grid. Energy minimizations (Polak-Ribiere conjugate gradient minimization, maximum of 5000 iterations) and conformational searches (systematic torsional sampling in water, maximum of 5000 steps) were provided by MacroModel for a series of DTE based derivatives. They were docked as ligands into the protein grid by

standard precision (SP) and extra precision (XP) modes with OPLS2005 as force field. The energy window for saving structures was set to 10 kJ/mol.

4.4.3 Photochemical Investigations

Photochemical syntheses of ring-closed isomers. Solutions of compounds **1**-**7** in MeOH (50 µM) were irradiated with a 312 nm lamp until complete conversion (36 s to 72 s) yielding pink solutions containing the ring-closed isomers. The changes in the UV/Vis absorption spectra are representatively shown for compound **4** in Figure 13 and for compounds **1**-**3** and **5**-**7** in the appendix in Figure A1.

Fatigue resistance studies. In order to test the robustness of the photochromic systems, photochemical cycling studies were recorded for all switches (see Figure 14 and appendix, Figure A2). In each case, a solution of ring-open inhibitor in MeOH (50 µM) was alternately irradiated with 312 nm light for 60 s and with visible light for 15 min over eight cycles. The absorption change at 525 nm was recorded after each cycle and plotted against the cycle number.

Thermal stability measurements: Absorption spectra were recorded in MeOH solutions (50 µM) in quartz cuvettes. Absorbances were recorded at 525 nm after storing the closed isomer compounds for 6 months at -20 °C in the dark and after subsequent UV irradiation for full photoconversion. The quotient of these two values gives the amount of closed isomer.

4.4.4 Enzymatic Reisomerization with ERK2

Purchased enzyme: ERK2/MAPK1, human recombinant, expressed in *E.coli*, untagged; 41.76 kDa, 0.223 mg/mL, 296.000 pmol/mg x min (=> 17.76 nm/µg in 1 hour). DTE **4** was dissolved in DMSO (10 mM, 1 mL DMSO) and diluted 1:200 with buffer (50 mM HEPES, pH 7.50, 100 mM NaCl, 5 mM DTT, 20% glycerol) giving a final DTE concentration of 50 µM. Buffer solutions of BSA (75 nM, 0.5 µg/mL) and ERK2 (0.12 µM, 0.5 µg/mL) were prepared. ERK2, BSA or buffer was incubated with the DTEs as open and closed isomers, respectively, and the absorbance at 260 nm (λ_{max} of open isomer) and 525 nm (λ_{max} of closed isomer) recorded over 16 h with time intervals of 30 min. Pure Buffer, BSA and ERK2 solutions were used to quantify the background absorption. Measurements were performed in triplicates in a 96-well Greiner flat bottom microtiter plate.

4.5 References

[1]   T. G. Boulton, S. H. Nye, D. J. Robbins, N. Y. Ip, E. Radzlejewska, S. D. Morgenbesser, R. A. DePinho, N. Panayotatos, M. H. Cobb, G. D. Yancopoulos, *Cell* **1991**, *65*, 663-675.

[2]   G. Manning, D. B. Whyte, R. Martinez, T. Hunter, S. Sudarsanam, *Science* **2002**, *298*, 1912-1934.

[3]   M. E. M. Noble, J. A. Endicott, L. N. Johnson, *Science* **2004**, *303*, 1800-1805.

[4]   S. Martic, H.-B. Kraatz, *Chemical Science* **2013**, *4*, 42-59.

[5]   P. Cohen, D. R. Alessi, *ACS Chem. Biol.* **2012**, *8*, 96-104.

[6]   J. S. Sebolt-Leopold, R. Herrera, *Nat. Rev. Cancer* **2004**, *4*, 937-947.

[7]   R. Roskoski Jr, *Pharmacol. Res.* **2012**, *66*, 105-143.

[8]   A. S. Little, P. D. Smith, S. J. Cook, *Oncogene* **2013**, *32*, 1207-1215.

[9]   G. Mayer, A. Heckel, *Angew. Chem. Int. Ed.* **2006**, *45*, 4900-4921.

[10]   D. D. Young, A. Deiters, *Org. Biomol. Chem.* **2007**, *5*, 999-1005.

[11]   C. Brieke, F. Rohrbach, A. Gottschalk, G. Mayer, A. Heckel, *Angew. Chem. Int. Ed.* **2012**, *51*, 8446-8476.

[12]   A. A. Beharry, G. A. Woolley, *Chem. Soc. Rev.* **2011**, *40*, 4422-4437.

[13]   T. Fehrentz, M. Schönberger, D. Trauner, *Angew. Chem. Int. Ed.* **2011**, *50*, 12156-12182.

[14]   A. Mourot, T. Fehrentz, Y. Le Feuvre, C. M. Smith, C. Herold, D. Dalkara, F. Nagy, D. Trauner, R. H. Kramer, *Nat Meth* **2012**, *advance online publication*.

[15]   I. Tochitsky, M. R. Banghart, A. Mourot, J. Z. Yao, B. Gaub, R. H. Kramer, D. Trauner, *Nat Chem* **2012**, *4*, 105-111.

[16]   M. Irie, *Chem. Rev. (Washington, DC, U. S.)* **2000**, *100*, 1685-1716.

[17]   D. Vomasta, C. Högner, N. R. Branda, B. König, *Angew. Chem. Int. Ed.* **2008**, *47*, 7644-7647.

[18]   D. Vomasta, A. Innocenti, B. König, C. T. Supuran, *Bioorg. Med. Chem. Lett.* **2009**, *19*, 1283-1286.

[19]   D. Wilson, N. R. Branda, *Angew. Chem. Int. Ed.* **2012**, *51*, 5431-5434.

[20]   U. Al-Atar, R. Fernandes, B. Johnsen, D. Baillie, N. R. Branda, *J. Am. Chem. Soc.* **2009**, *131*, 15966-15967.

[21]   M. Singer, A. Jäschke, *J. Am. Chem. Soc.* **2010**, *132*, 8372-8377.

[22]   S. Barrois, H.-A. Wagenknecht, *Beilstein J. Org. Chem.* **2012**, *8*, 905-914.

[23]   H. Cahová, A. Jäschke, *Angew. Chem. Int. Ed.* **2013**, *125*, 3268-3272.

[24]   B. Reisinger, N. Kuzmanovic, P. Löffler, R. Merkl, B. König, R. Sterner, *Angew. Chem. Int. Ed.* **2014**, *53*, 595-598.

[25]   M. Ohori, T. Kinoshita, M. Okubo, K. Sato, A. Yamazaki, H. Arakawa, S. Nishimura, N. Inamura, H. Nakajima, M. Neya, H. Miyake, T. Fujii, *Biochem. Biophys. Res. Commun.* **2005**, *336*, 357-363.

[26]   P. Puustinen, M. R. Junttila, S. Vanhatupa, A. A. Sablina, M. E. Hector, K. Teittinen, O. Raheem, K. Ketola, S. Lin, J. Kast, H. Haapasalo, W. C. Hahn, J. Westermarck, *Cancer Res.* **2009**, *69*, 2870-2877.

[27]   Schrödinger Maestro v. 9.0, LLC, 2010, http://www.schrodinger.com/. Nov. 26, 2013.

[28]   Linda N. Lucas, Jaap J. D. d. Jong, Jan H. v. Esch, Richard M. Kellogg, Ben L. Feringa, *Eur. J. Org. Chem.* **2003**, *2003*, 155-166.

[29]   W. R. Browne, J. J. D. de Jong, T. Kudernac, M. Walko, L. N. Lucas, K. Uchida, J. H. van Esch, B. L. Feringa, *Chemistry – A European Journal* **2005**, *11*, 6414-6429.

[30]   Agilent Technologies, Agilent Technologies, Inc., 900 South Taft Loveland, Colorado, USA, PathDetect in Vivo Signal Transduction Pathway trans-Reporting Systems, Instruction Manual, PathDetect trans Elk1 Reporter Gene Assay, Jun. 09, 2011. http://www.chem.agilent.com/Library/usermanuals/Public/219000.pdf. Nov. 26, 2013.

[31]   Millipore UK Ltd., Gemini Crescent, Dundee Technology Park, Dundee DD21SW, UK, KinaseProfiler™ Service Assay Protocols, GOU019Flex, Apr., 2011. http://www.millipore.com/techpublications/tech1/pf3036. Nov. 26, 2013.

[32]   Promega Corporation, Madison, WI, USA, ADP-Glo™ Kinase Assay Application Notes Ser-Thr Kinase Series: ERK2, Jan. 2011. http://www.promega.de/resources/protocols/product-information-sheets/n/erk2-kinase-enzyme-system-protocol/. Nov. 26, 2013.

CHAPTER 3

5 SYNTHESIS OF PHOTOCHROMIC DITHIENYLMALEIMIDE AMINO ACIDS‡

5.1 Introduction

Over the last decade photochromic molecules have increasingly been applied in biology to alter conformations or switch functions by light.[1-3] Photoinduced activation or deactivation of biomolecules, particularly with visible light, provides a high spatial and temporal resolution and is therefore a convenient method for investigating cellular processes or pathogeneses.[4] Two main concepts are applied: the irreversible release of caged compounds bearing photocleavable protecting groups[5] or the reversible switching between two structurally different photoisomers[6] (photoswitches) by light of certain wavelengths. In the latter field, most structures are based on azobenzene units due to easy synthetic access, high photostability and ultrafast kinetics.[7] The light-controlled regulation of neuronal activity by azobenzene containing ligands for ion channels and receptors were recently reported.[8-10] However, the photophysical properties of azobenzenes do not allow a complete photoisomerization in the photostationary state and in many cases the *cis* to *trans* thermal re-isomerization is fast.[7] Photochromic compounds based on the 1,2-dithienylethene (DTE) scaffold show nearly quantitative photochemical conversion and both photoisomers are thermally stable in the dark.[11] DTEs have been used to control enzyme activity,[12-15] Watson-Crick base pairing,[16-18] and even the agility of a living organism.[19] Irradiation with UV or visible light, respectively, toggles DTEs between the open and the closed photoisomer, which differ in conformational flexibility and electronic conjugation (Figure 19). Despite their interesting photophysical properties the application of DTEs as photoswitches in life science is still limited. The synthesis, particular of non-symmetric DTEs is laborious[18, 20] and the water-solubility of the typically used hydrophobic diaryl (perfluoro-)cyclopentene core is limited. Hence, we decided to develop a non-symmetric dithienylmaleimide based amino acid, which could easily be incorporated in any peptide by solid phase peptide synthesis (SPPS).
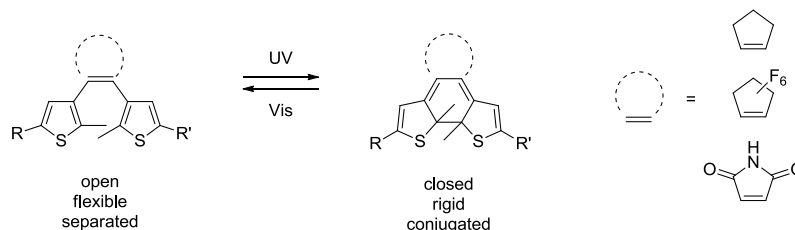

Figure 19. Photochemical interconversion of a DTE with cyclopentene, perfluoro-cyclopentene or maleimide ring structure.

DTEs with a central maleimide unit have been reported that are efficiently prepared via Perkin condensation allowing non-symmetric substitution of the thiophene rings.[21]

Compared to diarylcyclopentenes, the diarylmaleimides exhibit a higher hydrophilicity and hence offer a better water solubility. Meanwhile the diarylmaleimide's absorption maxima are shifted to higher wavelengths. The photoisomerization can thus be induced by light with lower energy reducing potential cell damage.[11] Moreover, the diarylmaleimides' biocompatibility is known from bisindoylmaleimides, e.g. the arcyriarubins and arcyriaflavins with antibiotic activities against bacteria and fungi, and several other highly potent protein kinase inhibitors.[22-26] Therefore the dithienylmaleimide structure was selected for the synthesis of a photoswitchable amino acid. The building block, Alloc protected at the amino group and with free carboxylic acid, is readily incorporated in peptides by solid phase synthesis as illustrated in Figure 20.
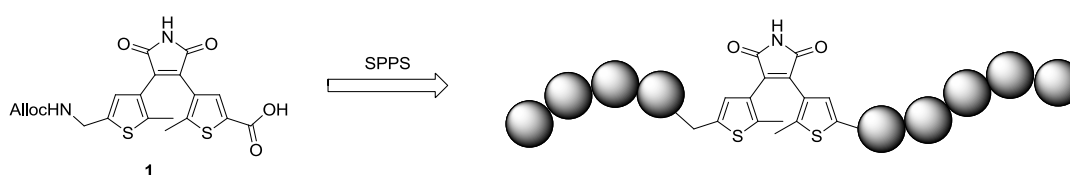
Figure 20. SPPS of the dithienylmaleimide amino acid **1** and natural amino acids (bowls).

5.2   Results and Discussion

5.2.1   Synthesis

To synthesize the amino acid functionalized dithienylmaleimide **2**, we chose to form the maleimide core by Perkin condensation allowing us to independently equip the thiophene precursors **3** and **4** with the desired amino or carboxylic group, respectively (Scheme 7).[21, 27-28] The glyoxylamide thiophene **3** carries the N-terminal amine via a methylene linker, which was necessary to introduce as all attempts to directly introduce the nitrogen atom at the thiophene failed.[29] Alloc was chosen as amino protecting group due to its stability against the applied conditions of further synthetic steps towards compound **2**. Furthermore, deprotection/peptide coupling protocols for solid phase peptide synthesis (SPPS) with Alloc-protected amines are well established.[30-31] As counterpart, the diester thiophene **4** bears the C-terminal carboxylic acid in 2-position and a second ester in 4-position. The latter forms the maleimide core and is thus fixed as methyl ester, which in turn restricts the choice of the C-terminal protective group as transesterification occurs during condensation. In particular, using a C-terminal ethyl ester led to a mixture of the ethyl and methyl ester as the condensation product (cf. Scheme A1 in the appendix). Consequently, we favoured the methyl ester as protecting group for the C-terminal carboxylic acid.
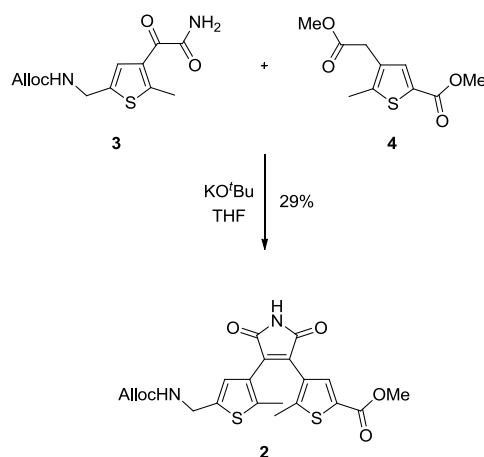
Scheme 7. Perkin condensation of the N-terminal precursor **3** and C-terminal precursor **4** to access the dithienylmaleimide **2**.
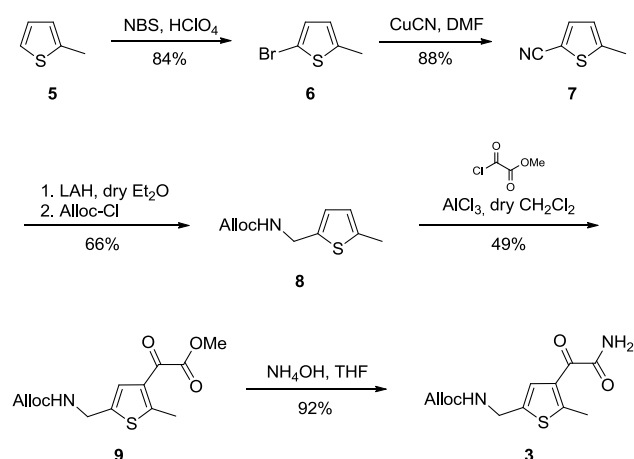
Scheme 8: Synthetic route for the preparation of the N-terminal precursor **3**.

The synthetic pathway to access the N-terminal precursor **3** is depicted in Scheme 8. To prepare the thiophene nitrile **7** bromination of 2-methyl thiophene **5** and subsequent Rosenmund-von Braun reaction were performed according to literature procedures.[32-33] Thereafter, reduction of the nitrile with lithium aluminium hydride followed by immediate protection with allyl chloroformate afforded carbamate **8** in good yield (66% for 2 steps). Using Fmoc chloride instead led to the respective Fmoc derivative, which was not only less efficient (38% yield) but also caused the formation of side products in the following Friedel-Crafts acylation. In particular, we observed simultaneous acylation of the Fmoc fluorene system (cf. Scheme A2 in the appendix). Even though the Alloc group should not be as prone to acylation, the Friedel-Crafts acylation was still the most challenging step of the synthesis. We noticed that the yield of glyoxylester **9** critically depends on the sequence of the addition of reagents. Best results (49%) were obtained by mixing **8** and methyl chlorooxoacetate prior to adding aluminium chloride slowly in small portions. Otherwise, the allyl carbamate was cleaved and the resulting primary amine was competitively acylated yielding compound **10** as main product (Figure 21). Additionally, quenching the reaction with saturated sodium hydrogen carbonate solution instead of neutral water suppressed the formation of compound **11** which is obtained by addition of hydrochloric acid to the allyl double bond (Figure 21). Obviously, the allyl carbamate is not as robust as expected towards the present acidic conditions.
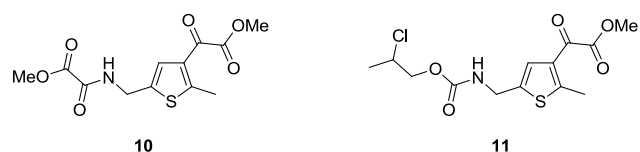

Figure 21: Undesired side products of the acylation reaction of carbamate **8**.

The use of zinc(II) chloride or iron(III) chloride as milder Lewis acids did not afford the desired product. Finally, aminolysis with aqueous ammonia converted the glyoxylester **9** into the desired N-terminal precursor **3** in 92% yield. All in all, we achieved moderate to high yields (49 to 92%) for the particular synthesis towards **3** resulting in an overall yield of 22% for six steps.
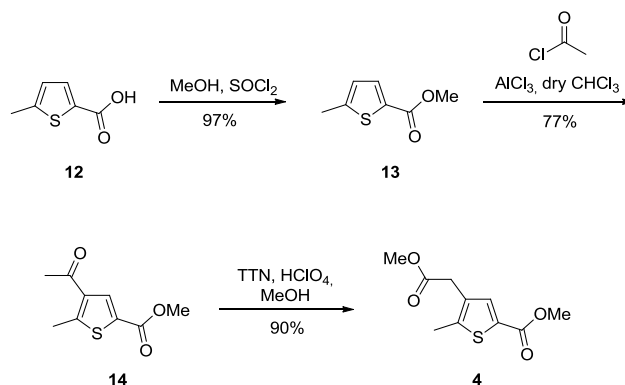
Scheme 9. Synthesis of the C-terminal precursor **4**.

The C-terminal precursor **4** was prepared by esterification of the methyl thiophene acid **12** in presence of thionyl chloride followed by Friedel-Crafts acylation and final thallium trinitrate mediated oxidative rearrangement (Scheme 9).[34-35] All intermediates could be isolated in good to excellent yields (77 to 97%) with an overall yield of 68% for three steps. It is noteworthy that initial yields of around 40% for the Friedel-Crafts acylation significantly increased to 77% after removal of stabilizers and reactive decomposition products from the solvent chloroform prior to drying and distillation (cf. Experimental Section).

The N-terminal precursor **3** and the C-terminal precursor **4** were combined by Perkin condensation (Scheme 7). In order to provide a photochromic amino acid with a free carboxylic group ready for SPPS, the methyl ester of **2** was cleaved (Scheme 10). Non-hydrolytic ester cleavage was required to avoid maleimide hydrolysis (cf. Scheme A4 in the appendix), which was achieved using lithium iodide in a polar aprotic solvent.[36] The S_N2 fashion C-O bond cleavage is based on the coordination of the lithium cation as hard acid at the oxygen atom (pulling factor) and the nucleophilic attack of the soft iodide at the carbon atom (pushing factor).[37] A large excess of lithium iodide and reflux conditions were necessary to achieve moderate conversion. The yield significantly changed with the solvent (Table 6). Best results (35%) could be achieved in acetone, whereas the reaction mixture mainly consisted of starting material in most other solvents. A more efficient deprotection protocol needs to be developed.

Table 6. Non-hydrolytic methyl ester deprotection of **2**.

Entry	eq. LiI	Solvent	T [°C]	Isolated yield[a] [%]
1	3.0	EtOAc	r.t.	--
2	3.0	EtOAc	reflux	--
3	30	EtOAc	reflux	26
4	3.0	acetone	reflux	--
5	30	acetone	reflux	35
6	30	MeCN	reflux	--
7	30	DMSO	100	--

[a] If conversion was too low the product **1** was not isolated.

5.2.2 Peptide Coupling
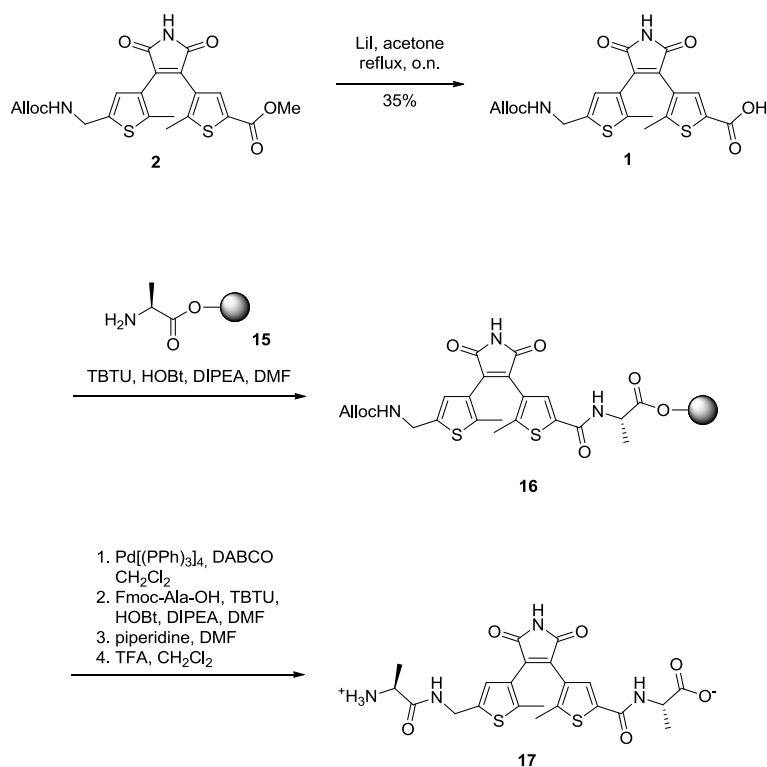
Scheme 10. Non-hydrolytic cleavage of the methyl ester **2** and subsequent solid phase peptide synthesis to access the photochromic tripeptide **17**.

To explore the applicability of the title compound **1** in SPPS, we used Wang resin bound alanine and attached it by standard coupling protocol (Scheme 10). Subsequently, the Alloc

protecting group was catalytically removed through coordination to palladium(0) and nucleophilic attack of DABCO as allyl scavenger.[30] After another coupling/deprotection step with Fmoc alanine, the photochromic tripeptide **17** was released from the resin (Scheme 10) and identified by mass spectrometry. Currently, purification and complete characterization of **17** is in progress.

5.2.3 Photochromism

The dithienylmaleimide core structure can reversibly be toggled between a ring-open and ring-closed photoisomer (Figure 19). The photochemical properties of compounds **1** and **2** were spectrophotometrically investigated. It is known that diarylmaleimides are not able to undergo photoisomerization in polar solvents due to a twisted intramolecular charge transfer (TICT).[38-39] However, the DTEs **1** and **2** showed excellent photochromic behavior in highly polar methanol (Figure 22 and Figure A4 in the appendix), which is in good accordance with the performance of other recently developed dithienylmaleimide derivatives.[21] This phenomenon can be explained by inductive and resonance effects of the substitution pattern on the aryl moieties.
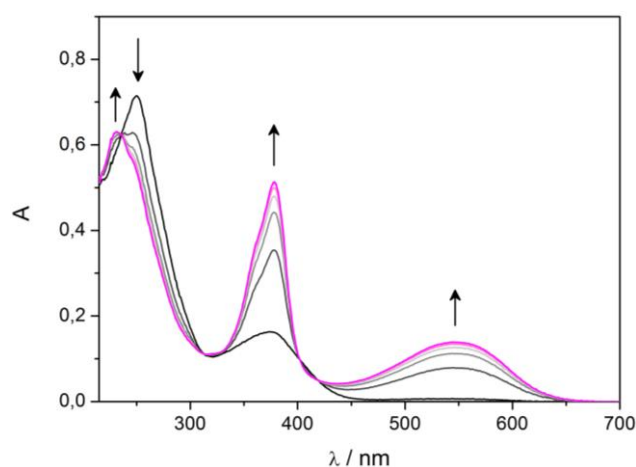
Figure 22: UV/Vis absorption spectra evolution of the dithienylmaleimide amino acid **1** (50 µM in MeOH) upon irradiation with 312 nm light; arrows indicate the changes of the absorption maxima with irradiation periods of 6 s.

Upon irradiating a methanol solution of the ring-open form of compound **1** with UV light (312 nm), the absorption band at 250 nm immediately decreases. Simultaneously, new absorption maxima at 232 nm, 378 nm and 550 nm arise causing the color change from colorless to purple (Figure 22). Compared to the common DTE-cyclopentenes the absorption maxima are red shifted by approximately 25 nm.[11] The photostationary state was reached after 36 s of irradiation and the open form can be reobtained by irradiation

with visible light (> 420 nm) for 5 min. The photoswitchable amino acid **1** is stable over several closing/opening cycles (see Figure 23).
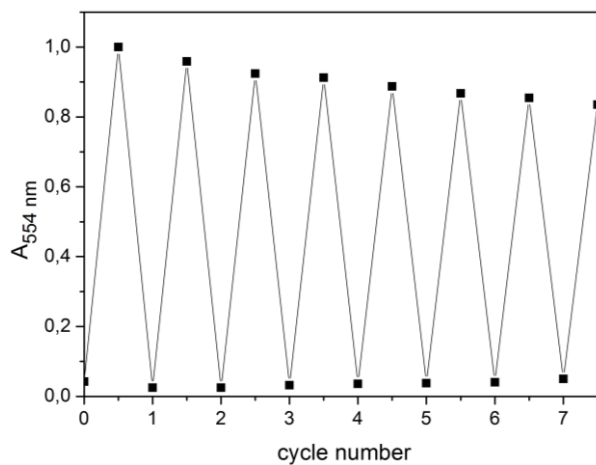

Figure 23: Cycle performance of the dithienylmaleimide amino acid **1** (50 µM in MeOH). Changes in absorption at 554 nm were measured during an alternated irradiation with 312 nm light for 60 s and greater than 420 nm light for 5 min.

5.3 Conclusion

We have developed an efficient synthesis of a photochromic dithienylmaleimide amino acid. The compound shows an increased hydrophilicity and water solubility compared to DTEs bearing a perfluorocyclopentene unit. Its absorption is bathochromically shifted and the irradiation with light of 312 nm and greater than 420 nm converts the open and closed photoisomers completely. As a protected amino acid the compound can conveniently be conjugated to biological molecules or incorporated in peptides by solid phase synthesis, as exemplarily demonstrated by coupling to alanine at the amino and carboxy function. Applications of the dithienylmaleimide amino acid in the photoregulation of peptide conformations or interactions can be envisaged.

5.4 Experimental Section

5.4.1 General

Commercial reagents and starting materials were purchased from Acros Organics, Alpha-Aesar, Fluka, Sigma Aldrich or VWR and used without further purification. Solvents were used in p.a. quality and dried according to common procedures, if necessary. To purify the chloroform for Friedel-Crafts acylations, it was extracted with sulfuric acid (1 M), dried over calcium chloride, filtered through silica, subsequently refluxed with phosphorous pentoxide (5 – 10 g/L) and distilled under nitrogen atmosphere. Thienyl nitrile **7** and thienyl methyl ester **13** were prepared according to previously reported procedures.[33-34] Flash column chromatography was performed on a Biotage Isolera One automated flash purification system with UV/Vis detector using Sigma Aldrich MN silica gel 60 M (40-63 μm, 230-400 grain diameter) for normal phase or pre-packed Biotage SNAP cartridges (KP-C18-HS) for reversed phase chromatography. Reaction monitoring via TLC was performed on alumina plates coated with silica gel (Merck silica gel 60 F_{254}, 0.2 mm). Melting points were determined using a Stanford Research Systems OptiMelt MPA 100. NMR spectra were recorded on Bruker Avance 300 (^{1}H 300.13 MHz, ^{13}C 75.48 MHz) and Bruker Avance 400 (^{1}H 400.13 MHz, ^{13}C 100.61 MHz) instruments. The spectra are referenced against the NMR-solvent, chemical shifts δ are reported in ppm and coupling constants J are given in Hz. Resonance multiplicity is abbreviated as: s (singlet), d (doublet), t (triplet), m (multiplet) and b (broad). Carbon NMR signals are reported using DEPT 135 spectra with (+) for primary/tertiary, (−) for secondary and (q) for quaternary carbons. Mass spectra were recorded on Finnigan MAT95 (EI-MS), Agilent Q-TOF 6540 UHD (ESI-MS, APCI-MS), Finnigan MAT SSQ 710 A (EI-MS, CI-MS) or ThermoQuest Finnigan TSQ 7000 (ES-MS, APCI-MS) spectrometer. UV/Vis absorption spectroscopy was performed using a Varian Cary BIO 50 UV/Vis/NIR spectrometer. IR-spectra were recorded with a Specac Golden Gate Diamond Single Reflection ATR System in a Bio-Rad FT-IR-Spectrometer Excalibur FTS 3000. Signal intensity is abbreviated with s = strong, m = medium and w = weak. Standard hand-held lamps (Herolab, 312 nm, 6 W) were used for visualizing TLC plates and to carry out the ring-closure reactions at 312 nm. The ring-opening reactions were performed with the light of a 200 W tungsten light bulb which was passed through a 420 nm cut-off filter to eliminate higher energy light. The power of the light is given based on the specifications supplied by the company when the lamps were purchased. A light detector was not used to measure the intensity during the irradiation experiments.

5.4.2 New Compounds
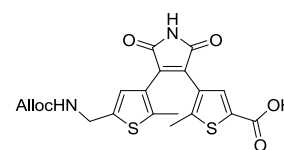
4-(4-(5-((((Allyloxy)carbonyl)amino)methyl)-2-methylthiophen-3-yl)-2,5-dioxo-2,5-dihydro-1H-pyrrol-3-yl)-5-methylthiophene-2-carboxylic acid (1): Compound **2** (40 mg, 0.09 mmol, 1.0 eq.) was dissolved in acetone (10 mL) and LiI (350 mg, 2.60 mmol, 30 eq.) was added. The mixture was heated to 100 °C overnight. After cooling to room temperature it was quenched with 1 M HCl (5 mL) and diluted with CH_2Cl_2 (5 mL). The phases were separated and the aqueous phase was extracted with CH_2Cl_2 (3 x 5 mL). The combined organic phases were dried over sodium sulfate and the solvent was removed at the rotary evaporator. Automated reversed phase flash column chromatography (MeCN/H_2O with 0.05% TFA, 3 - 100% MeCN) yielded compound **1** (14 mg, 0.03 mmol, 35%) as yellow foam; R_f: 0.04 (PE/EtOAc : 1/1); **^{1}H-NMR (300 MHz, CD$_3$CN):** δ = 1.93 (3H, s, thiophene-CH_3), 1.97 (3H, s, thiophene-CH_3), 4.33 (2H, d, J = 6.3 Hz, thiophene-CH_2NH), 4.52 (2H, d, J = 5.3 Hz, CH$_2$=CHCH_2O), 5.18 (1H, dd, J = 10.5, 1.4 Hz, CH_2=CHCH$_2$), 5.27 (1H, dd, J = 17.3, 1.6 Hz, CH_2=CHCH$_2$), 5.74 – 6.05 (1H, m, CH$_2$=CHCH$_2$), 6.14 (1H, bs, CH$_2$NHCO), 6.79 (1H, s, thiophene-H), 7.60 (1H, s, thiophene-H), 8.80 (1H, bs, COOH); **^{13}C-NMR (75 MHz, CD$_3$CN):** δ = 14.7 (+), 15.1 (+), 40.0 (−), 65.9 (−), 117.4 (−), 127.2 (q), 127.4 (+), 129.0 (q), 131.3 (q), 134.0 (q), 134.3 (+), 136.0 (+), 136.1 (q), 141.1 (q), 141.7 (q), 149.5 (q), 157.0 (q), 162.8 (q), 171.5 (q); **IR ṽ [cm^{-1}]:** 2926 (w), 1981 (w), 1769 (w), 1709 (s), 1544 (m), 1459 (m), 1344 (m), 1246 (m), 1185 (m), 1150 (m), 1049 (w), 991 (m), 849 (w), 762 (m); **UV/Vis (50 μM in MeOH):** open isomer: λ_{max} = 250 nm; closed isomer: λ_{max} = 232 nm, 378 nm, 550 nm; **MS (ESI):** m/z (%) = 346.0 (100, [M-AllocNH]$^+$), 447.1 (60, MH$^+$); **HR-MS (ESI):** calcd. for $C_{20}H_{18}N_2O_6S_2$ (M+H)$^+$, m/z = 447.0679; found 447.0676.
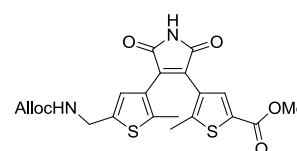

Methyl 4-(4-(5-((((allyloxy)carbonyl)amino)methyl)-2-methyl-thiophen-3-yl)-2,5-dioxo-2,5-dihydro-1H-pyrrol-3-yl)-5-methylthiophene-2-carboxylate (2): KOtBu (1 M in THF, 0.12 mL, 0.12 mmol, 1.2 eq.) was added to a solution of glyoxylamide **3** (28 mg, 0.10 mmol, 1.0 eq.) in dry THF (1 mL) at 0 °C under nitrogen atmosphere. After stirring for 90 min at 0 °C, diester **4** (27 mg, 0.12 mmol, 1.2 eq.) in THF (0.5 mL) was added at 0 °C and stirred for 24 h at room temperature. Then the reaction was heated to reflux for 1 h,

quenched with 1 M HCl solution (3 mL) and diluted with EtOAc (5 mL). The organic phase was washed with water (2 x 5 mL), brine (5 mL) and dried over $MgSO_4$. The solvent was removed under reduced pressure and purification of the crude product by automated reversed phase flash column chromatography (H_2O/EtOH, 20% - 45% EtOH) yielded **2** (53 mg, 0.05 mmol, 50%) as yellow foam; R_f: 0.20 (PE/EtOAc : 2/1); **¹H-NMR (400 MHz, CDCl₃):** δ = 1.90 (3H, s, thiophene-CH_3); 1.98 (3H, s, thiophene-CH_3), 3.87 (1H, s, OCH_3), 4.45 (2H, d, J = 6.0 Hz, thiophene-CH_2NH), 4.60 (2H, d, J = 4.9 Hz, CH_2=CHCH_2O), 5.13 – 5.27 (2H, m, CH_2=CHCH$_2$ and CH_2NHCO), 5.31 (1H, dd, J = 17.2, 1.2 Hz, CH_2=CHCH$_2$), 5.92 (1H, ddt, J = 16.2, 10.8, 5.5 Hz, CH_2=CHCH$_2$), 6.90 (1H, s, thiophene-H), 7.74 (1H, s, thiophene-H), 8.30 (1H, bs, CONHCO); **¹³C-NMR (101 MHz, CDCl₃):** δ = 15.0 (+), 15.3 (+), 39.9 (−), 52.3 (+), 65.9 (−), 117.9 (−), 125.8 (q), 126.7 (+), 127.5 (q), 130.9 (q), 132.7 (+), 134.8 (q), 134.9 (+), 139.4 (q), 142.1 (q), 148.6 (q), 156.0 (q), 162.1 (q), 170.0 (q), 170.2 (q); **IR ṽ [cm⁻¹]:** 3289 (w), 3070 (w), 2952 (w), 1703 (s), 1540 (m), 1458 (w), 1339 (m), 1248 (m), 994 (w), 909 (m), 727 (m); **UV/Vis (50 µM in MeOH):** open isomer: λ_{max} = 250 nm; closed isomer: λ_{max} = 232 nm, 378 nm, 550 nm; **MS (ESI):** m/z (%) = 461.1 (100, MH⁺), 360.0 (98, [M-AllocNH]⁺), 483.1 (26), 519.1 (25), 462.1 (24), 571.3 (21), 361.0 (21), 270.1 (21); **HR-MS (ESI):** calcd. for $C_{21}H_{21}N_2O_6S_2$ (M+H)⁺, m/z = 461.0838; found 461.0386.
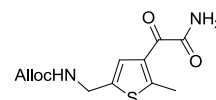
Allyl ((4-(2-amino-2-oxoacetyl)-5-methylthiophen-2-yl)methyl) carbamate (3): To a solution of oxoacetate **9** (282 mg, 0.95 mmol, 1.0 eq.) in THF (5 mL) was added a NH_4OH solution (32% in H_2O) (1.18 mL, 9.50 mmol, 10.0 eq.) at 0 °C. The reaction was stirred for 90 min at room temperature and then quenched with water (5 mL). The aqueous phase was extracted with EtOAc (3 x 10 mL). The combined organic phases were dried over $MgSO_4$ and the solvent was removed under reduced pressure. Compound **3** (253 mg, 0.90 mmol, 94%) was obtained as yellow solid and used without further purification; R_f: 0.21 (PE/EtOAc : 1/1); **m.p.:** 108 °C; **¹H-NMR (400 MHz, CDCl₃):** δ = 2.70 (3H, s, thiophene-CH_3), 4.44 (2H, d, J = 6.1 Hz, thiophene-CH_2NH), 4.59 (2H, d, J = 5.1 Hz, CH_2=CHCH_2O), 5.21 (1H, d, J = 10.4 Hz, CH_2=CHCH$_2$), 5.24 – 5.43 (2H, m, CH_2=CHCH$_2$ and NH), 5.90 (1H, ddt, J = 16.2, 10.7, 5.5 Hz, CH_2=CHCH$_2$), 6.05 (1H, bs, NH_2), 7.06 (1H, bs, NH_2), 7.86 (1H, s, thiophene-H); **¹³C-NMR (101 MHz, CDCl₃):** δ = 16.7 (+), 39.8 (−), 65.9 (−), 117.9 (−), 129.0 (+), 130.8 (q), 132.7 (+), 137.0 (q), 155.7 (q), 156.1 (q), 164.4 (q), 182.1 (q); **IR ṽ [cm⁻¹]:** 3402 (m), 3301 (m), 3167 (w), 2962 (w), 1750 (m), 1686 (s), 1649 (s), 1535 (m), 1460 (m), 1254 (m), 1047 (m), 796 (m); **MS (ESI):** m/z (%) = 300.1 (100, MNH₄⁺), 283.1 (60, MH⁺),182 (30)

588.1 (27, 2MNa$^+$); **HR-MS (ESI):** calcd. for C$_{12}$H$_{18}$N$_3$O$_4$S (M+NH$_4$)$^+$, m/z = 300.1013; found 300.1012.
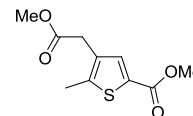

Methyl 4-(2-methoxy-2-oxoethyl)-5-methylthiophene-2-carboxylate (4): Thallium trinitrate (850 mg, 1.91 mmol, 1.2 eq.) and 70% HClO$_4$ (0.30 mL) were added to a suspension of **14** (316 mg, 1.59 mmol, 1.0 eq.) in MeOH (3 mL) at room temperature. After stirring for 24 h the mixture was concentrated under vacuum and diluted with water (5 mL). The aqueous phase was diluted with EtOAc (5 mL), extracted with EtOAc (3 x 5 mL) and dried over MgSO$_4$. The solvent was evaporated and purification of the crude product by automated flash column chromatography (PE/EtOAc, 3% - 15% EtOAc) yielded compound **4** (331 mg, 1.45 mmol, 91%) as colorless oil; *R$_f$*: 0.34 (PE/EtOAc : 5/1); **^{1}H-NMR (300 MHz, CDCl$_3$):** δ = 2.43 (3H, s, thiophene-C*H$_3$*), 3.54 (2H, s, thiophene-C*H$_2$*C(O)OCH$_3$), 3.70 (3H, s, thiophene-CH$_2$C(O)OC*H$_3$*), 3.85 (3H, s, C(O)OC*H$_3$*), 7.61 (1H, s, thiophene-*H*); **^{13}C-NMR (75 MHz, CDCl$_3$):** δ = 13.8 (+), 33.8 (−), 52.0 (+), 52.1 (+), 129.0 (q), 130.7 (q), 135.6 (+), 144.0 (q), 162.6 (q), 170.9 (q); **IR ṽ [cm^{-1}]:** 2997 (w), 2953 (m), 2845 (w), 1736 (w), 1704 (s), 1535 (w), 1457 (s), 1392 (w), 1331 (w), 1291 (m), 1250 (s), 1194 (s), 1132 (w), 1063 (s), 1006 (m), 927 (w), 874 (w), 785 (w), 751 (s); **MS (APCI):** m/z (%) = 229.1 (100, MH$^+$); **HR-MS (APCI):** calcd. for C$_{10}$H$_{12}$O$_4$S (M+H)$^+$, m/z = 229.0529; found 229.0531.
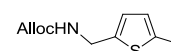
Allyl ((5-methylthiophen-2-yl)methyl)carbamate (8): LAH (2.78 g, 73.2 mmol, 1.0 eq.) was added in portions to a solution of nitrile **7** (3.01 g, 24.4 mmol, 3.0 eq.) in dry Et$_2$O (250 mL) at 0 °C under nitrogen atmosphere. After stirring for 4 h at room temperature the reaction was quenched with water (80 mL) and saturated NaHCO$_3$ solution (50 mL) at 0 °C. The suspension was filtered and the aqueous phase was extracted with Et$_2$O (3 x 80 mL). The combined organic phases were dried over MgSO$_4$ and concentrated *in vacuo*. Then the residue was dissolved in dry THF (100 mL) and pyridine (2.47 mL, 30.50 mmol, 1.25 eq.) was added at 0 °C. Within 1 h allyl chloroformate (4.02 mL, 37.82 mmol, 1.55 eq.) in dry THF (5 mL) was dropped to the solution *via* a syringe pump at 0 °C. After stirring for 14 h at room temperature the reaction was quenched cautiously with water (50 mL) and extracted with EtOAc (3 x 30 mL). The combined organic phases were dried over MgSO$_4$ and the solvent was removed under reduced pressure. Purification of the crude product by

automated flash column chromatography (PE/EtOAc, 8% - 15% EtOAc) yielded **8** (3.40 g, 16.1 mmol, 66%) as yellow oil; R_f: 0.20 (PE/EtOAc : 9/1); **^{1}H-NMR (400 MHz, CDCl$_3$):** δ = 2.44 (3H, s, thiophene-CH_3), 4.44 (2H, d, J = 5.7 Hz, thiophene-CH_2NH), 4.59 (2H, d, J = 5.1 Hz, CH$_2$=CHCH_2O), 5.05 (1H, bs, NH), 5.21 (1H, d, J = 10.4 Hz, CH_2=CHCH$_2$), 5.30 (1H, d, J = 16.1 Hz, CH_2=CHCH$_2$), 5.92 (1H, ddt, J = 16.3, 10.8, 5.5 Hz, CH$_2$=CHCH$_2$), 6.57 (1H, dd, J = 3.2, 0.8 Hz, 4-thiophene-H), 6.74 (1H, d, J = 3.0 Hz, 3-thiophene-H); **^{13}C-NMR (101 MHz, CDCl$_3$):** δ = 15.4 (+), 40.1 (−), 65.6 (−), 117.8 (−), 124.8 (+), 125.7 (+), 132.8 (+), 138.8 (q), 139.9 (q), 155.9 (q); **IR ṽ [cm^{-1}]:** 3335 (m), 3073 (w), 2922 (w), 1695 (s), 1514 (m), 1426 (w), 1236 (s), 982 (m), 799 (m); **MS (ESI):** m/z (%) = 212.1 (100, MH$^+$), 151.1 (48), 114.1 (47), 111.0 (35), 234.1 (27, MNa$^+$); **HR-MS (ESI):** calcd. for C$_{10}$H$_{14}$NO$_2$S (M+H)$^+$, m/z = 212.0740; found 212.0740.
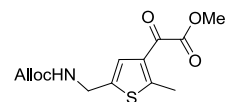
Methyl 2-(5-((((allyloxy)carbonyl)amino)methyl)-2-methylthiophen-3-yl)-2-oxoacetate (9): Carbamate **8** (169 mg, 0.80 mmol, 1.0 eq.) and methyl chlorooxoacetate (81 μL, 0.88 mmol, 1.1 eq.) were dissolved in dry CH$_2$Cl$_2$ (6 mL) under nitrogen atmosphere. Then aluminium chloride (427 mg, 3.20 mmol, 4.0 eq.) was added in portions at 0 °C and the suspension was stirred for 20 h at room temperature. The reaction was quenched with saturated NaHCO$_3$ solution (1 mL) at 0 °C and diluted with water (5 mL). The aqueous phase was extracted with CH$_2$Cl$_2$ (3 x 5 mL), the combined organic layers were washed with brine (10 mL) and dried over MgSO$_4$. After evaporation of the solvent the crude product was purified by automated flash column chromatography (PE/EtOAc, 15% - 40% EtOAc) to obtain **9** (117 mg, 0.39 mmol, 49%) as brown oil; R_f: 0.22 (PE/EtOAc : 3/1); **^{1}H-NMR (400 MHz, CDCl$_3$):** δ = 2.70 (3H, s, thiophene-CH_3) 3.91 (3H, s, OCH_3), 4.42 (2H, d, J = 6.1 Hz, thiophene-CH_2NH), 4.58 (2H, d, J = 5.3 Hz, CH$_2$=CHCH_2O), 5.16 – 5.34 (3H, m, CH_2=CHCH$_2$ and NH), 5.90 (1H, ddt, J = 16.3, 10.8, 5.6 Hz, CH$_2$=CHCH$_2$), 7.32 (1H, s, thiophene-H); **^{13}C-NMR (101 MHz, CDCl$_3$):** δ = 16.3 (+), 39.7 (−), 52.8 (+), 65.9 (−), 118.0 (−), 127.5 (+), 131.0 (q), 132.6 (+), 138.0 (q), 154.8 (q), 156.1 (q), 164.0 (q), 180.0 (q); **IR ṽ [cm^{-1}]:** 3395 (m), 2954 (w), 1726 (s), 1670 (s), 1517 (m), 1434 (m), 1242 (s), 1200 (s), 1112 (s), 984 (m), 757 (m); **MS (ESI):** m/z (%) = 298.1 (100, MH$^+$), 315.1 (58, MNH$_4$$^+$), 320.1 (48, MNa$^+$), 185.0 (37); **HR-MS (ESI):** calcd. for C$_{13}$H$_{16}$NO$_5$S (M+H)$^+$, m/z = 298.0744; found 298.0744.
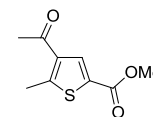
Methyl 4-acetyl-5-methylthiophene-2-carboxylate (14): Thiophene **13** (800 mg, 5.12 mmol, 1.0 eq.) and acetyl chloride (550 µL, 7.68 mmol, 1.5 eq.) were dissolved in purified anhydrous $CHCl_3$ (10 mL) under nitrogen atmosphere. After cooling to 0 °C aluminium chloride (2.05 g, 15.4 mmol, 3.0 eq.) was added in small portions. The yellow suspension was heated to 45 °C overnight upon turning bright red, then the reaction was quenched with ice/water and the aqueous phase was extracted with ethyl acetate (3 x 10 mL). The combined organic phases were washed with a saturated solution of $NaHCO_3$ (10 mL) and brine (10 mL). The organic phase was dried over $MgSO_4$ and the solvent was evaporated. The crude product was purified by automated flash column chromatography (PE/EtOAc, 5% - 25% EtOAc) and **14** (781 mg, 3.94 mmol, 77%) was obtained as colorless solid; *R*f: 0.41 (PE/EtOAc : 3/1); **m.p.:** 84 °C; **¹H-NMR (300 MHz, CDCl₃):** δ = 2.52 (3H, s, thiophene-C*H₃*), 2.76 (3H, s, acetyl-C*H₃*), 3.88 (3H, s, OC*H₃*), 8.03 (1H, s, thiophene-*H*); **¹³C-NMR (75 MHz, CDCl₃):** δ = 16.8 (+), 29.6 (+), 52.3 (+),128.5 (q), 135.0 (+), 136.3 (q), 155.8 (q), 162.0 (q), 193.7 (q); **IR ṽ [cm⁻¹]:** 3007 (w), 2957 (w), 1717 (s), 1678 (s), 1539 (s), 1457 (m), 1439 (m), 1254 (s), 1233 (s), 1074 (m), 1021 (w), 745 (s); **MS (EI):** m/z (%) = 183.1 (100, [M-(CH₃)]⁺), 198.1 (41, M⁺); **HRMS (APCI):** m/z (%) = 199.0 (100, MH⁺); calcd. for $C_9H_{10}O_3S$ (M+H)⁺, m/z = 199.0423; found 199.0424.

5.4.3 Solid Phase Peptide Synthesis

Solid phase peptide synthesis was carried out manually on 50 mg Wang resin (loading 1.0 – 1.2 mmol) using the Fmoc strategy in BD Discardit II syringes (Becton Dickinson GmbH). Solvents and soluble reagents were removed by suction. A syringe was equipped with Wang resin (50 mg, 0.05 – 0.06 mmol) as solid phase, which was initially allowed to swell for 60 min in DMF (3 mL).

The amino acid coupling steps were performed in DMF (3 mL) with Fmoc-S-alanine (93 mg, 0.30 mmol, 10 eq.), TBTU (94 mg, 0.29 mmol, 9.8 eq.), HOBt (46 mg, 0.30 mmol, 10 eq.) and DIPEA (11 µL, 0.60 mmol, 20 eq.). After shaking for 90 min another portion of TBTU (62 mg, 0.19 mmol, 6.0 eq.) was added to complete the coupling step and the shaking was continued for further 30 min. The resin was washed with DMF/CH_2Cl_2/DMF (4 x 3 mL each) and the coupling step was repeated.

Fmoc removal followed with piperidine/DMF (4:6, 3 mL) for 5 min, washing with DMF (2 x 3 mL) and further 5 min of piperidine/DMF (2:8, 3 mL). After completion, the resin was washed with DMF/CH_2Cl_2/MeOH/DMF (4 x 3 mL each).

The dithienylmaleimide amino acid **1** (13 mg, 0.03 mmol, 1.0 eq.) was attached to Wang-Ala-NH_2 **15** (0.05 – 0.06 mmol, 1.7 – 2.0 eq.) by dissolving in DMF (2 mL) and adding TBTU (9 mg, 0.03 mmol, 1.0 eq.), HOBt (5 mg, 0.03 mmol, 1.0 eq) and DIPEA (10 µL, 0.06 mmol, 2.0 eq.). After shaking for 90 min another portion of TBTU (6 mg, 0.02 mmol, 0.6 eq.) was added and the shaking continued for further 30 min. The resin was washed with DMF/CH_2Cl_2/DMF (4 x 3 mL each).

Alloc was deprotected under nitrogen atmosphere using $Pd(PPh_3)_4$ (7 mg, 0.01 mmol, 20 mol%) and DABCO (17 mg, 0.15 mmol, 5.0 eq.) in anhydrous CH_2Cl_2 (2.5 mL). After shaking for 90 min it was washed with CH_2Cl_2/DMF (5 x 3 mL each).

Following the completion of the sequence the tripeptide **17** was released from the resin by treatment with TFA/CH_2Cl_2 (95:5, 1 mL) for 60 min. It was repeated and the solvent of the combined filtrates was removed by nitrogen purge.

The tripeptide **17** was separated from byproducts by automated reversed phase flash column chromatography (MeCN/H_2O with 0.05% TFA, 3-100% MeCN) and requires further purification by preparative HPLC.

5.4.4 Photochemical Investigations

Photochemical syntheses of the ring-closed isomers. Solutions of compounds **1** and **2** in MeOH (50 μM) were irradiated with a 312 nm lamp until complete conversion (36 s) yielding pink solutions containing the ring-closed isomers. The changes in the UV/Vis absorption spectra are representatively shown for compound **1** in Figure 22 and for compound **2** in the appendix in Figure A4.

Fatigue resistance studies. In order to test the robustness of the photochromic systems, photochemical cycling studies were recorded for the dithienylmaleimides **1** and **2** (see Figure 23 and appendix, Figure A4). In each case, a solution of the ring-open photoswitch in MeOH (50 μM) was alternately irradiated with 312 nm light for 60 s and with visible light >420 nm for 5 min over eight cycles. The absorption change at 565 nm was recorded after each cycle and plotted against the cycle number.

5.5 References

[1]   G. Mayer, A. Heckel, *Angew. Chem. Int. Ed.* **2006**, *45*, 4900-4921.

[2]   C. Brieke, F. Rohrbach, A. Gottschalk, G. Mayer, A. Heckel, *Angew. Chem. Int. Ed.* **2012**, *51*, 8446-8476.

[3]   I. Ahmed, L. Fruk, *Mol. BioSyst.* **2013**, *9*, 565-570.

[4]   D. D. Young, A. Deiters, *Org. Biomol. Chem.* **2007**, *5*, 999-1005.

[5]   A. Deiters, *ChemBioChem* **2010**, *11*, 47-53.

[6]   W. Szymański, J. M. Beierle, H. A. V. Kistemaker, W. A. Velema, B. L. Feringa, *Chem. Rev. (Washington, DC, U. S.)* **2013**, *113*, 6114-6178.

[7]   A. A. Beharry, G. A. Woolley, *Chem. Soc. Rev.* **2011**, *40*, 4422-4437.

[8]   T. Fehrentz, M. Schönberger, D. Trauner, *Angew. Chem. Int. Ed.* **2011**, *50*, 12156-12182.

[9]   I. Tochitsky, M. R. Banghart, A. Mourot, J. Z. Yao, B. Gaub, R. H. Kramer, D. Trauner, *Nat Chem* **2012**, *4*, 105-111.

[10]   A. Mourot, T. Fehrentz, Y. Le Feuvre, C. M. Smith, C. Herold, D. Dalkara, F. Nagy, D. Trauner, R. H. Kramer, *Nat Meth* **2012**, *9*, 396-402.

[11]   M. Irie, *Chem. Rev. (Washington, DC, U. S.)* **2000**, *100*, 1685-1716.

[12]   D. Vomasta, C. Högner, N. R. Branda, B. König, *Angew. Chem. Int. Ed.* **2008**, *47*, 7644-7647.

[13]   D. Vomasta, A. Innocenti, B. König, C. T. Supuran, *Bioorg. Med. Chem. Lett.* **2009**, *19*, 1283-1286.

[14]   D. Wilson, N. R. Branda, *Angew. Chem. Int. Ed.* **2012**, *51*, 5431-5434.

[15]   B. Reisinger, N. Kuzmanovic, P. Löffler, R. Merkl, B. König, R. Sterner, *Angew. Chem. Int. Ed.* **2014**, *53*, 595-598.

[16]   M. Singer, A. Jäschke, *J. Am. Chem. Soc.* **2010**, *132*, 8372-8377.

[17]   S. Barrois, H.-A. Wagenknecht, *Beilstein J. Org. Chem.* **2012**, *8*, 905-914.

[18]   H. Cahová, A. Jäschke, *Angew. Chem. Int. Ed.* **2013**, *125*, 3268-3272.

[19]   U. Al-Atar, R. Fernandes, B. Johnsen, D. Baillie, N. R. Branda, *J. Am. Chem. Soc.* **2009**, *131*, 15966-15967.

[20]   P. Raster, S. Weiss, G. Hilt, B. König, *Synthesis* **2011**, *2011*, 905-908.

[21]   C. Falenczyk, Master thesis, University of Regensburg **2012**.

[22]   W. Steglich, *Pure & Appl. Chem.* **1989**, *81*, 281-288.

[23]   T. Tamaoki, H. Nakano, *Nat Biotech* **1990**, *8*, 732-735.

[24]   P. D. Davis, C. H. Hill, G. Lawton, J. S. Nixon, S. E. Wilkinson, S. A. Hurst, E. Keech, S. E. Turner, *J. Med. Chem.* **1992**, *35*, 177-184.

[25]   D. A. E. Cross, A. A. Culbert, K. A. Chalmers, L. Facci, S. D. Skaper, A. D. Reith, *J. Neurochem.* **2001**, *77*, 94-102.

[26]   L. Meijer, M. Flajolet, P. Greengard, *Trends Pharmacol. Sci.* **2004**, *25*, 471-480.

[27]   M. M. Faul, L. L. Winneroski, C. A. Krumrich, *The Journal of Organic Chemistry* **1998**, *63*, 6053-6058.

[28]   M. M. Faul, L. L. Winneroski, C. A. Krumrich, *Tetrahedron Lett.* **1999**, *40*, 1109-1112.

[29]   D. Wutz, Master thesis, University of Regensburg **2013**.

[30]   C. Zorn, F. Gnad, S. Salmen, T. Herpin, O. Reiser, *Tetrahedron Lett.* **2001**, *42*, 7049-7053.

[31]   N. Thieriet, J. Alsina, E. Giralt, F. Guibé, F. Albericio, *Tetrahedron Lett.* **1997**, *38*, 7275-7278.

[32]   Y. Goldberg, H. Alper, *The Journal of Organic Chemistry* **1993**, *58*, 3072-3075.

[33]   O. E. Levy, E. L. Madison, J. E. Semple, A. P. Tamiz, M. Weinhouse, **2002**, *WO0214349 (A2)*.

[34]   G. A. R. Y. Suaifan, C. L. M. Goodyer, M. D. Threadgill, *Molecules* **2010**, *15*, 3121-3134.

[35]   A. McKillop, B. P. Swann, E. C. Taylor, *J. Am. Chem. Soc.* **1973**, *95*, 3340-3343.

[36]   J. W. Fisher, K. L. Trinkle, *Tetrahedron Lett.* **1994**, *35*, 2505-2508.

[37]   K. Fuji, T. Kawabata, E. Fujita, *Chem. Pharm. Bull.* **1980**, *28*, 3662-3664.

[38]   T. Yamaguchi, K. Uchida, M. Irie, *J. Am. Chem. Soc.* **1997**, *119*, 6066-6071.

[39]   T. Yamaguchi, M. Irie, *Chem. Lett.* **2004**, *33*, 1398-1399.

CHAPTER 4

6 NEW PHOTOCHROMIC DITHIENYL MALEIC HYDRAZIDES

6.1 Introduction

Maleic hydrazide is a well-established plant growth inhibitor that was first reported in 1949.[1] Agriculture exploits its ability to prevent sprouting during growth or storage. It is usually applied on potatoes, onions and tobacco, or to prevent weed spread.[2-5] Even if its uptake and metabolization by mammalians has been investigated for decades, the impact on human health is still not fully examined and subject of ongoing research.[6-9] Maleic anhydride suppresses cell proliferation in plants by inhibiting their DNA and protein synthesis.[7] Moreover, its structural similarity with pyrimidine bases suggests intercalation into the DNA.[10]
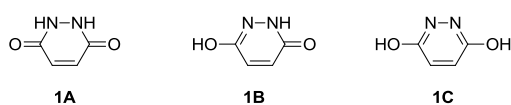
Figure 24. Tautomers of maleic hydrazide; diketo **1A**, monolactim **1B** and dihydroxy tautomer **1C**.

Analogous to nucleic bases, maleic hydrazide exhibits different tautomers appearing as diketo, monolactim or dihydroxy form (Figure 24). Experimental[10-11] and theoretical[12-14] studies indicate a predominance of the diketo **1A** and the monolactim tautomer **1B** as they seem similarly stable in solid state, solution and gas phase, whereas the dihydroxy form **1C** is less populated.[14] NMR studies revealed that **1B** is favored in polar solvents,[15] which is supported by the hypothesis that contiguous heteroatoms of the same hybridization type are strongly destabilizing.[16] Interestingly, new investigations on 2,3-diaryl-substituted maleic hydrazides report the exclusive formation of maleic hydrazide **1A** without any monolactim byproduct.[17] Furthermore, it was recently shown, that UV irradiation generates the *N*-aminomaleimide tautomer **1D** (Scheme 11).[18]
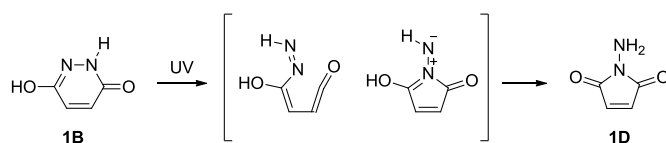
Scheme 11. UV-induced unimolecular transformations of **1B** into the *N*-aminomaleimide **1D**.[18]

In the course of exploring the reactivity of dithienylmaleimides, we discovered photochromic dithienyl maleic hydrazides as a new generation of DTE photoswitches. They comprise a six-membered core cycle, which is able to adopt different tautomeric structures as known for maleic hydrazide. We therefore wanted to investigate the interplay of photochromism and tautomerism of a dithienyl maleic hydrazide upon irradiation with UV and visible light.

6.2 Initial Results and Discussion

To develop a new generation of photochromic dithienylethenes, we treated the bischloro dithienylmaleimide **1** with hydrazine under acidic conditions to afford the respective dithienyl maleic hydrazide **2** (Scheme 12).[19-20] We obtained two products that exhibited the same mass, in particular a photochromic blue fraction and a yellow fraction that was stable towards UV irradiation. The latter was not further investigated. According to the reported investigations on the diphenyl-substituted maleic hydrazide, the reaction product is estimated to appear as diketo form **2A**.[17] This may be the case if the tautomerism equilibrium is dependent on the substitution at the 2- and 3-position of the maleic hydrazide. Else, the monolactim tautomer **2B** is expected to be predominant as it is the preferred tautomer of maleic hydrazide.[15-16]
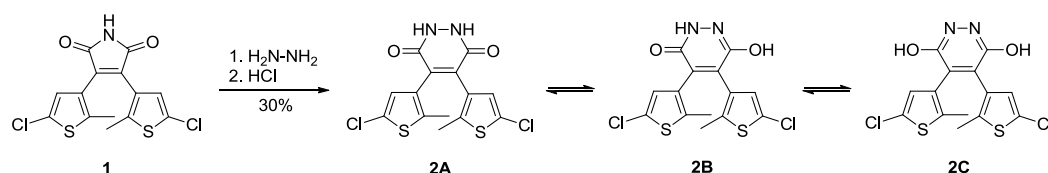
Scheme 12. Synthesis of the dithienyl maleic hydrazide **2A** and its tautomers **2B** and **2C**.[19]

To get further insight into the proton distribution on the dithienyl maleic hydrazide **2**, we applied NMR spectroscopy. Thereby, dimethylsulfoxide-d$_6$ was used as aprotic polar solvent. The ¹H-NMR spectra shows two separated broad singlets with the same intensity and high chemical shifts (11.14 and 12.24 ppm), thus indicating the existence of two different groups with hydrogen bonding ability (Figure 25).
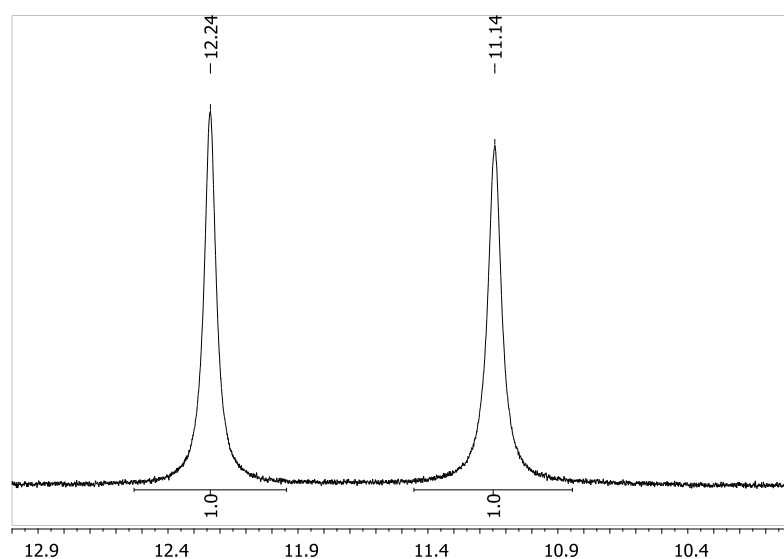
Figure 25. ¹H-NMR spectra (10 to 13 ppm) of the dithienyl maleic hydrazide **2** in DMSO-d₆.

In the case of a symmetric molecule as in **2A** or **2C**, only one signal is expected for both hydrazide protons. We could hence conclude that the title compound may mainly be present as tautomer **2B** in a DMSO solution. Additionally, the thienyl and methyl protons appear as broad singlets, which may result from proton exchange implying the existence of a tautomerism equilibrium. Using methanol-d$_4$ as polar protic solvent shows only the broadened signals for the methyl and thienyl protons, the resonance signals at 11 and 12 ppm disappear.

The physicochemical properties of the new dithienyl maleic hydrazide **2** were spectrophotometrically investigated by alternate irradiation with 312 nm or greater than 420 nm light, respectively. Similar to known photochromic dithienylethenes, it can reversibly be toggled between two photoisomers (Scheme 13, upper reaction). Surprisingly, the color of the closed isomer of compound **2** in solution changed with the solvent, e.g. it appeared purple in methanol and blue in chloroform (Figure 26). The observed solvatochromism may be due to a solvent induced shift in the tautomerism equilibrium (Scheme 12).
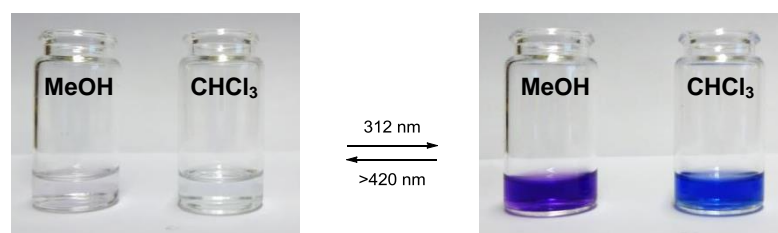
Figure 26. Coloration and decoloration of dithienyl maleic hydrazide **2** dissolved in methanol or chloroform upon irradiation with UV or visible light, respectively. The color is dependent on the solvent, appearing purple in methanol and blue in chloroform.

Table 7. Absorption maxima of the closed isomer of compound **2** dependent on the solvent.

Entry	Solvent	λ_{max} [nm]
1	MeOH	351, 560
2	CHCl$_3$	340, 592
3	acetone	342, 551
3	toluene[a]	362, 590, 612
4	toluene[b]	323, 555, 612

[a] up to 40 s of UV irradiation; [b] more than 40 s of UV irradiation.

Upon irradiating a solution of the ring-open form of compound **2** in the respective solvent with UV light (312 nm), new absorption maxima arise causing the color change (Figure 26 and Figure 27). The position of this absorption band is strongly dependent on the solvent (Table 7). Compared to the common DTE-cyclopentenes the absorption maxima are red shifted by approximately 25 nm, which is in good accordance with the related dithienylmaleimdes (see Chapter 3).[21] The photostationary state was reached after 71 to 90 s of irradiation. Particularly in toluene, we observed a maximum shift after 40 s of UV irradiation, which could be due to UV-light induced photoisomerization according to Reva *et al*. (Scheme 13).[18] The open form can be reobtained by irradiation with visible light (> 420 nm) for 10 min.
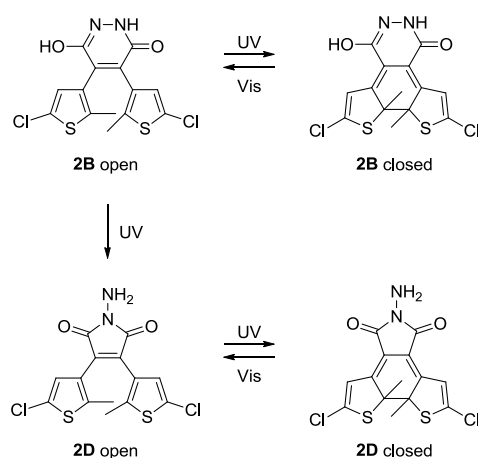
Scheme 13. Possible UV-light induced reactions of **2B**.
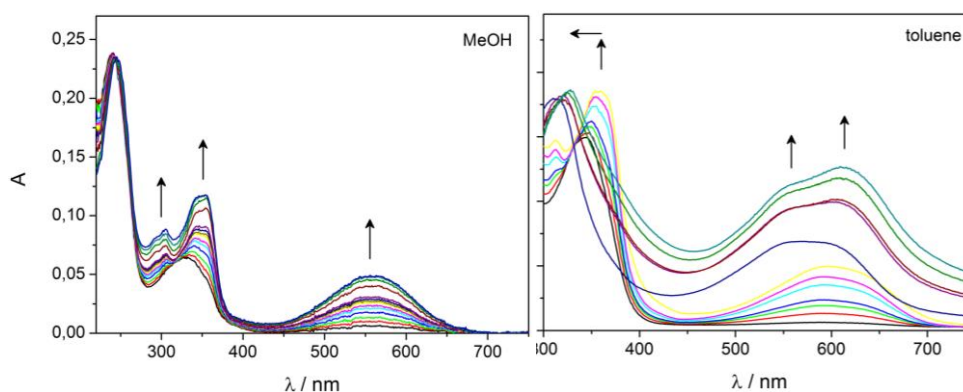
Figure 27. Absorption spectra evolution of maleic hydrazide **2** (25 µM in MeOH or toluene) upon irradiation with 312 nm light; arrows indicate the changes of the absorption maxima with irradiation periods of 6 s.

In contrast to the highly fatigue-resistant dithienylmaleimides (c.f. Chapter 3), the dithienyl maleic hydrazide **2** shows rather low photostability. It is almost completely degraded after eight iterations of alternate ring-closing/-opening cycles (Figure 28).
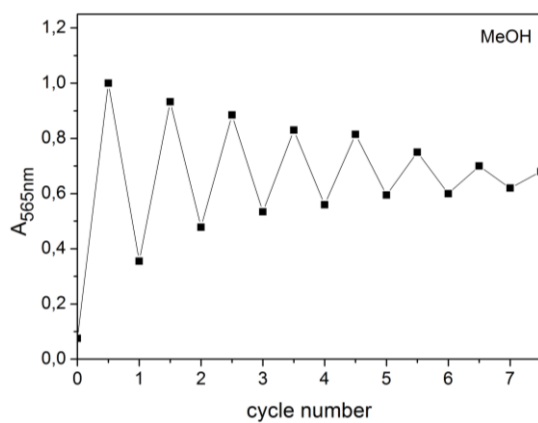
Figure 28. Cycle performance of maleic hydrazide **2.** Changes in absorption at 565 nm were measured during an alternated irradiation the inhibitor solution (25 µM in MeOH) with 312 nm light for 60 s and greater than 420 nm light for 10 min.

6.3 Conclusion

In summary, we discovered a new type of dithienylethenes. According to the present data it is presumably a dithienyl maleic hydrazide, which adopts its monolactim tautomer as preferred structure. Irradiation with UV or visible light, respectively, toggles the resulting compound reversibly between two photoisomers, whereby we observed a solvatochromism of the ring-closed form. However, it only exhibits rather low photostability compared to other dithienylethenes. To draw conclusions about the interplay of tautomerism, solvatochromism and photoisomerization, more detailed investigations are necessary, e.g. temperature-dependent 2D NMR measurements in different solvents before and after UV irradiation. Additionally, it would be interesting if the hydrazide moiety can be derivatized, thus establishing new possibilities to functionalize this new type of photoswitches.

6.4 Experimental Section
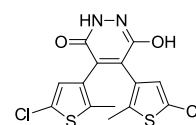
4,5-Bis(5-chloro-2-methylthiophene-3-yl) maleic hydrazide (2). Hydrazine monohydrate (16 μL, 0.34 mmol, 1.2 eq.) was dissolved in MeOH/THF (5:1, 12 mL) and cooled to 0 °C. Fuming hydrochloric acid (0.1 mL) was added dropwise, after which the bath was removed and dithienylmaleimide **1** (100 mg, 0.28 mmol, 1.0 eq.) was added. It was refluxed for 24 h. After cooling to r.t. it was extracted with ethyl acetate (2 x 10 mL), dried over magnesium sulfate and the volatiles removed. The crude product was obtained as yellow powder and purification by automated column chromatography (PE/EtOAc, 30% – 60% EtOAc) yielded 31 mg (0.08 mmol, 30%) of **2B** as blue powder. **¹H-NMR (300 MHz, MeOD):** δ = 2.09 (6H, bs, 2 thiophene-CH_3), 6.54 (1H, bs, thiophene-H), 6.62 (1H, bs, thiophene-H); **¹H-NMR (400 MHz, DMSO):** δ = 2.11 – 1.92 (6.3 H, m, 2 thiophene-CH_3), 2.17 (0.3H, s), 6.70 (2.1H, bm, 2 thiophene-H), 7.40 (0.1 H, s), 11.14 (1H, bs), 12.24 (1H, bs); **MS (ESI):** m/z (%) = 373.0 (100, [MH+]), 375.0 (70, [MH+]).

6.5   References

[1]   D. L. Schoene, O. L. Hoffmann, *Science* **1949**, *109*, 588-590.

[2]   H. B. Currier, A. S. Crafts, *Science* **1950**, *111*, 152-153.

[3]   A. C. Leopold, W. H. Klein, *Science* **1951**, *114*, 9-10.

[4]   F. M. R. Isenberg, C. O. Jensen, M. L. Odland, *Science* **1954**, *120*, 464-465.

[5]   Y.-Y. Liu, D. Hoffmann, *Anal. Chem.* **1973**, *45*, 2270-2273.

[6]   S. S. Epstein, J. Andrea, H. Jaffe, S. Joshi, H. Falk, N. Mantel, *Nature* **1967**, *215*, 1388-1390.

[7]   Z. Swietlińska, J. Žuk, *Mutation Research/Reviews in Genetic Toxicology* **1978**, *55*, 15-30.

[8]   C. Mamani Moreno, T. Stadler, A. A. da Silva, L. C. A. Barbosa, M. E. L. R. de Queiroz, *Talanta* **2012**, *89*, 369-376.

[9]   H. Zhang, G. Tang, N. Liu, Z. Bian, Q. Hu, *The Scientific World Journal* **2012**, *2012*, 5.

[10]   P. D. Cradwick, *Nature* **1975**, *258*, 774-774.

[11]   P. Beak, F. S. Fry, J. Lee, F. Steele, *J. Am. Chem. Soc.* **1976**, *98*, 171-179.

[12]   H.-J. Hofmann, R. Cimiraglia, J. Tomasi, R. Bonaccorsi, *Journal of Molecular Structure: THEOCHEM* **1991**, *227*, 321-326.

[13]   M. Shabanian, H. Moghanian, M. Hajibeygi, A. Mohamadi, *E-Journal of Chemistry* **2012**, *9*, 107-112.

[14]   N. A. Burton, D. V. S. Green, I. H. Millier, P. J. Taylor, M. A. Vincent, S. Woodcock, *Journal of the Chemical Society, Perkin Transactions 2* **1993**, 331-335.

[15]   H. P. Fritz, F. H. Köhler, B. Lippert, *Chem. Ber.* **1973**, *106*, 2918-2924.

[16]   R. W. Taft, F. Anvia, M. Taagepera, J. Catalan, J. Elguero, *J. Am. Chem. Soc.* **1986**, *108*, 3237-3239.

[17]   H. Shih, R. J. Shih, D. A. Carson, *J. Heterocycl. Chem.* **2011**, *48*, 1243-1250.

[18]   I. Reva, B. J. A. N. Almeida, L. Lapinski, R. Fausto, *J. Mol. Struct.* **2012**, *1025*, 74-83.

[19]   H. Feuer, E. H. White, J. E. Wyman, *J. Am. Chem. Soc.* **1958**, *80*, 3790-3792.

[20]   R. Sun, Y. Zhang, F. Bi, Q. Wang, *J. Agric. Food Chem.* **2009**, *57*, 6356-6361.

[21]   M. Irie, *Chem. Rev. (Washington, DC, U. S.)* **2000**, *100*, 1685-1716.
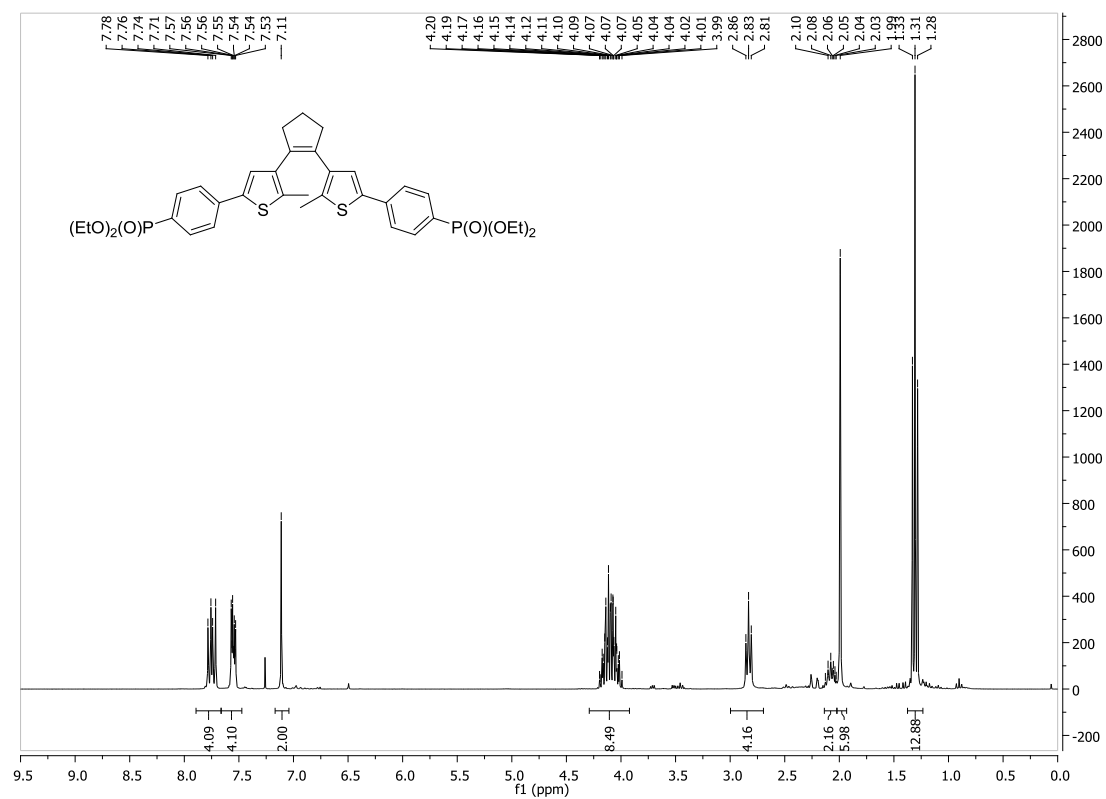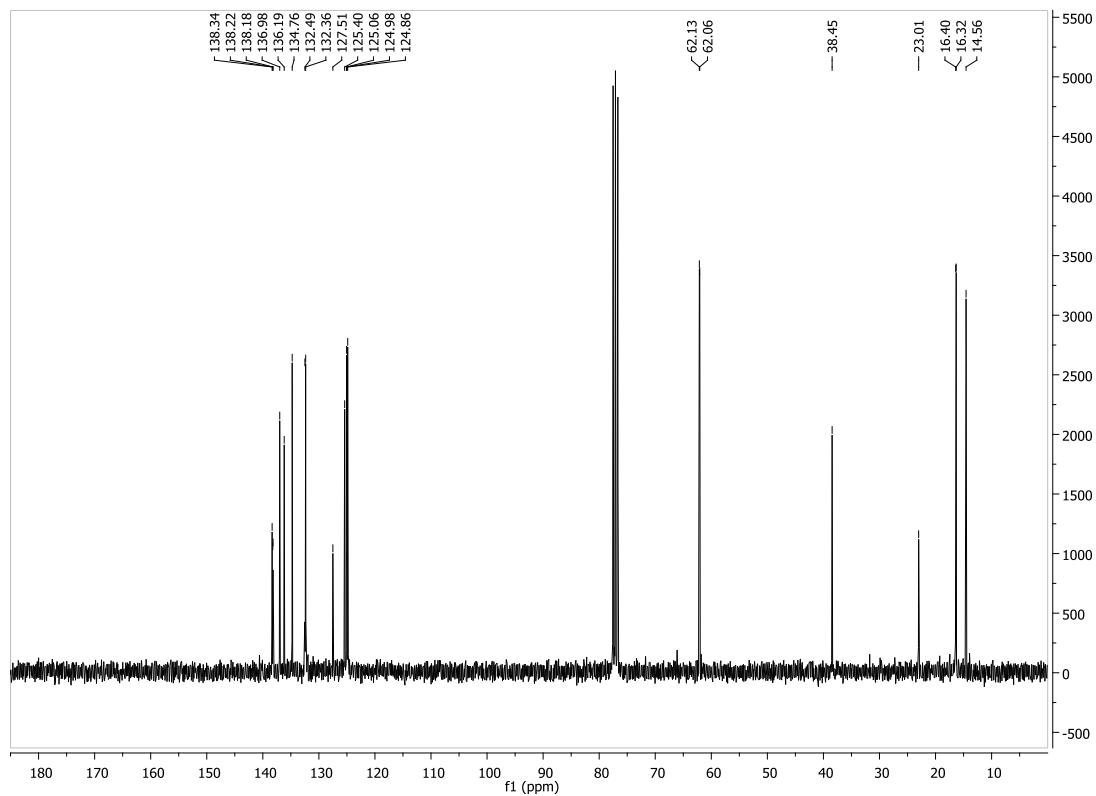
APPENDIX

7 APPENDIX

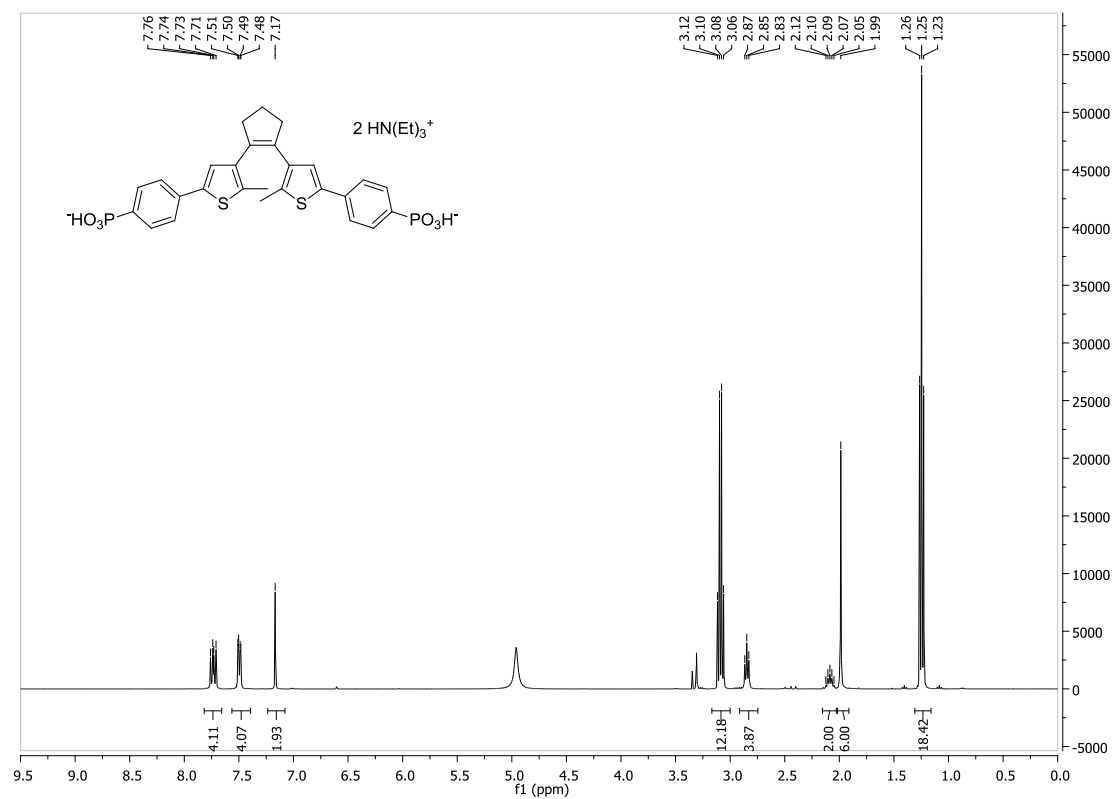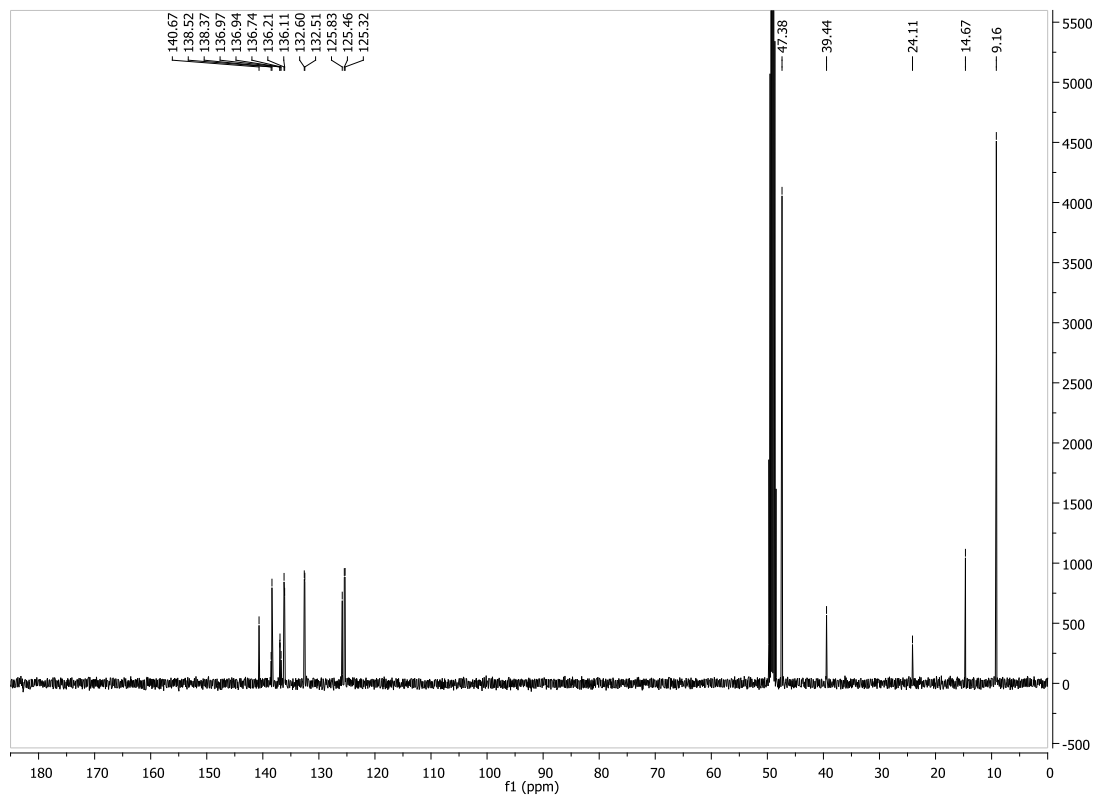## 7.1   Supplementary NMR spectra for Chapter 1

¹H-NMR for compound **2**:

¹³C-NMR for compound **2**:

¹H-NMR for compound **3**:

¹³C-NMR for compound **3**:

1H-NMR for compound **4**:

13C-NMR for compound **4**:

¹H-NMR for compound **5**:

¹³C-NMR for compound **5**:

^{1}H-NMR for compound **6**:

4 HN(Et)$_3$$^+$
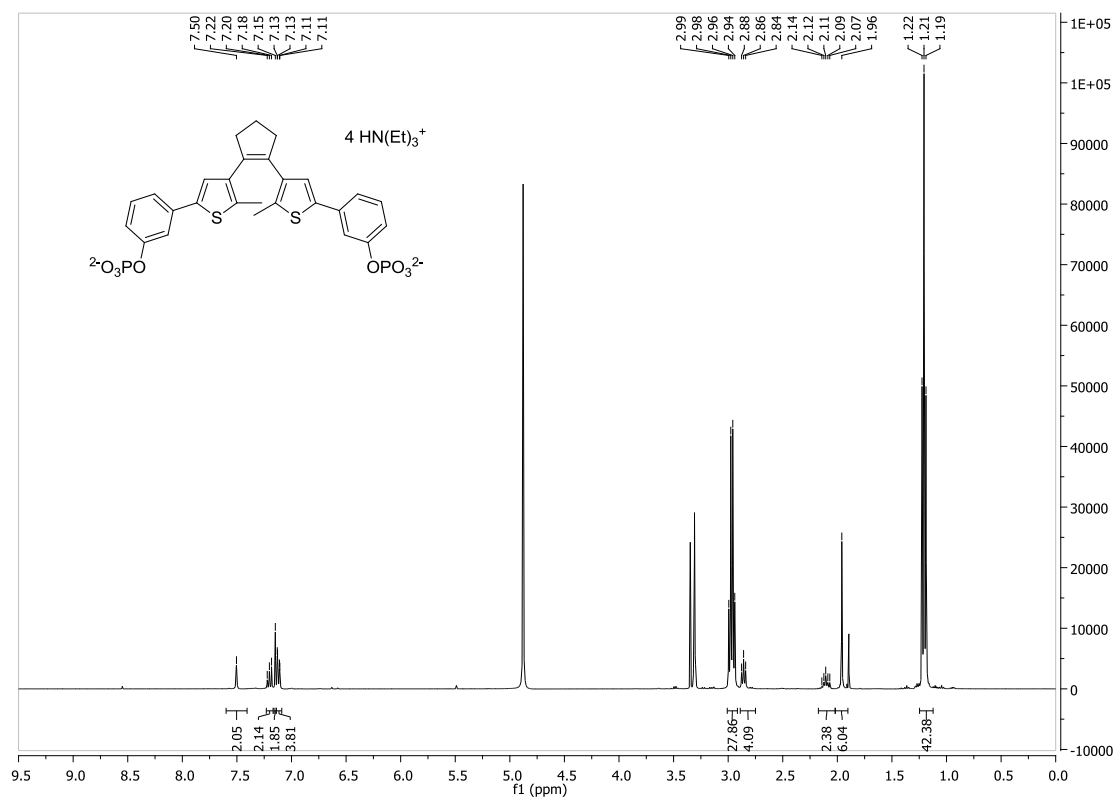
^{13}C-NMR for compound **6**:

¹H-NMR for compound **7**:

¹³C-NMR for compound **7**:

1H-NMR for compound **10**:

13C-NMR for compound **10**:

Appendix
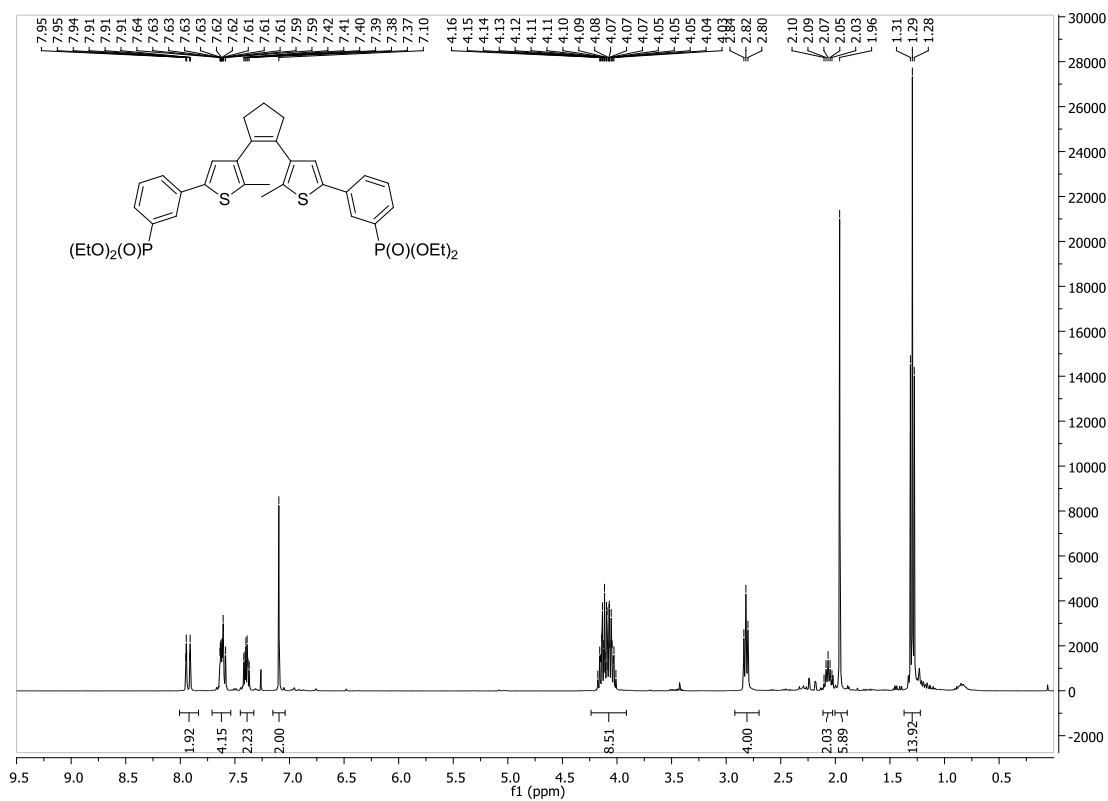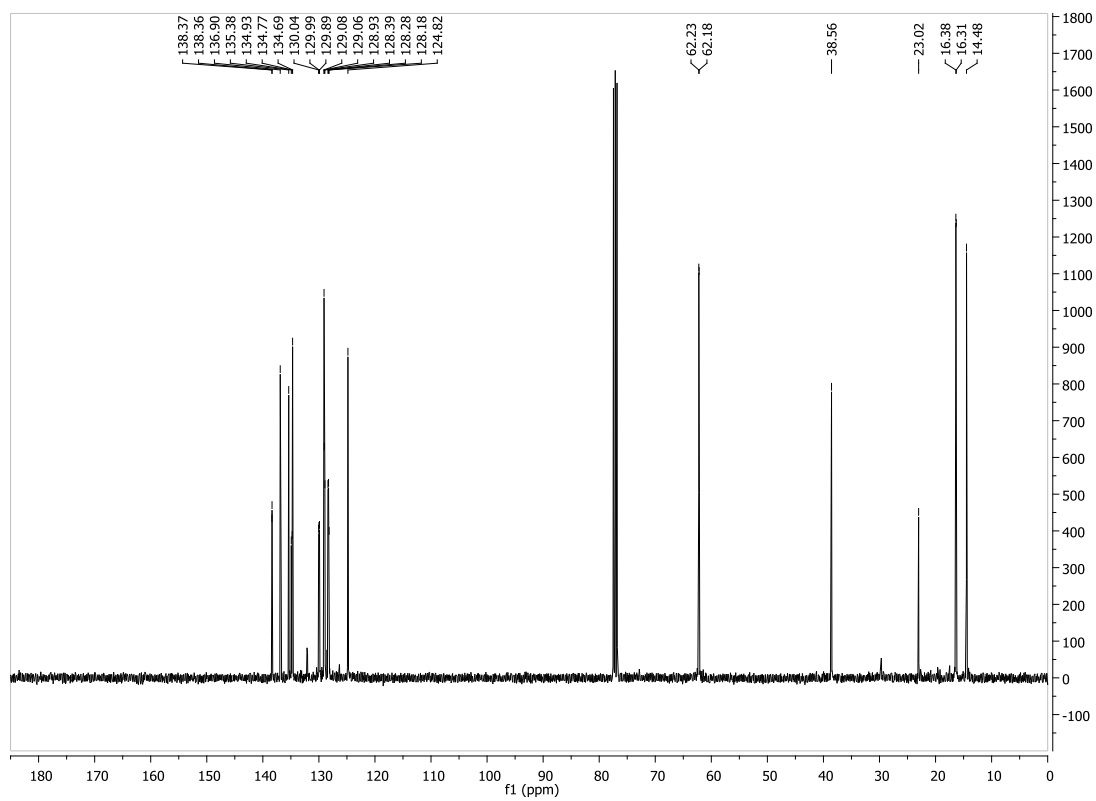
^{1}H-NMR for compound **11**:

^{13}C-NMR for compound **11**:

98

1H-NMR for compound **12**:
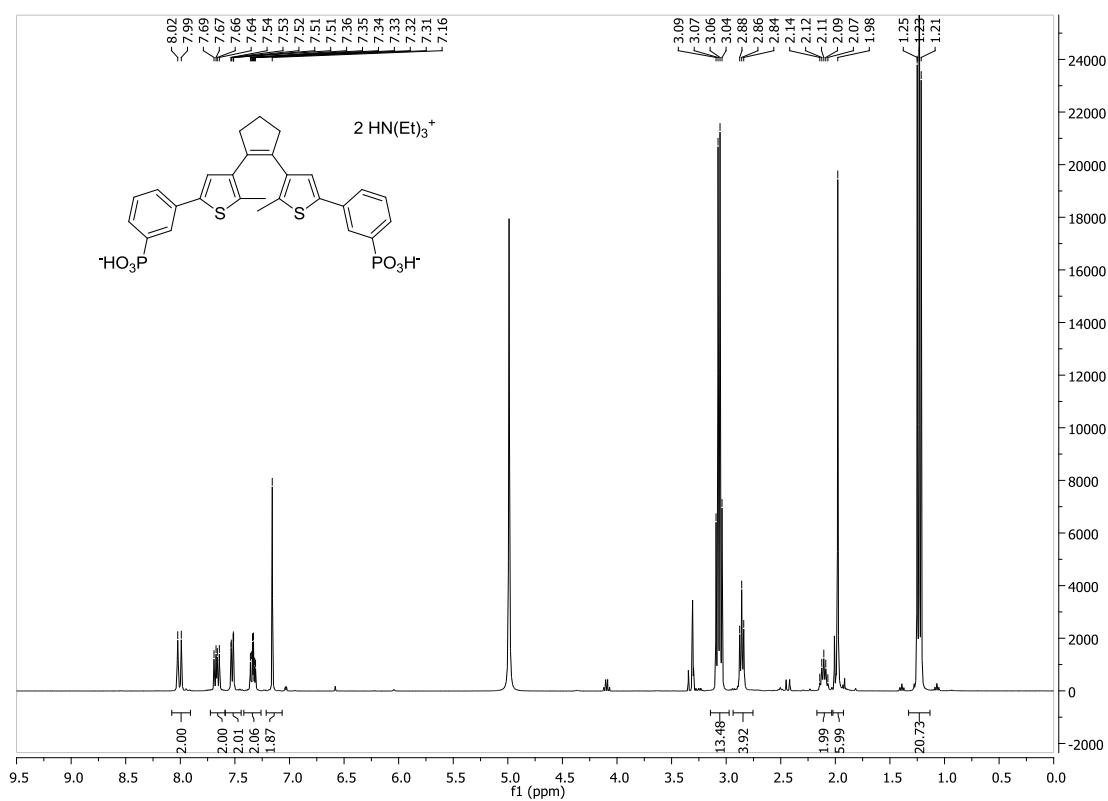
13C-NMR for compound **12**:

¹H-NMR for compound **13**:

7.76 7.74 7.73 7.71 7.51 7.50 7.49 7.48 7.17

3.12 3.10 3.08 3.06 2.87 2.85 2.83 2.12 2.10 2.09 2.07 2.05 1.99 1.26 1.25 1.23

2 HN(Et)₃⁺

⁻HO₃P — PO₃H⁻

4.11 4.07 1.93 12.18 3.87 2.00 6.00 18.42

f1 (ppm)

¹³C-NMR for compound **13**:

140.67 138.52 138.37 136.97 136.94 136.74 136.21 136.11 132.60 132.51 125.83 125.46 125.32

47.38 39.44 24.11 14.67 9.16

f1 (ppm)
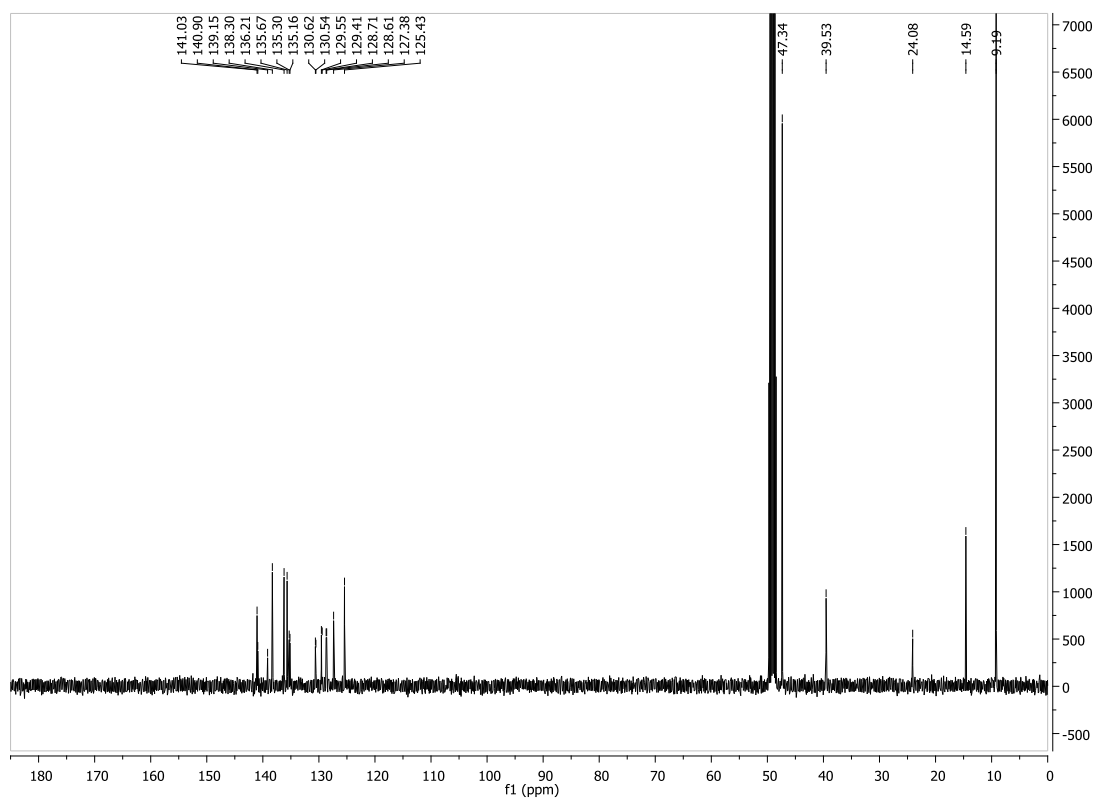
7.2   Supporting Information for Chapter 2

7.2.1   Supplementary Figures
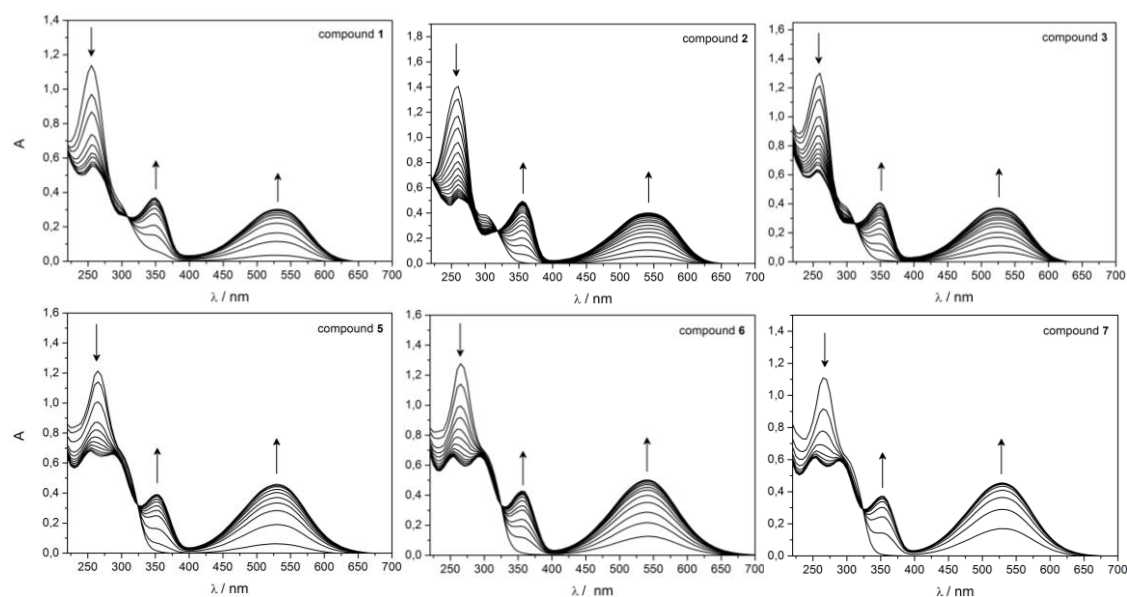
Figure A1. UV/Vis absorption spectra evolution of DTEs **1**-**3** and **5**-**7** (50 μM in MeOH) upon irradiation with 312 nm light; arrows indicate the changes of the absorption maxima with irradiation periods of 6 s; the colors of the respective solutions are depicted.
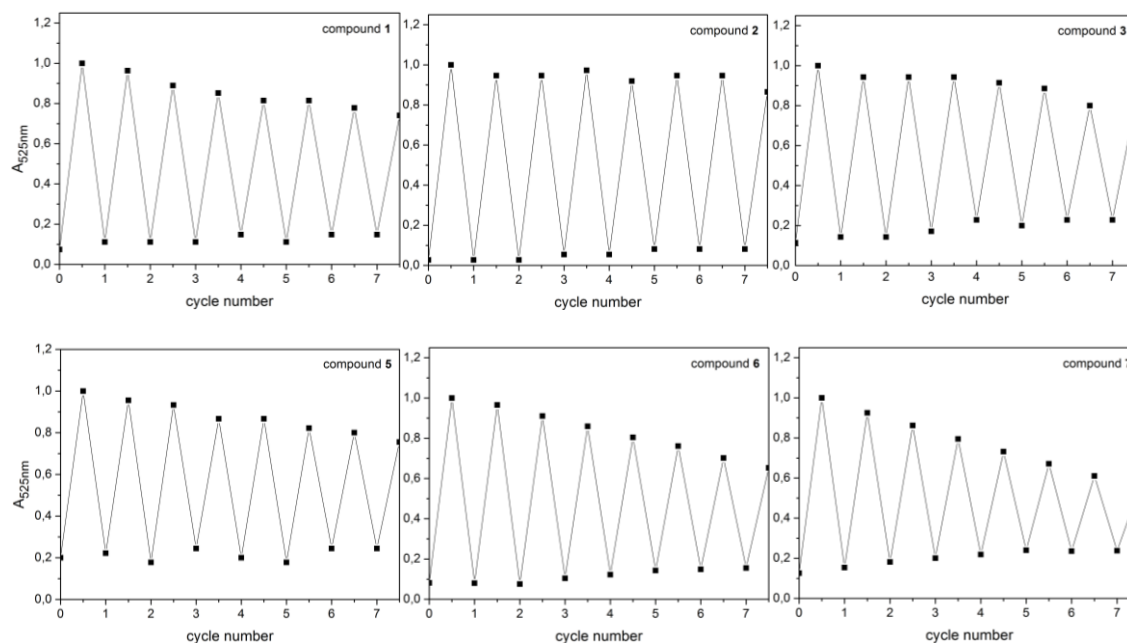
Figure A2. Cycle performances of compounds **1**-**3** and **5**-**7**. Changes in absorption at 525 nm were measured during an alternated irradiation the inhibitor solution (50 μM in MeOH) with 312 nm light for 60 s and greater than 420 nm light for 15 min.
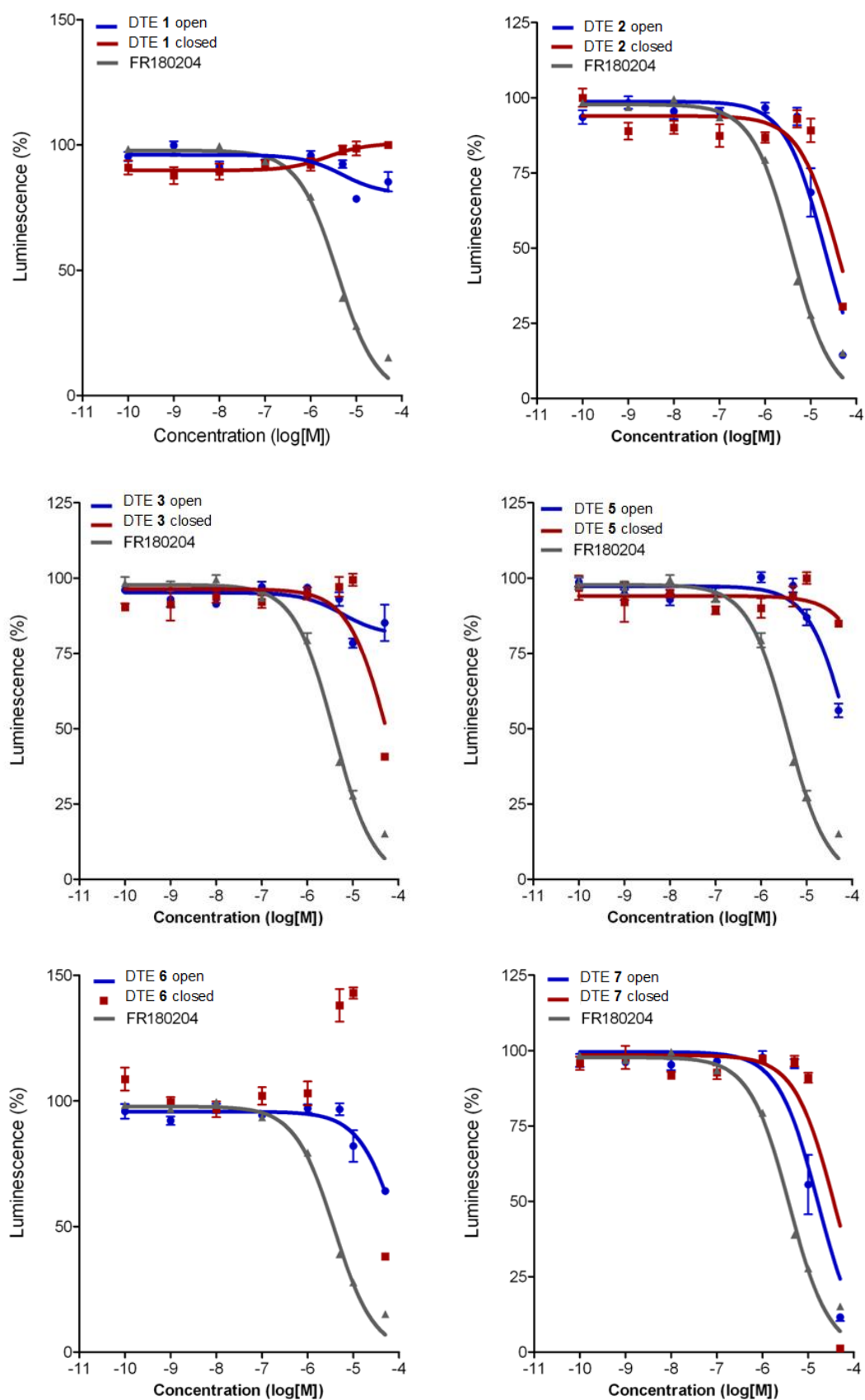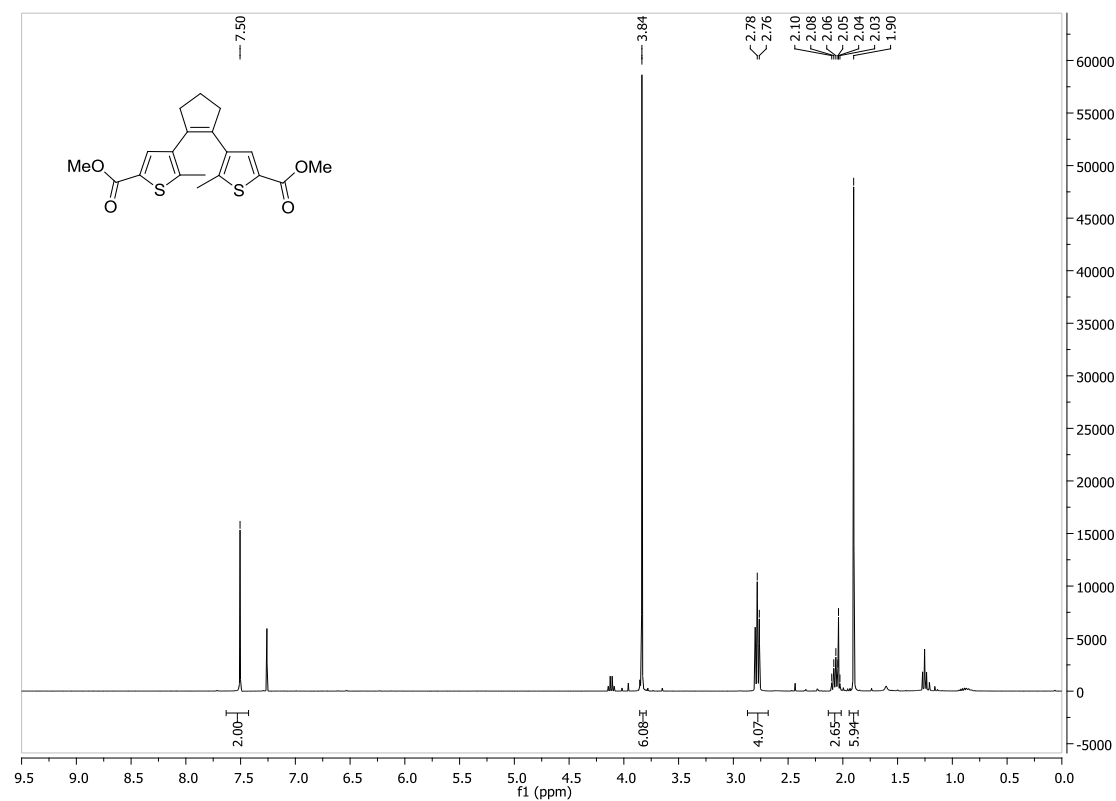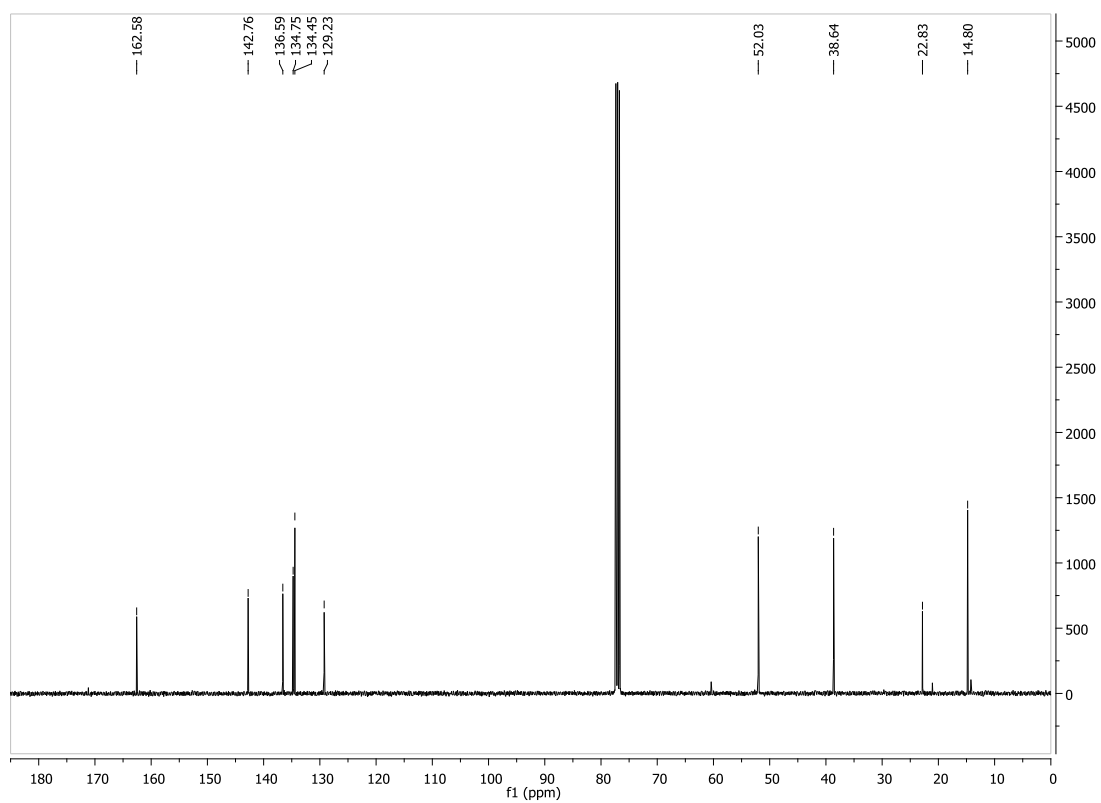
Figure A3. Dose-response curves for DTEs **1-3** and **5-7** in their open (blue) and closed (red) photoisomers with **FR180204** as reference.
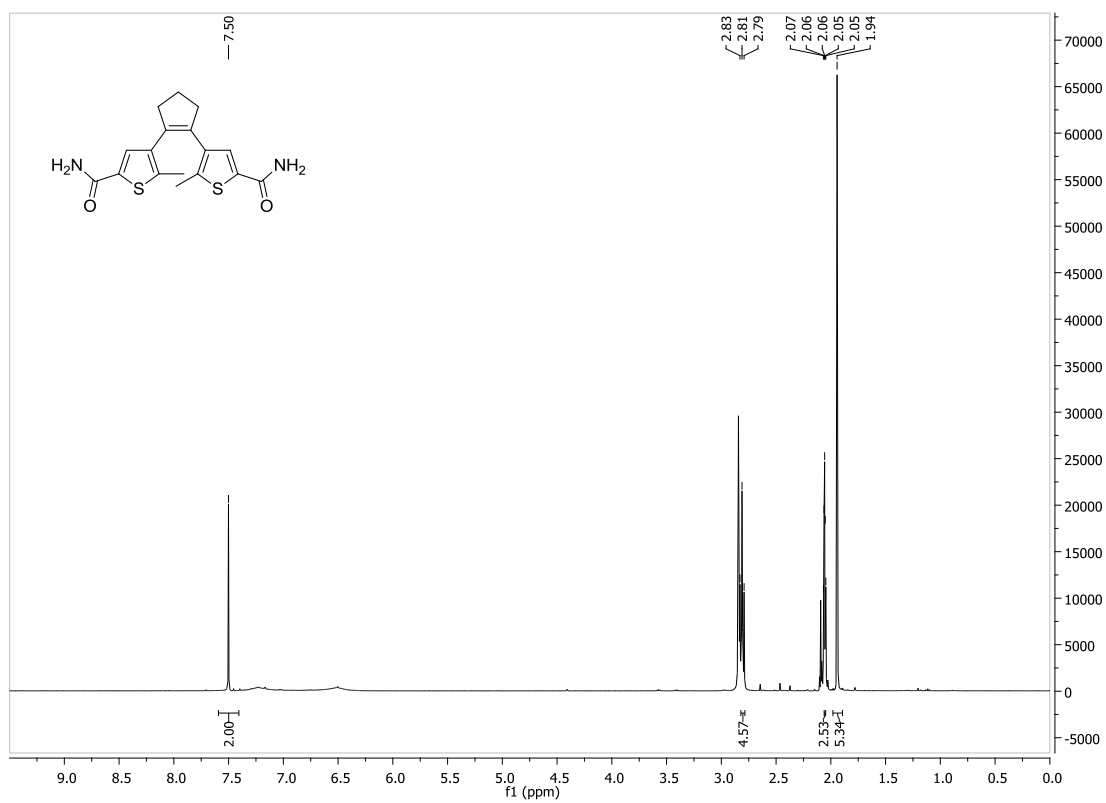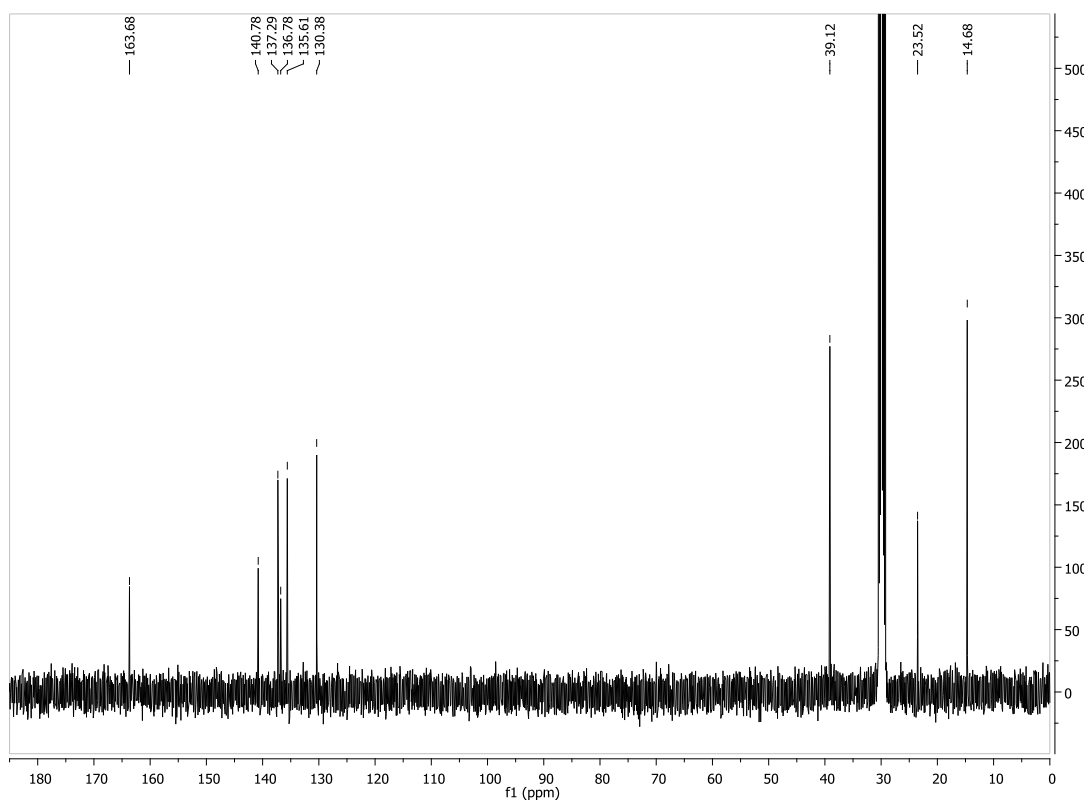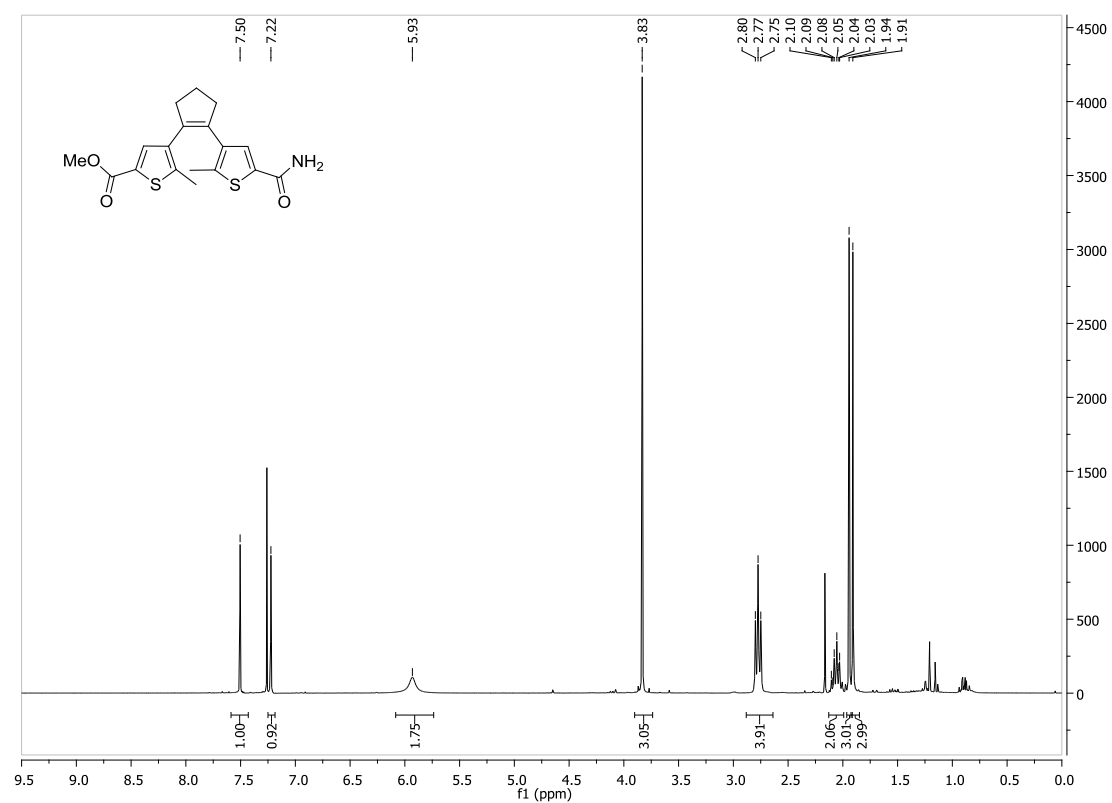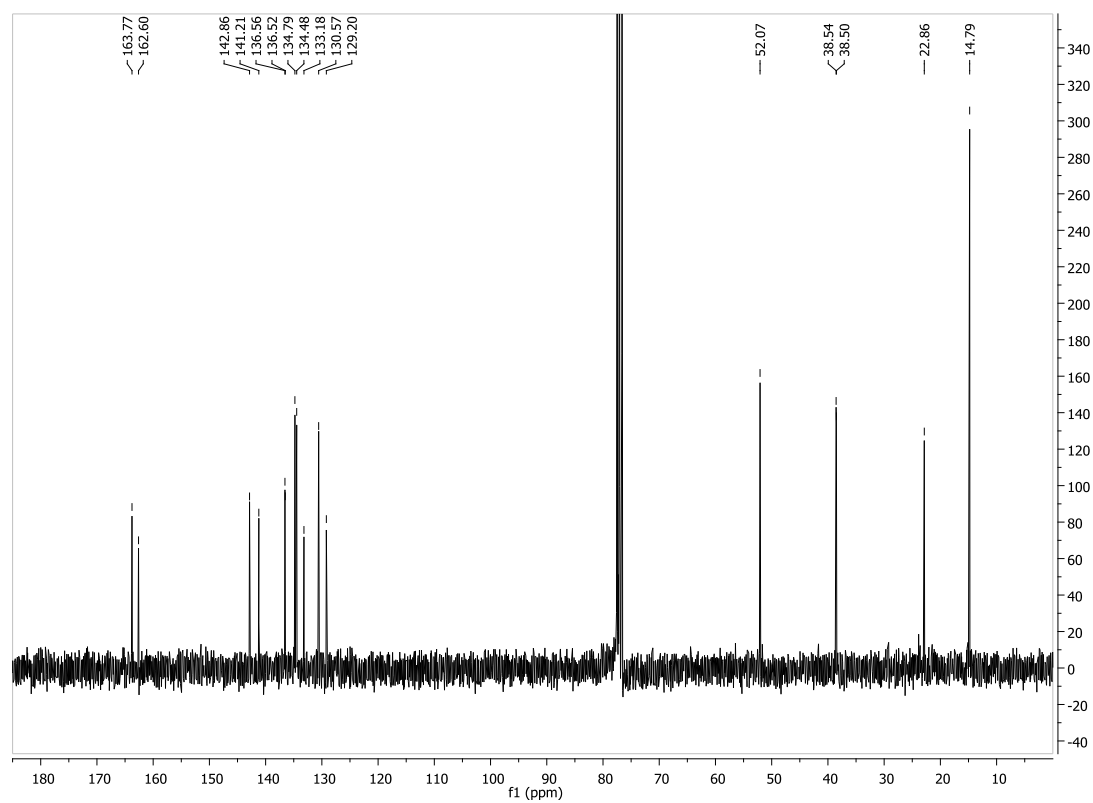
7.2.2   Supplementary NMR spectra

^{1}H-NMR for compound **2**:

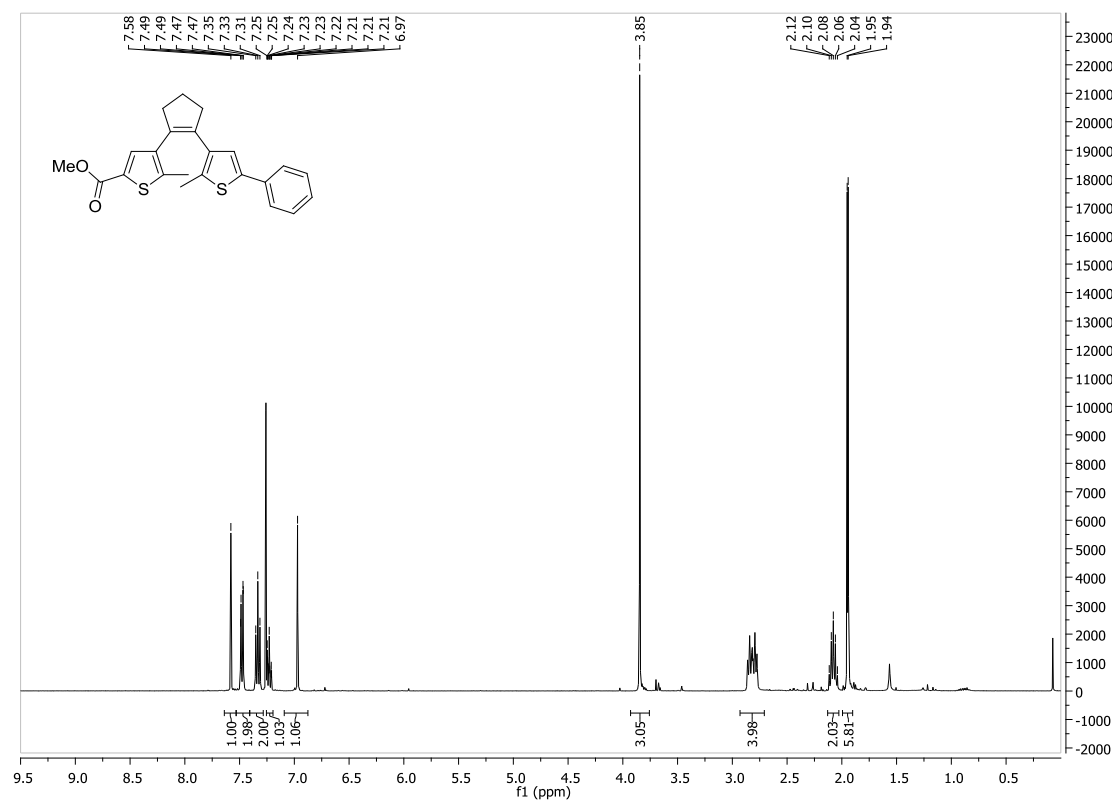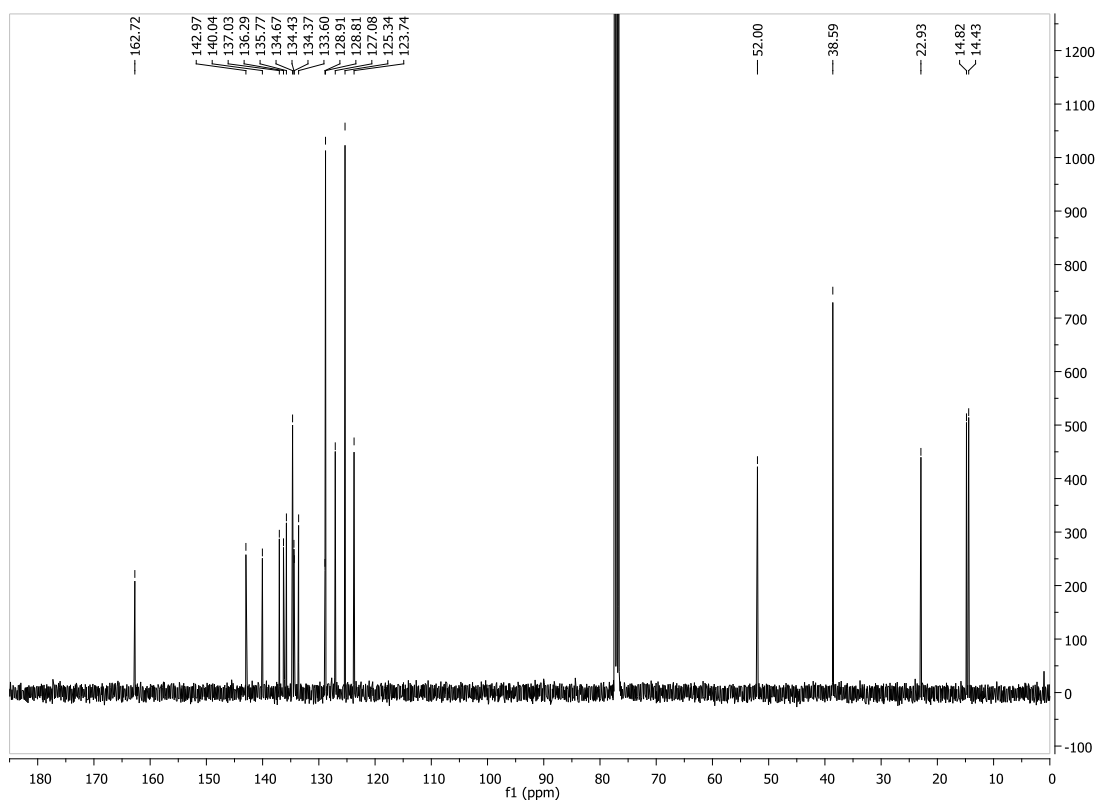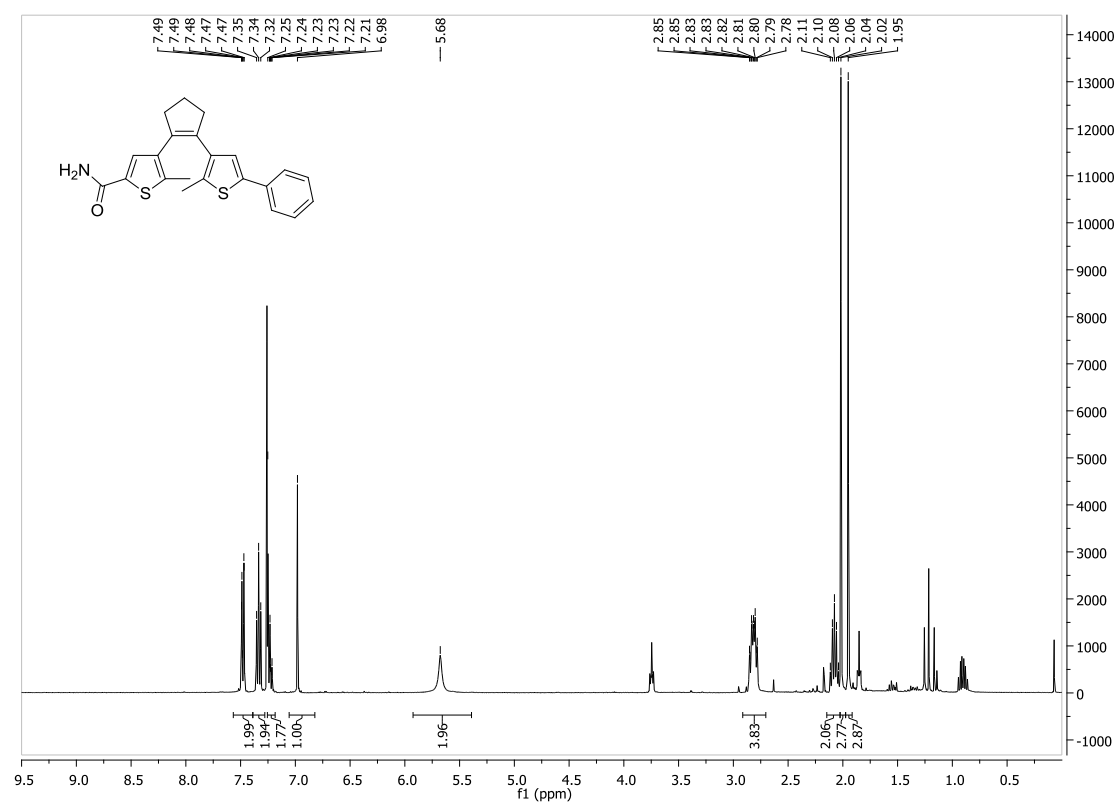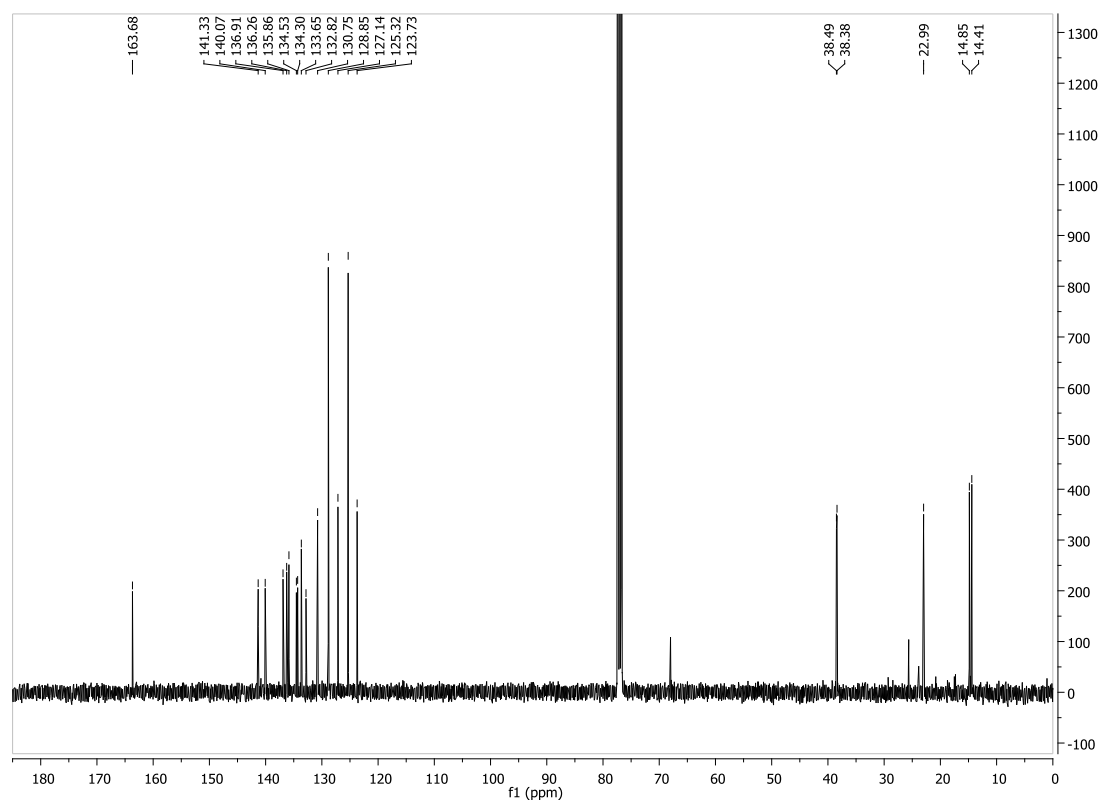^{13}C-NMR for compound **2**:

1H-NMR for compound **3:**

13C-NMR for compound **3**:

1H-NMR for compound **4:**

13C-NMR for compound **4:**

^{1}H-NMR for compound **6**:

^{13}C-NMR for compound **6**:

¹H-NMR for compound **7:**

¹³C-NMR for compound **7:**

7.3 Supporting Information for Chapter 3

7.3.1 Supplementary Synthetic Data
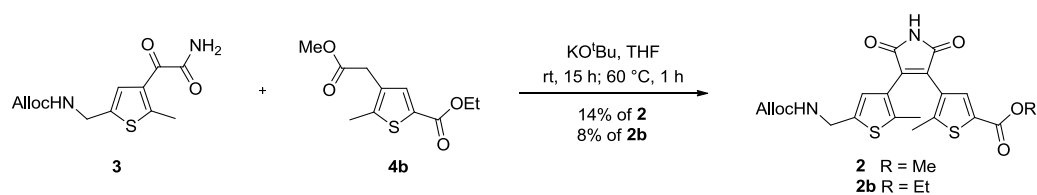
Scheme A1. Perkin condensation of the N-terminal precursor **3** and C-terminal precursor **4b** to access the dithienylmaleimide **2** and **2b**.
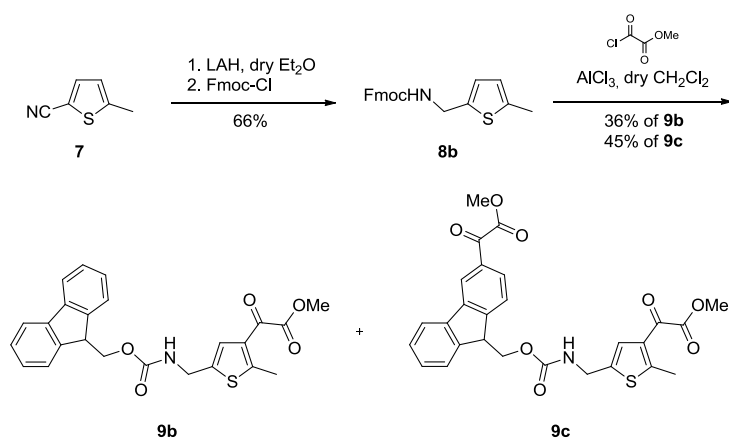
Scheme A2. Synthesis of the N-terminal precursor **9b** using Fmoc protection. Double acylated **9c** occurred as main product.
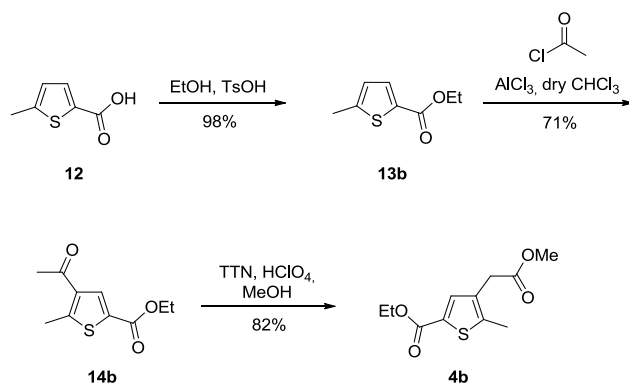
Scheme A3. Synthesis of the C-terminal ethyl ester precursor **4b**.

Scheme A4. Hydrolytic ester cleavage yielded the anhydride **1b**.

4-(4-(5-((((Allyloxy)carbonyl)amino)methyl)-2-methylthiophen-3-yl)-2,5-dioxo-2,5-dihydrofuran-3-yl)-5-methylthiophene-2-carboxylic acid (1b): A mixture of **2** and **2b** (62 mg) in 10 mL of H_2O/MeOH/THF (2:5:3, v/v/v) was stirred for 20 h with NaOH (78 mg, 1.95 mmol) at room temperature. After addition of water (10 mL) the reaction mixture was washed with EtOAc (2 x 10 mL) and then acidified with conc. HCl to pH 1. The aqueous phase was e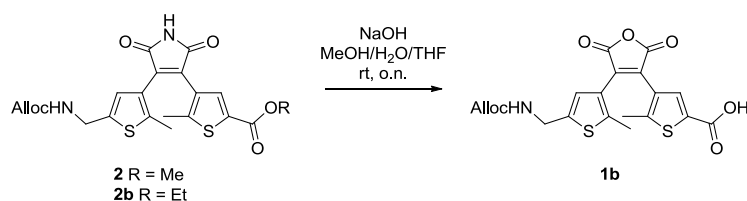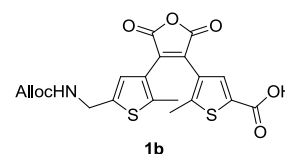xtracted with EtOAc (3 x 10 mL) and the combined organic phases were dried over magnesium sulfate. Evaporation of the solvent and purification of the crude product by automated reversed phase flash column chromatography (H_2O/MeCN, 20% - 55% MeCN) yielded **1b** (29 mg, 0.06 mmol) as green solid; R_f: 0.02 (PE/EtOAc : 1/1); **m.p.:** 84 °C; **^{1}H-NMR (400 MHz, DMSO-d$_6$):** δ = 1.92 (3H, s, thiophene-CH_3), 1.97 (3H, s, thiophene-CH_3), 4.28 (2H, d, J = 6.1 Hz, thiophene-CH_2NH), 4.49 (2H, d, J = 5.3 Hz, CH$_2$=CHCH_2O), 5.18 (1H, dd, J = 10.5, 1.4 Hz, CH_2=CHCH$_2$), 5.27 (1H, dd, J = 17.2, 1.5 Hz, CH_2=CHCH$_2$), 5.90 (1H, ddt, J = 17.2, 10.6, 5.3 Hz, CH$_2$=CHCH$_2$), 6.87 (1H, s, thiophene-H), 7.65 (1H, s, thiophene-H), 7.90 (1H, t, J = 6.0 Hz, CH$_2$NHCO), 13.27 (1H, bs, COOH); **^{13}C-NMR (75 MHz, DMSO-d$_6$):** δ = 14.1 (+), 14.5 (+), 38.8 (−), 64.4 (−), 116.9 (−), 124.9 (q), 125.5 (+), 126.8 (q), 131.6 (q), 133.5 (+), 133.9 (+), 135.6 (q), 140.8 (q), 141.4 (q), 148.6 (q), 155.9 (q), 162.2 (q), 164.9 (q), 164.9 (q); **IR ṽ [cm^{-1}]:** 3327 (w), 3164 (w), 3020 (w), 2925 (m), 1764 (s), 1702 (m), 1541 (m), 1458 (w), 1254 (m), 931 (m), 750 (w); **UV/Vis (50 μM in MeOH):** open isomer: $λ_{max}$ = 246 nm; closed isomer: $λ_{max}$ = 384 nm, 568 nm; **MS (ESI):** m/z (%) = 448.1 (100, MH$^+$), 347.0 (98, [M-AllocNH]$^+$); **HR-MS (ESI):** calcd. for $C_{20}H_{18}NO_7S_2$ (M+H)$^+$, m/z = 448.0519; found 448.0516.
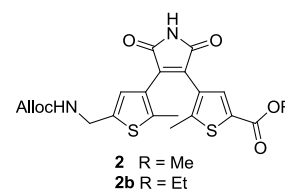
Ethyl/Methyl 4-(4-(5-(((((allyloxy)carbonyl)amino)methyl)-2-methyl-thiophen-3-yl)-2,5-dioxo-2,5-dihydro-1H-pyrrol-3-yl)-5-methylthiophene-2-carboxylate (2/2b).
KO^{t}Bu (1 M in THF) (1.34 mL, 1.34 mmol, 1.2 eq.) was added to a solution of **3** (316 mg, 1.12 mmol, 1.0 eq.) in dry THF (6 mL) at 0 °C under nitrogen atmosphere. After stirring for 90 min at 0 °C, diester **4b** (326 mg, 1.34 mmol, 1.2 eq.) was added at 0 °C and stirred for 15 h at room temperature. Then the reaction was heated to 60 °C for 1 h, quenched with 1 M

HCl solution (4 mL) and diluted with EtOAc (10 mL). The organic phase was washed with water (3 x 5 mL), brine (5 mL) and dried over magnesium sulfate. The solvent was removed under reduced pressure and purification of the crude product by automated reversed phase flash column chromatography (H_2O/EtOH, 20% - 45% EtOH) yielded **2b** (40 mg, 0.08 mmol, 8%) as orange foam, **2** (74 mg, 0.16 mmol, 14%) as yellow foam and a mixed fraction of both (65 mg); Analysis of **1b**: R_f: 0.25 (PE/EtOAc : 2/1); **^{1}H-NMR (400 MHz, CDCl$_3$):** δ = 1.36 (3H, t, J = 7.1 Hz, O−CH$_2$−CH_3), 1.91 (3H, s, thiophene-CH_3), 1.97 (3H, s, thiophene-CH_3), 4.33 (2H, q, J = 7.1 Hz, O−CH_2−CH$_3$), 4.45 (2H, d, J = 5.9 Hz, C−CH_2−NH), 4.60 (2H, d, J = 4.8 Hz, O−CH_2−CH), 5.14 −5.26 (2H, m, CH_2=CH−CH$_2$ and CH$_2$−NH−CO), 5.31 (1H, dd, J = 17.2, 1.1 Hz, CH_2=CH−CH$_2$), 5.92 (1H, ddt, J = 16.3, 10.8, 5.6 Hz, CH$_2$=CH−CH$_2$), 6.90 (1H, s, thiophene-H), 7.75 (1H, s, thiophene-H), 7.97 (1H, bs, CO−NH−CO); **^{13}C-NMR (101 MHz, CDCl$_3$):** δ = 14.3 (+), 15.0 (+), 15.3 (+), 39.9 (−), 61.4 (−), 65.9 (−), 117.9 (−), 125.8 (q), 126.7 (+), 127.4 (q), 131.4 (q), 132.7 (+), 132.8 (q), 134.7 (+), 139.4 (q), 142.1 (q), 148.4 (q), 156.0 (q), 161.7 (q), 170.0 (q), 170.1 (q); **IR ṽ [cm^{-1}]:** 3288 (w), 3071 (w), 2980 (w), 1710 (s), 1541 (m), 1458 (w), 1252 (m), 995 (w), 916 (w), 760 (w); **UV/Vis** (50 µM in MeOH): open isomer: λ$_{max}$ = 250 nm; closed isomer: λ$_{max}$ = 232 nm, 378 nm, 554 nm; **MS (ESI):** m/z (%) = 475.1 (100, MH$^+$), 374.1 (78, [M-AllocNH]$^+$), 476.1 (26), 533.2 (24, [MNH$_4$ + MeCN]$^+$), 497.1 (21); **HR-MS (ESI):** calcd. for C$_{22}$H$_{23}$N$_2$O$_6$S$_2$ (M+H)$^+$, m/z = 475.0993; found 475.0992.

4b
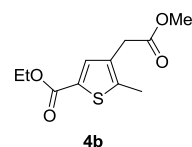
Ethyl 4-(2-methoxy-2-oxoethyl)-5-methylthiophene-2-carboxylate (4b). Thallium tri-nitrate (2.20 g, 4.94 mmol, 1.2 eq.) and 70% HClO$_4$ (2 mL) were added to a suspension of **14b** (875 mg, 4.12 mmol, 1.0 eq.) in MeOH (20 mL) at room temperature. After stirring for 24 h the mixture was concentrated under vacuum and diluted with water (5 mL). The aqueous phase was extracted with chloroform (3 x 5 mL) and dried over magnesium sulfate. The solvent was evaporated and purification of the crude product by automated flash column chromatography (PE/EtOAc, 3% - 15% EtOAc) yielded 816 mg (3.37 mmol, 82%) of compound **4b** as yellowish oil; R_f: 0.23 (PE/EtOAc : 9/1); **^{1}H-NMR (400 MHz, CDCl$_3$):** δ = 1.35 (3H, t, J = 7.1 Hz, O−CH$_2$−CH_3), 2.42 (3H, s, thiophene-CH_3), 3.54 (2H, s, C−CH_2−CO), 3.70 (3H, s, CO−O−CH_3), 4.31 (2H, q, J = 7.1 Hz, O−CH_2−CH$_3$), 7.60 (1H, s, thiophene-H); **^{13}C-NMR** (75 MHz, CDCl$_3$): δ = 13.8 (+), 14.4 (+), 33.8 (−), 52.2 (+), 61.0 (−), 129.6 (q), 130.6 (q), 135.4 (+), 143.8 (q), 162.2 (q), 171.0 (q); **IR ṽ [cm^{-1}]:** 3081 (w), 2987 (w), 2922 (w), 1730 (s), 1705 (s), 1460 (m), 1254 (s), 1201 (s), 1172 (s), 1061 (s); **MS (EI):** m/z (%) =

183.1 (100, [M-(CO$_2$Me)]$^+$), 242.1 (67, M$^+$), 155.1 (61), 197.0 (49, [M-(EtO)]$^+$), 182.1 (47); **HR-MS (ESI):** calcd. for C$_{11}$H$_{14}$NaO$_4$S (M+Na)$^+$, m/z = 265.0505; found 265.0502.

8b

(9H-Fluoren-9-yl)methyl ((5-methylthiophen-2-yl)methyl)carbamate (8b). To an ice-bath cooled solution of nitrile **7** (2.00 g, 16.24 mmol, 1.0 eq) in anhydrous Et$_2$O (200 mL), LAH (1.85 g, 48.71 mmol, 3.0 eq) was slowly added. After stirring for 2 h at room temperature the reaction mixture was quenched with water (6 mL). The precipitate was filtered off and the aqueous phase was extracted with Et$_2$O (2 x 10 mL). 9-Fluorenylmethyl chloroformate (4.20 g, 16.24 mmol, 1.0 eq) was added to the combined organic phases and the reaction mixture was stirred at room temperature overnight. The solvent was removed under reduced pressure and the crude product was purified by automated flash column chromatography (PE/EtOAc, 5 - 25% EtOAc) affording 2.14 g (6.12 mmol, 38%) of **8b** as beige solid. **^{1}H-NMR (400 MHz, CDCl$_3$):** δ = 2.45 (3H, s, thiophene-CH_3), 4.23 (1H, t, J = 6.6 Hz, fluorenyl-H), 4.43 – 4.47 (4H, m, fluorenyl-CH_2 and thiophene-CH_2), 5.17 (1H, bs, Fmoc-NH), 6.59 (1H, bs, thiophene-H), 6.74 (1H, bs, thiophene-H), 7.31 (2H, t, J = 7.4 Hz, 2 phenyl-H), 7.41 (2H, t, J = 7.4 Hz, 2 phenyl-H), 7.59 (2H, d, J = 7.4 Hz, 2 phenyl-H), 7.77 (2H, d, J = 7.6 Hz, 2 phenyl-H); **^{13}C-NMR (100 MHz, CDCl$_3$):** δ = 15.4 (+), 40.2 (−), 47.3 (+), 66.8 (−), 120.0 (+), 124.9 (+), 125.1 (+), 125.8 (+), 127.1 (+), 127.7 (+), 138.8 (q), 139.9 (q), 141.4 (q), 143.9 (q), 156.1 (q); **MS (ESI):** m/z (%) = 350.1 (100, [MH$^+$]), 372.1 (94, [MNa$^+$]), 721.1 (50, [2 MNa$^+$]), 699.2 (37, [2 MH$^+$]); **HR-MS (ESI):** calcd. for C$_{21}$H$_{20}$NO$_2$S (MH$^+$), m/z = 350.1209; found 350.1206.

9b   **9c**

Methyl-2-(5-(((((9H-fluoren-9-yl)methoxy)carbonyl)amino)methyl)-2-methylthio-phen-3-yl)-2-oxoacetate (9b/9c). In a crimp top vial a solution of methyl-chlorooxoacetate (19 mg, 0.15 mmol, 1.1 eq) in anhydrous CH$_2$Cl$_2$ (2 mL) was added to AlCl$_3$ (75 mg, 0.56 mmol, 4.0 eq) under nitrogen atmosphere. It was cooled by ice-bath and a solution of **8b** (50 mg, 0.14 mmol, 1.0 eq) in anhydrous CH$_2$Cl$_2$ (2 mL) was added dropwise via syringe. The reaction mixture was stirred for 2 h at 0 °C, and subsequently quenched by

addition of ice water (5 mL), which led to decoloration. The aqueous phase was extracted with CH_2Cl_2 (2 x 5 mL) and the combined organic phases were washed with saturated $NaHCO_3$ and brine (each 5 mL) and dried over magnesium sulfate. Purification by flash chromatography (PE/EtOAc, 5-15% EtOAc) provided 22 mg (0.05 mmol, 36%) of **9b** and 35 mg (0.07 mmol, 45%) of **9c**, both as slightly yellow oil. Analysis of **9b**: **¹H-NMR (400 MHz, CDCl₃):** δ = 2.72 (3H, s, thiophene-C*H*₃), 3.93 (3H, s, oxoacetyl-OC*H*₃), 4.23 (1H, t, *J* = 6.6 Hz, fluorenyl-*H*), 4.44 – 4.46 (4H, m, fluorenyl-C*H*₂ and thiophene-C*H*₂), 5.20 (1H, bs, Fmoc-N*H*), 7.31 (2H, t, *J* = 7.4 Hz, 2 fluorenyl-*H*), 7.35 (1H, s, thiophene-*H*), 7.40 (2H, t, *J* = 7.3 Hz, 2 fluorenyl-*H*), 7.58 (2H, d, *J* = 7.3 Hz, 2 fluorenyl-*H*), 7.76 (2H, d, *J* = 7.5 Hz, 2 fluorenyl-*H*); **¹³C-NMR (100 MHz, CDCl₃):** δ = 16.3 (+), 39.7 (−), 47.2 (+), 52.8 (+), 67.0 (−), 120.0 (+), 125.0 (+), 127.1 (+), 127.6 (+), 127.8 (+), 131.0 (q), 137.9 (q), 141.4 (q), 143.8 (q), 164.0 (q), 179.9 (q); MS (ESI): m/z (%) = 436.1 (100, [MH⁺]); Analysis of **9c**: **¹H NMR (300 MHz, CDCl₃):** δ = 2.72 (3H, s, thiophene-C*H*₃), 3.92 (3H, s, oxoacetyl-OC*H*₃), 3.99 (3H, s, oxoacetyl-OC*H*₃), 4.38 – 4.24 (2H, m, C*H*₂), 4.46 (2H, d, *J* = 5.9 Hz, C*H*₂), 4.72 – 4.50 (1H, m, fluorenyl-*H*), 5.30 (1H, bs, Fmoc-N*H*), 7.35 (1H, s, thiophene-*H*), 7.53 – 7.38 (2H, m, 2 fluorenyl-*H*), 7.62 (1H, d, *J* = 7.4 Hz, fluorenyl-*H*), 7.85 (2 H, dd, *J* = 7.4, 3.8 Hz, 2 fluorenyl-*H*), 8.08 (1 H, dd, *J* = 8.0, 1.4 Hz, fluorenyl-*H*), 8.28 (1H, s, fluorenyl-*H*); **MS (ESI):** m/z (%) = 522.1 (100, [MH⁺]), 539.1 (63, [MNH₄⁺]), 544.1 (36, [MNa⁺]).

14b
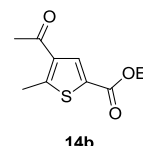
Ethyl 4-acetyl-5-methylthiophene-2-carboxylate (14b). A solution of acetyl chloride (128 μL, 1.80 mmol, 1.5 eq.) in dry chloroform (2 mL) was added to $AlCl_3$ (480 mg, 3.60 mmol, 3.0 eq.) at room temperature under nitrogen atmosphere. After stirring for 10 min a solution of **13b** (204 mg, 1.20 mmol, 1.0 eq.) in dry chloroform (2 mL) was dropped to the suspension. The mixture was heated to 60 °C for 9 h, then the reaction was quenched with ice/water and the aqueous phase was extracted with chloroform (2 x 30 mL). The combined organic phases were washed with a saturated solution of $NaHCO_3$ (50 mL) and brine (50 mL). The organic phase was dried over magnesium sulfate and the solvent was evaporated. The crude product was purified by automated flash column chromatography (PE/EtOAc, 8% - 30% EtOAc) and 180 mg of **14b** (180 mg, 0.85 mmol, 71%) were obtained as colorless solid; *R*f: 0.15 (PE/EtOAc : 9/1); **m.p.:** 103 °C; **¹H-NMR (400 MHz, CDCl₃):** δ = 1.37 (3H, t, *J* = 7.1 Hz, O−CH₂−C*H*₃), 2.52 (3H, s, thiophene-C*H*₃), 2.75 (3H, s, acetyl-C*H*₃), 4.34 (2H, q, *J* = 7.1 Hz, O−C*H*₂−CH₃), 8.02 (1H, s, thiophene-*H*); **¹³C-NMR (101 MHz, CDCl₃):** δ = 14.3 (+), 16.8 (+), 29.6 (+), 61.4 (−), 129.0 (q), 134.7 (+), 136.3 (q),

155.6 (q), 161.6 (q), 193.7 (q); **IR ṽ [cm⁻¹]:** 3008 (w), 2985 (w), 2944 (w), 1713 (s), 1670 (s), 1540 (s), 1452 (m), 1250 (s), 1236 (s), 1082 (s), 1021 (w), 747 (s); **MS (EI):** m/z (%) = 197.0 (100, [M-(CH$_3$)]$^+$), 169.0 (70, [M-(COCH$_3$)]$^+$), 212.1 (63, M$^+$), 167.1 (43), 43.1 (27); **HR-MS** (ESI): calcd. for C$_{10}$H$_{13}$O$_3$S (M+H)$^+$, m/z = 213.0580; found 213.0581.

7.3.2 Supplementary Figures
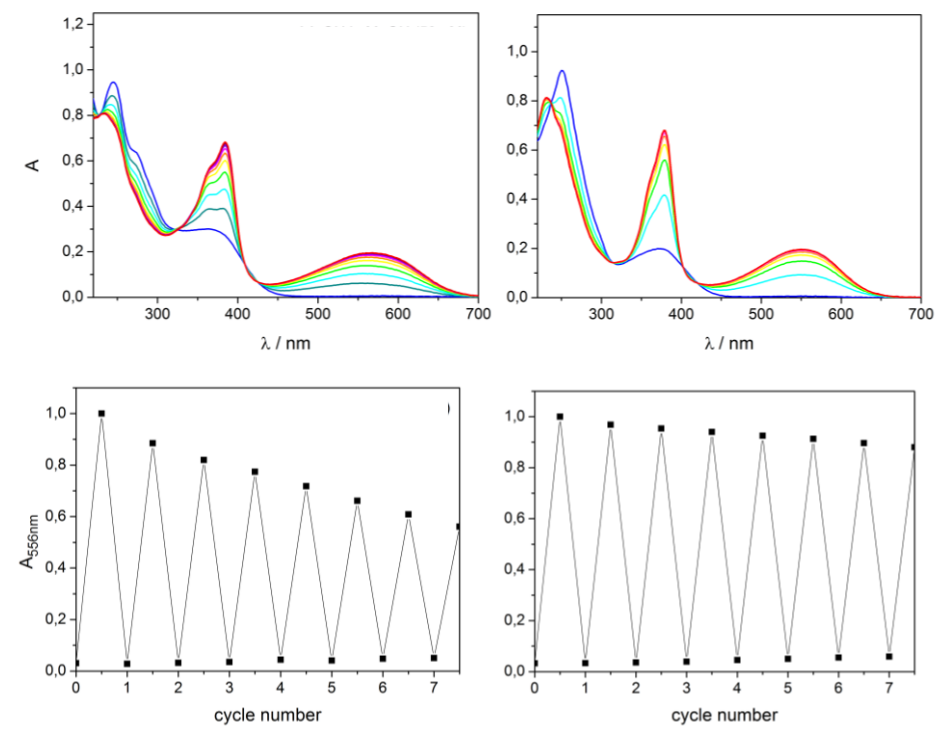
Figure A4. Upper spectra: UV/Vis absorption spectra evolution of the dithienylanhydride **1b** (left) and the dithienylmaleimide **2** (right), each 50 µM in MeOH, upon irradiation with 312 nm light; arrows indicate the changes of the absorption maxima with irradiation periods of 6 s. Lower spectra: Cycle performance of the dithienylanhydride **1b** (left) and dithienylmaleimide **2** (right). Changes in absorption at 556 nm were measured during an alternated irradiation with 312 nm light for 60 s and greater than 420 nm light for 5 min.
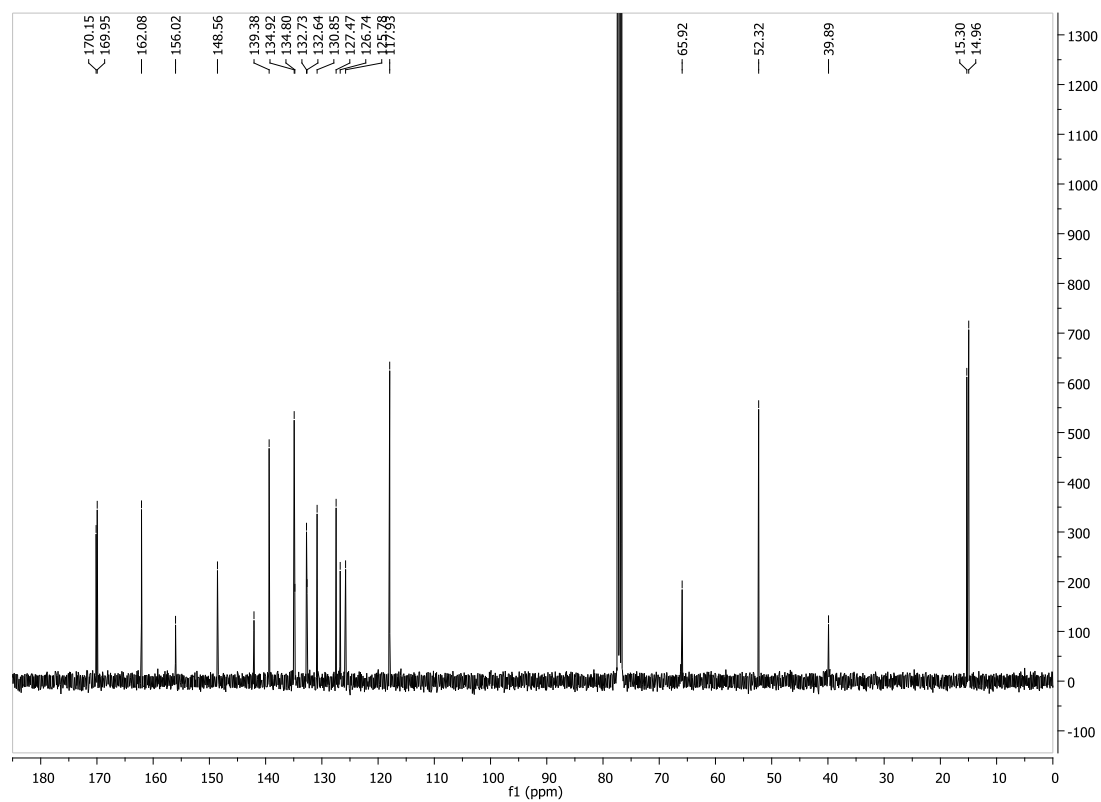
7.3.3 Supplementary NMR spectra

¹H-NMR for compound **1**:
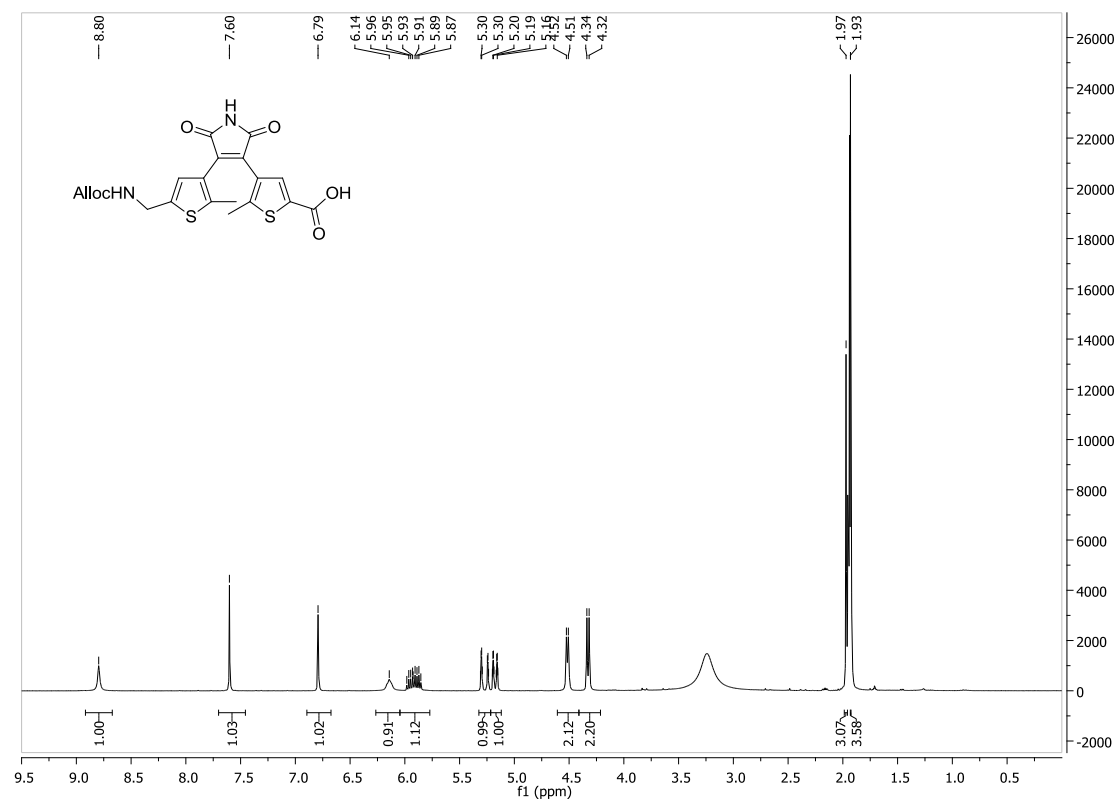
¹³C-NMR for compound **1**:
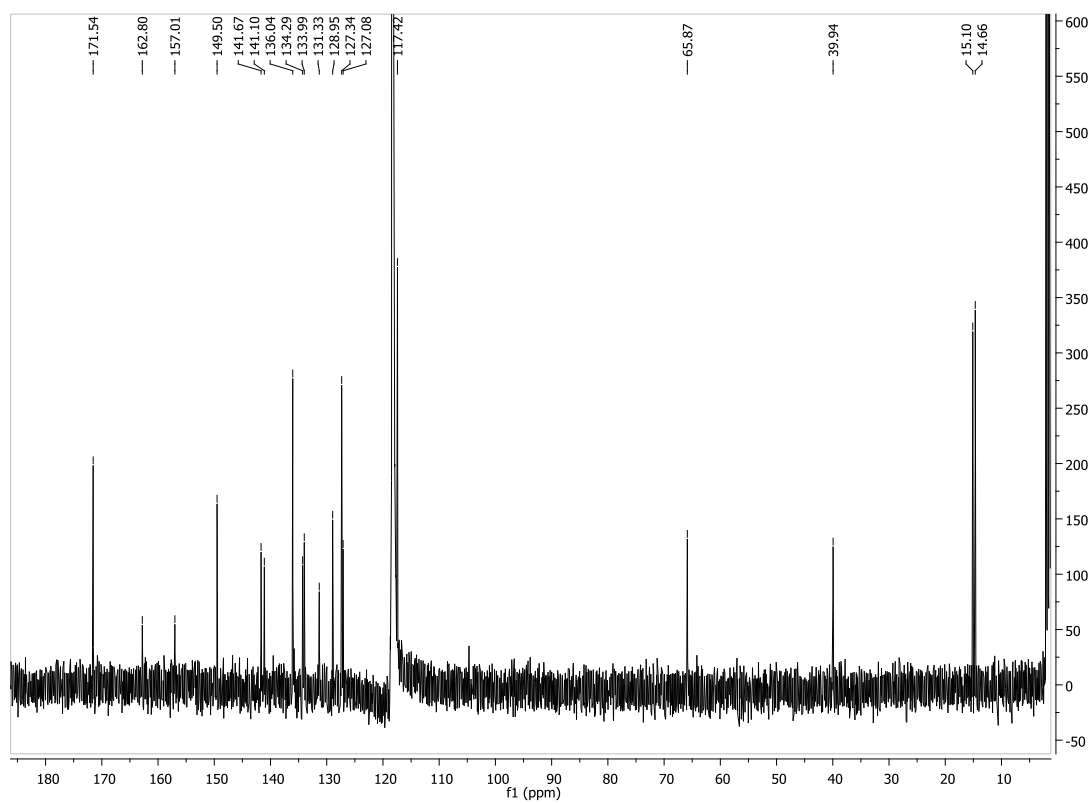
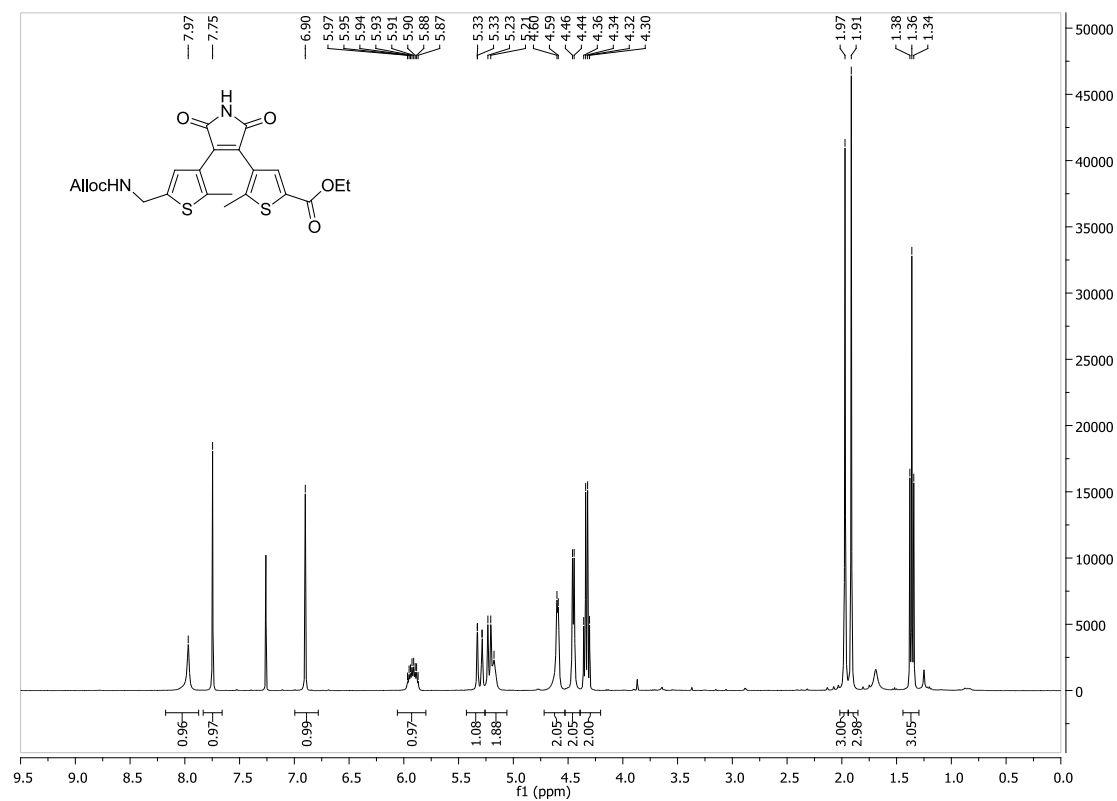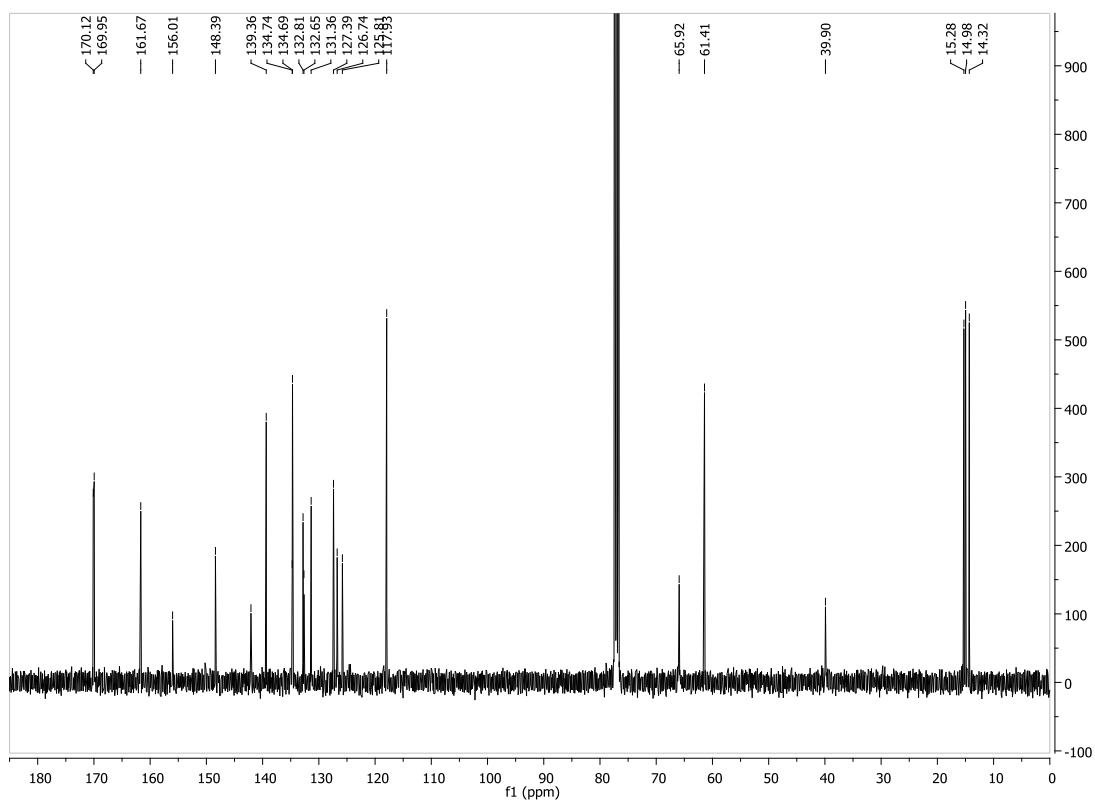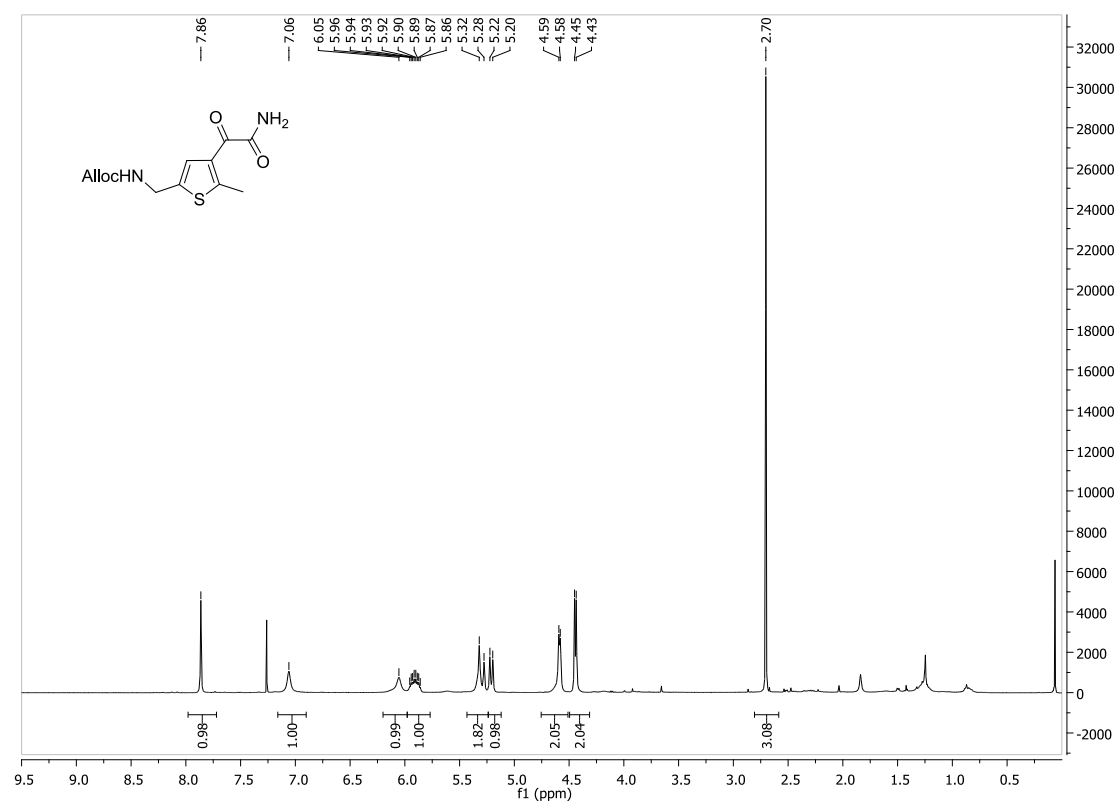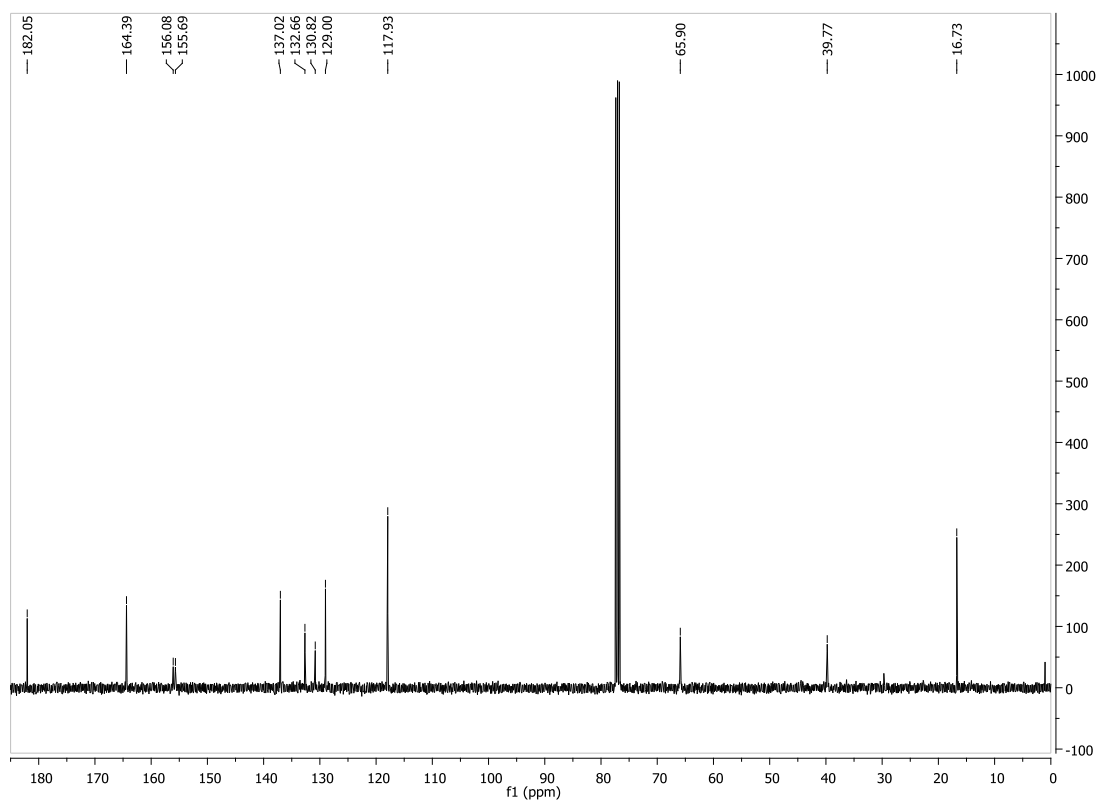1H-NMR for compound **1b**:
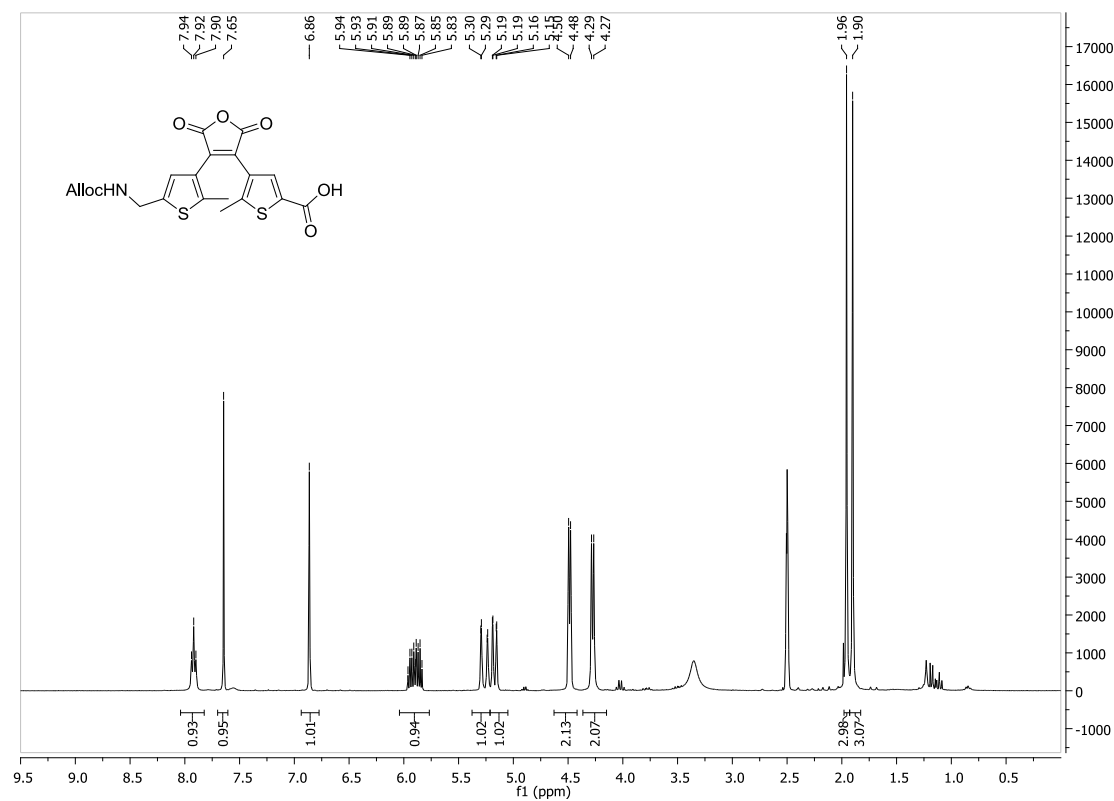
13C-NMR for compound **1b**:
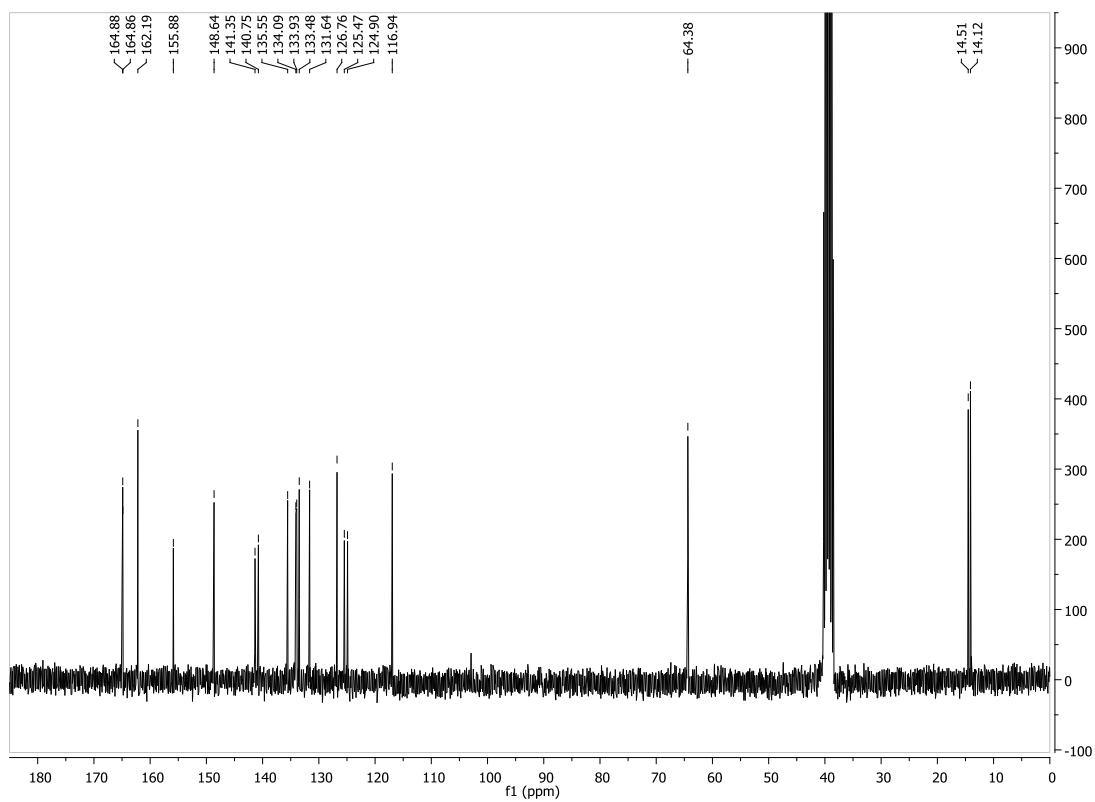
^{1}H-NMR for compound **2**:
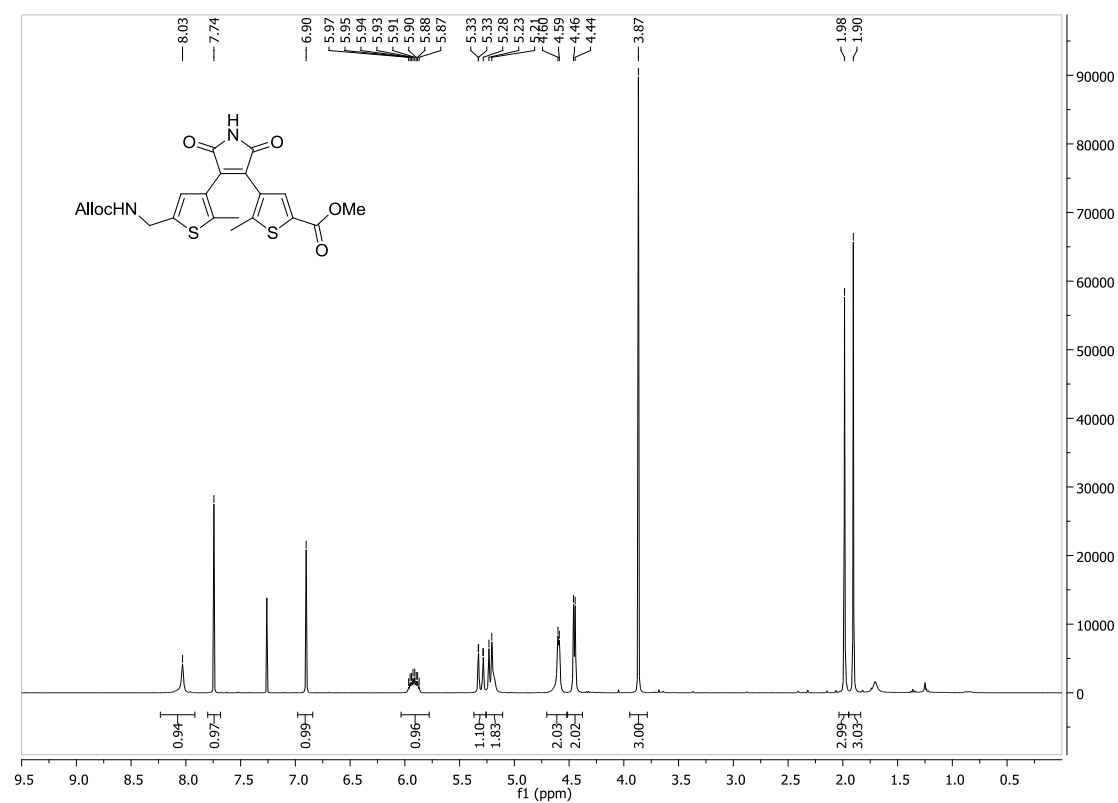
^{13}C-NMR for compound **2**:

¹H-NMR for compound **2b**:

¹³C-NMR for compound **2b**:

^{1}H-NMR for compound **3**:

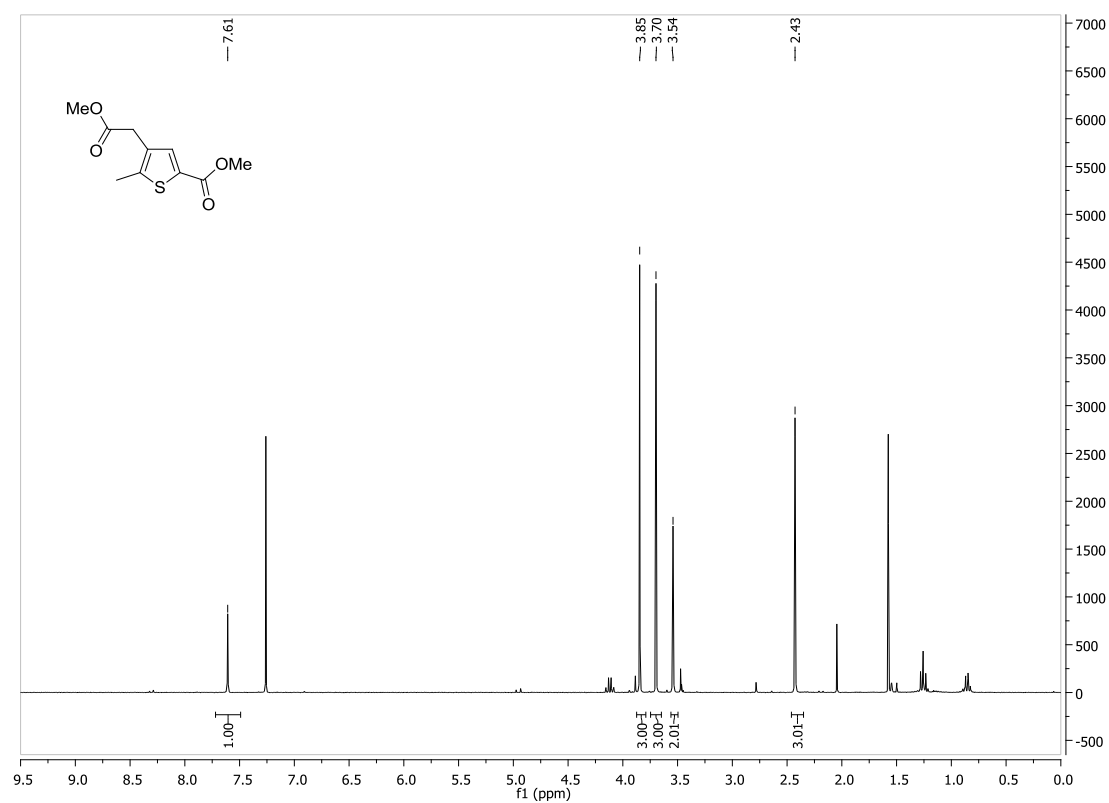^{13}C-NMR for compound **3**:

1H-NMR for compound **4**:

13C-NMR for compound **4**:

¹H-NMR for compound **8**:
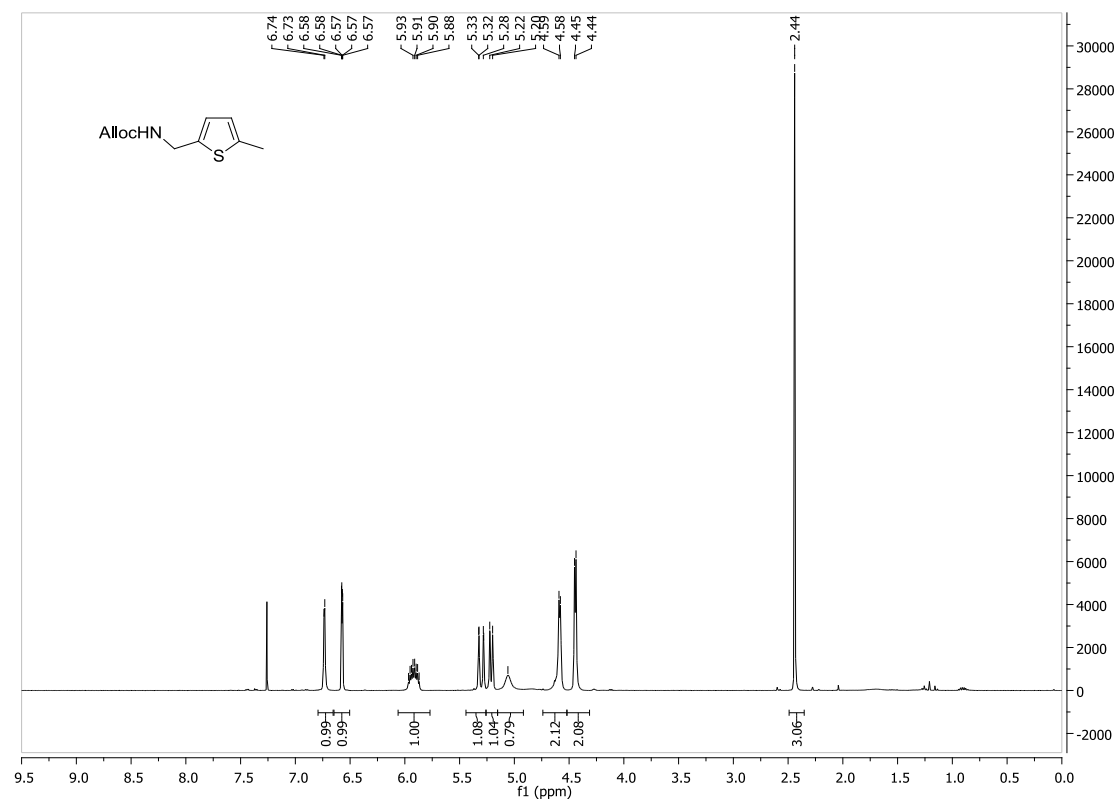
¹³C-NMR for compound **8**:

¹H-NMR for compound **8b**:

FmocHN — thiophene — CH₃
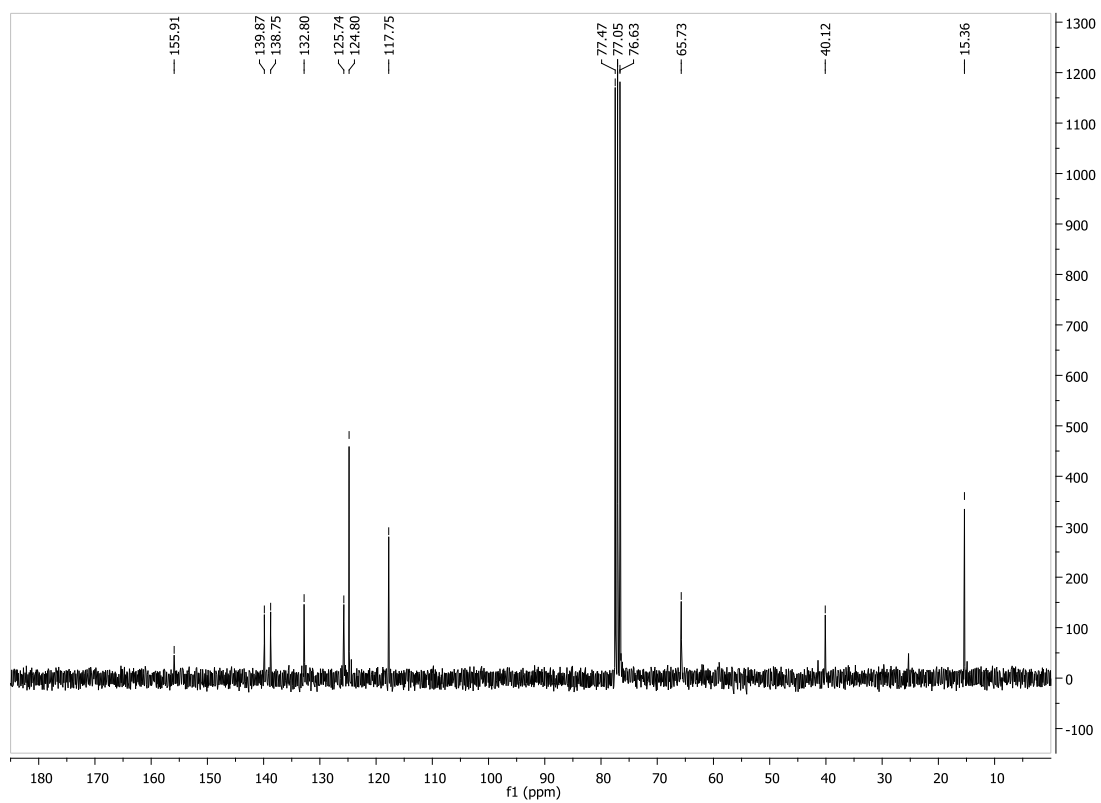
¹³C-NMR for compound **8b**:
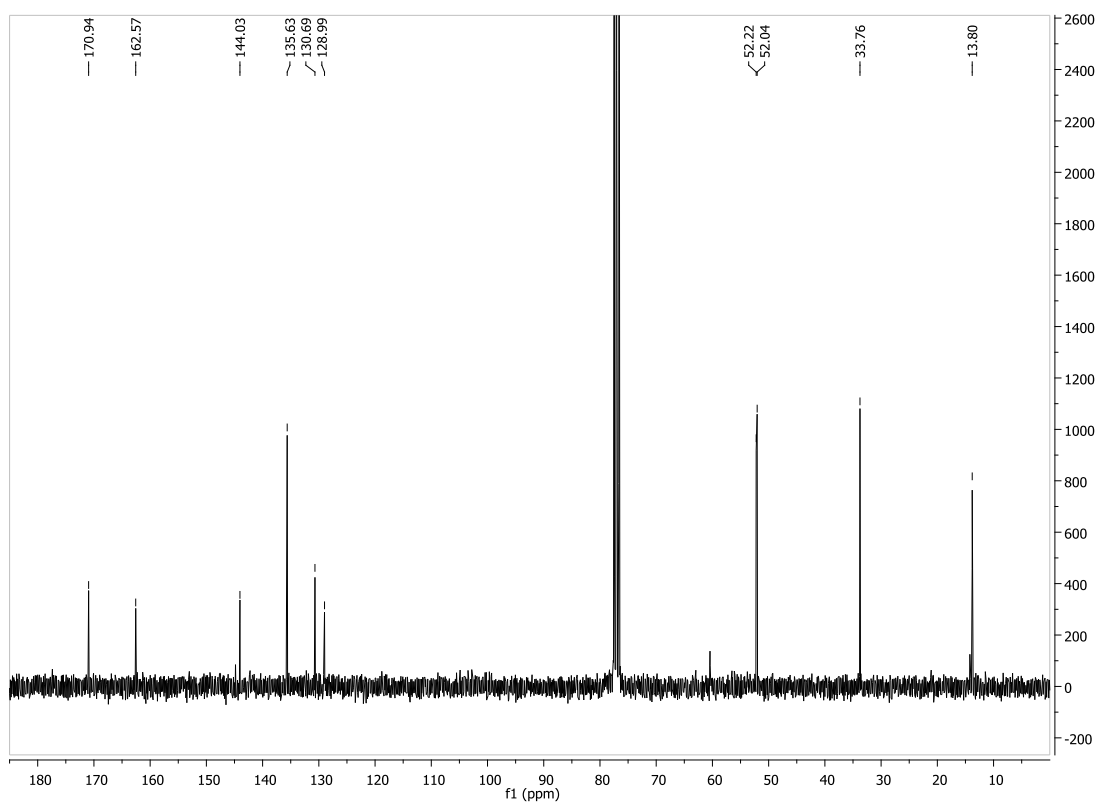
1H-NMR for compound **9**:

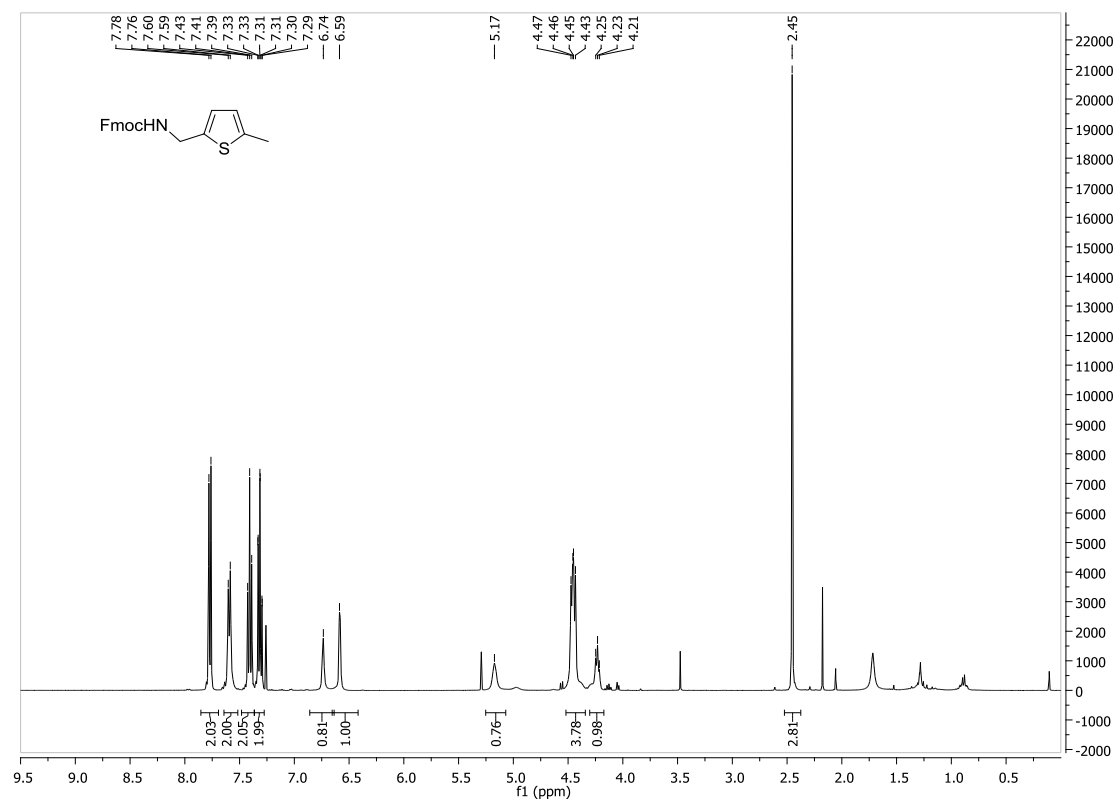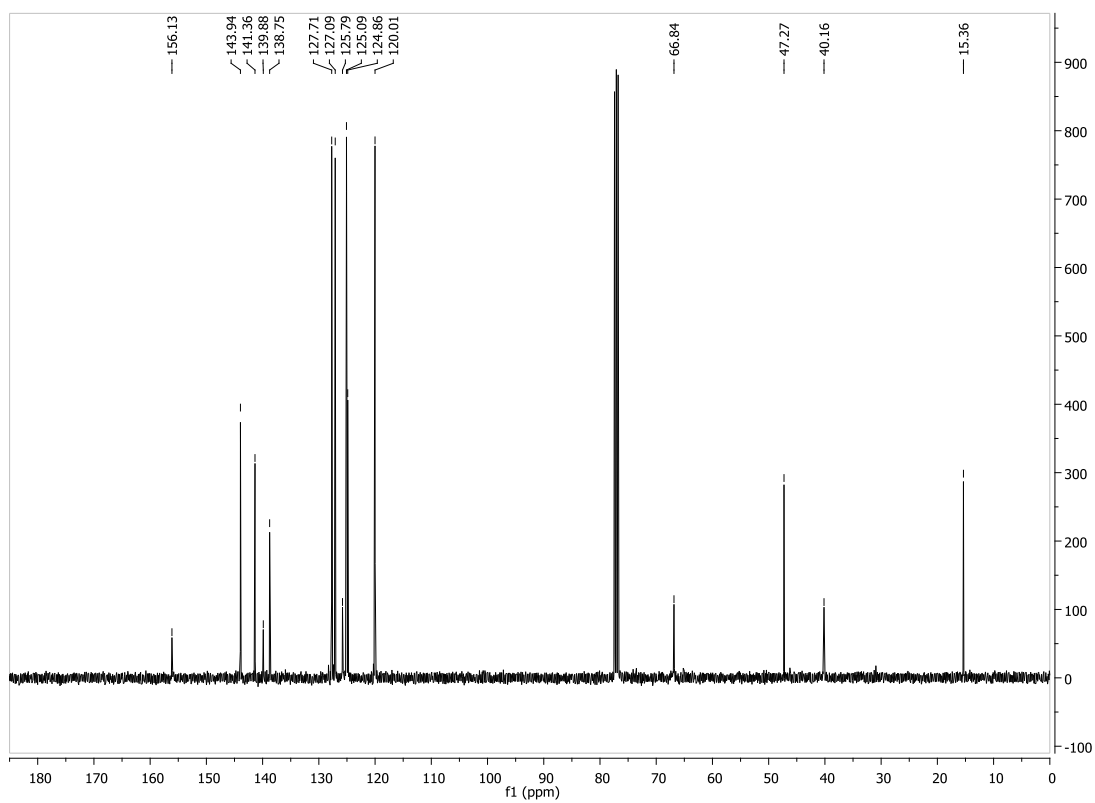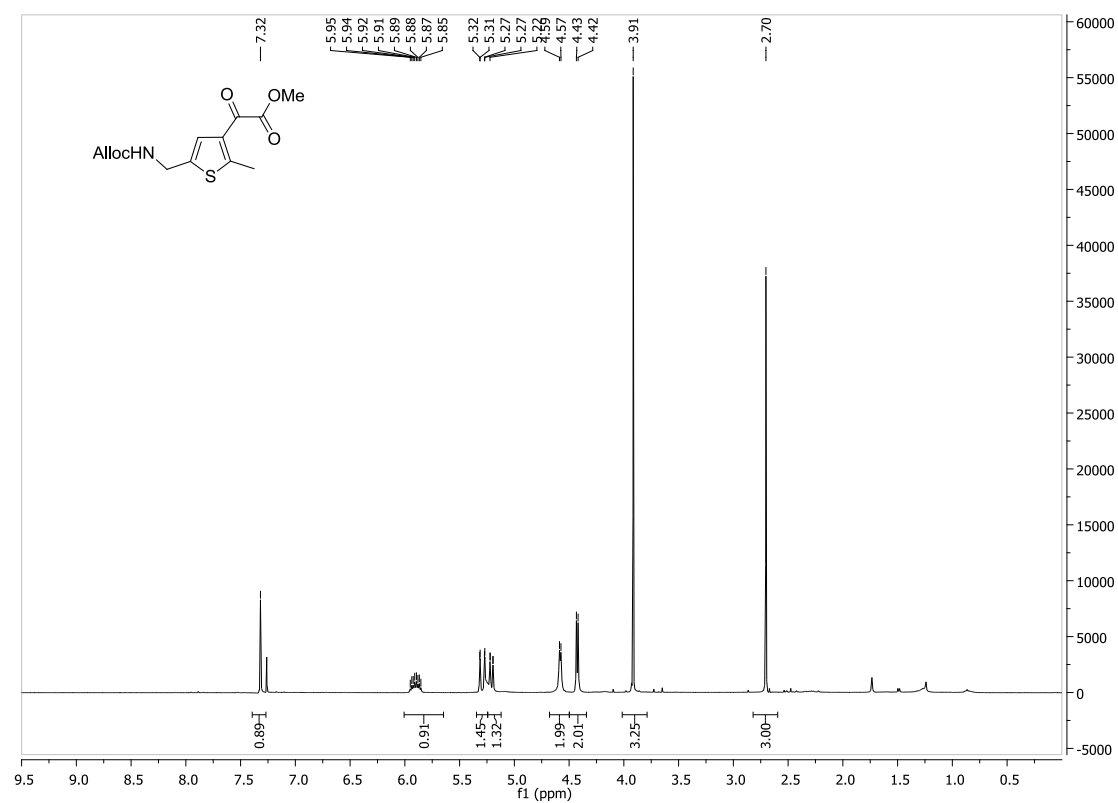

13C-NMR for compound **9**:

¹H-NMR for compound **9b**:

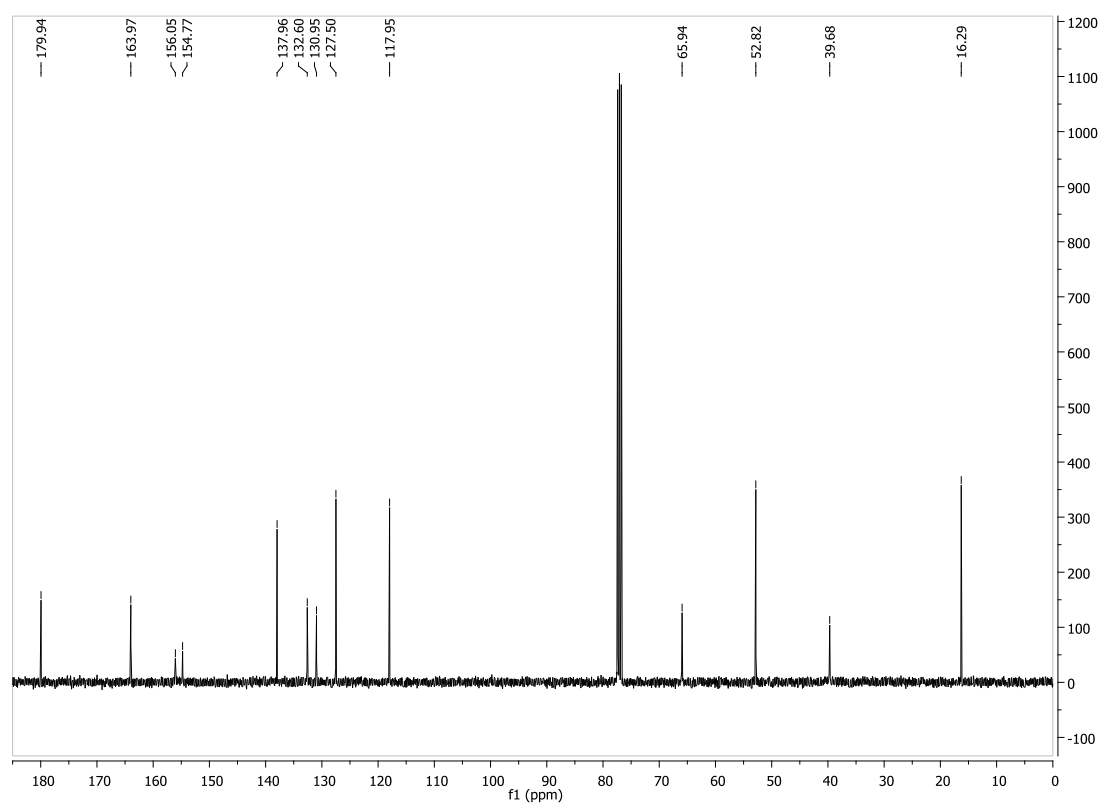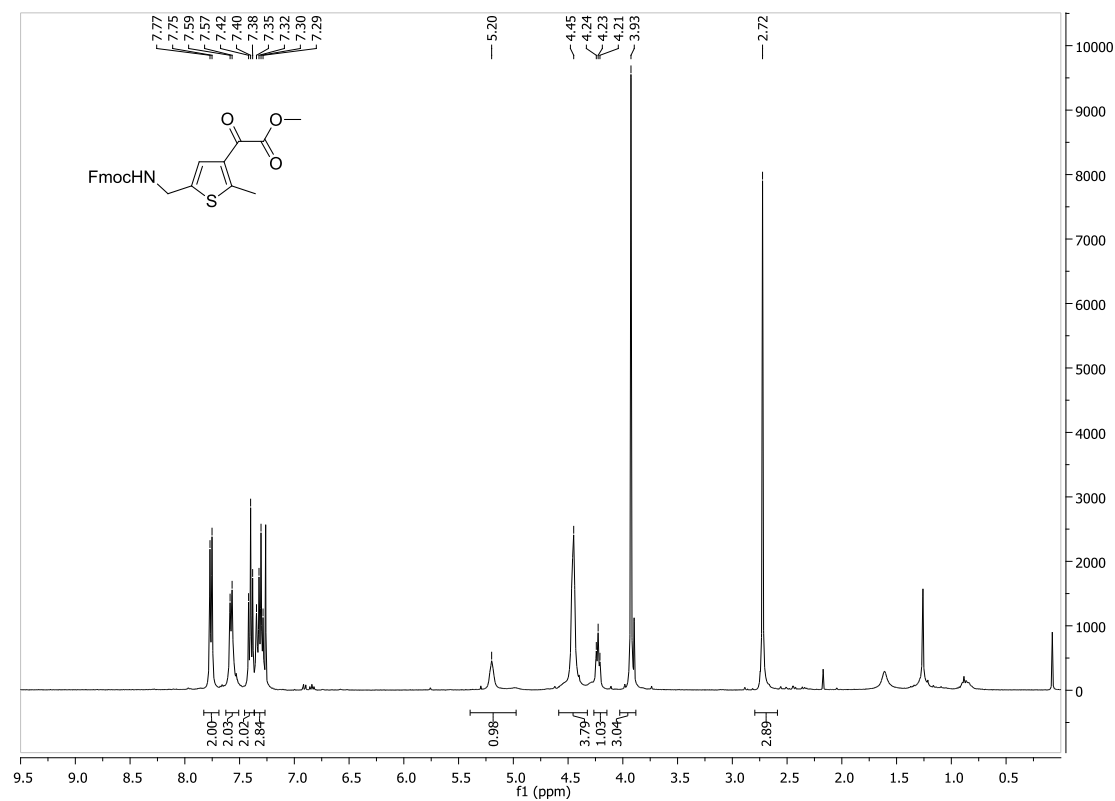
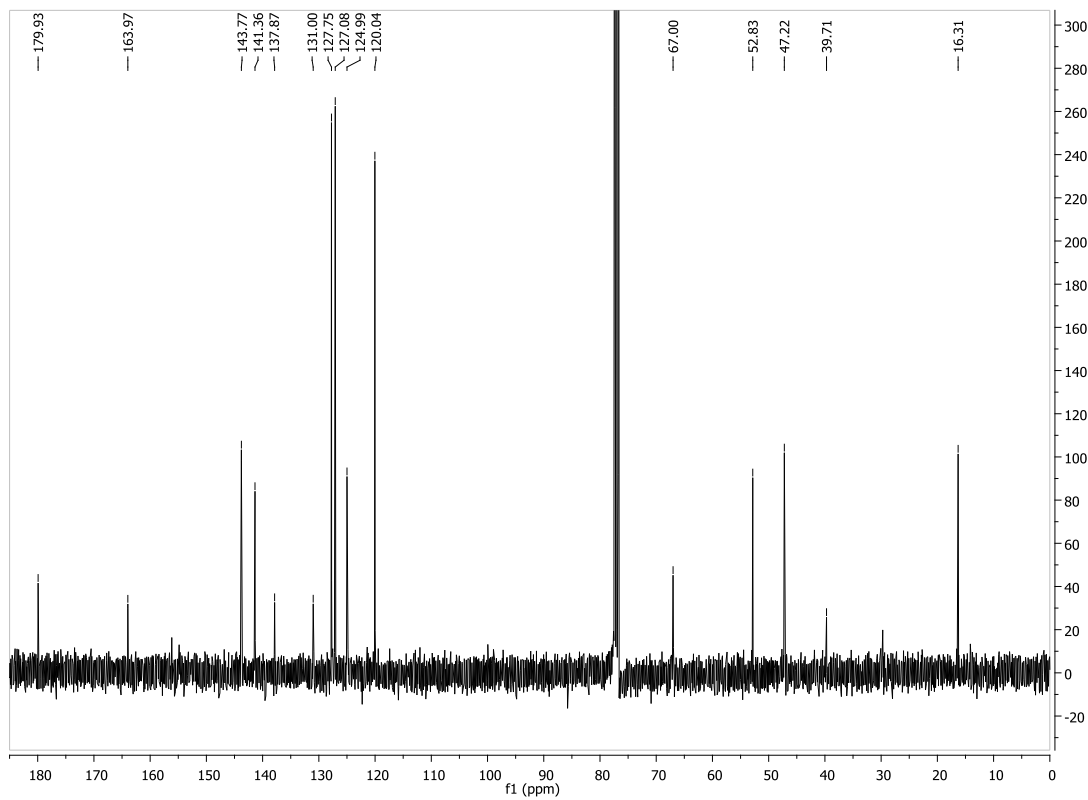
¹³C-NMR for compound **9b**:

1H-NMR of compound **9c**:
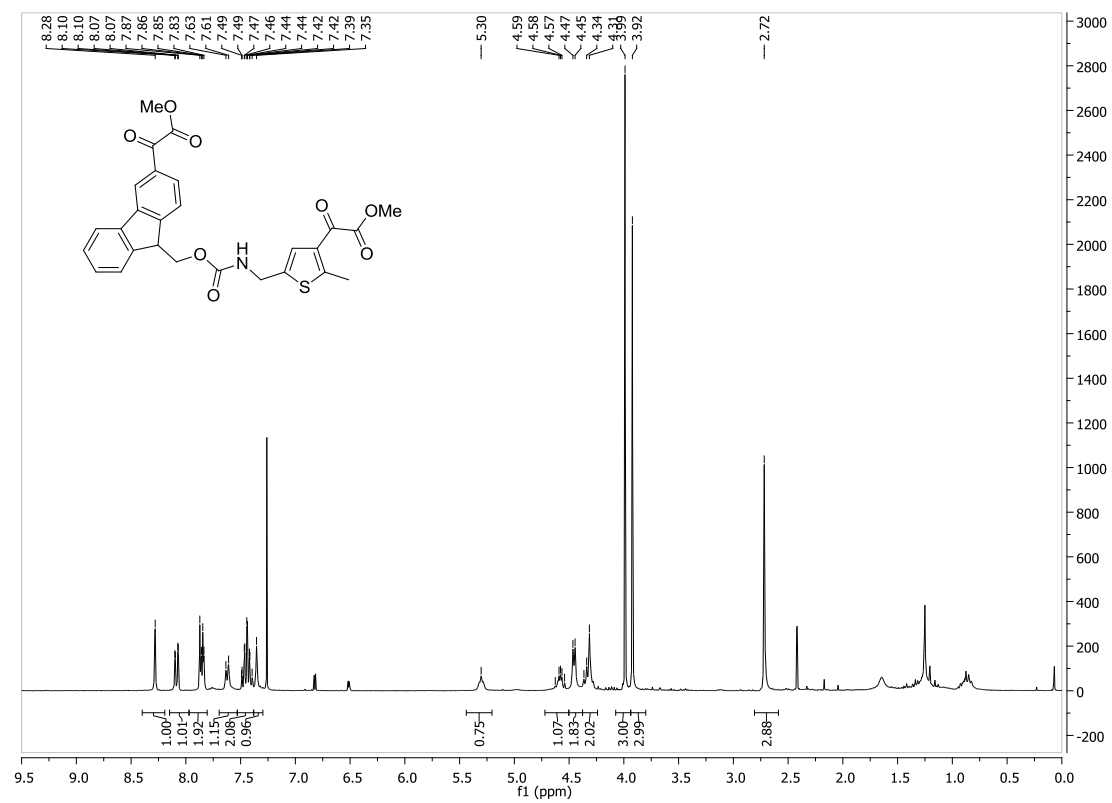
1H-NMR for compound **14**:
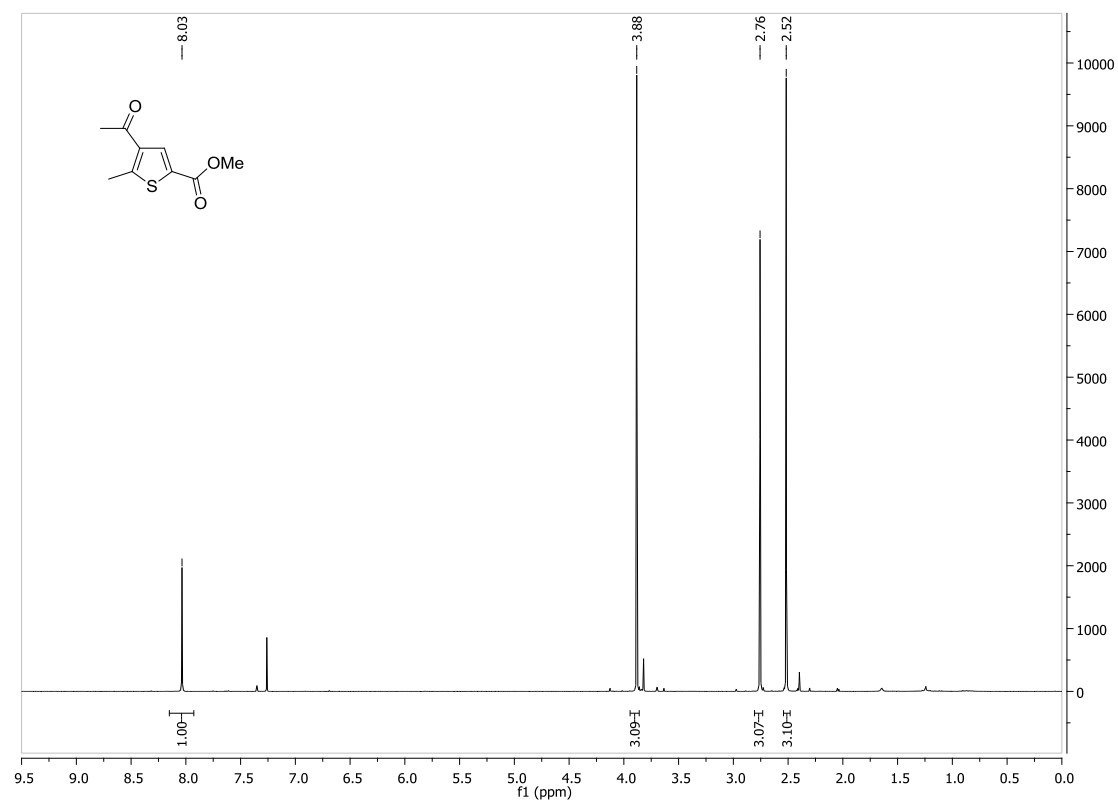
13C-NMR for compound **14**:
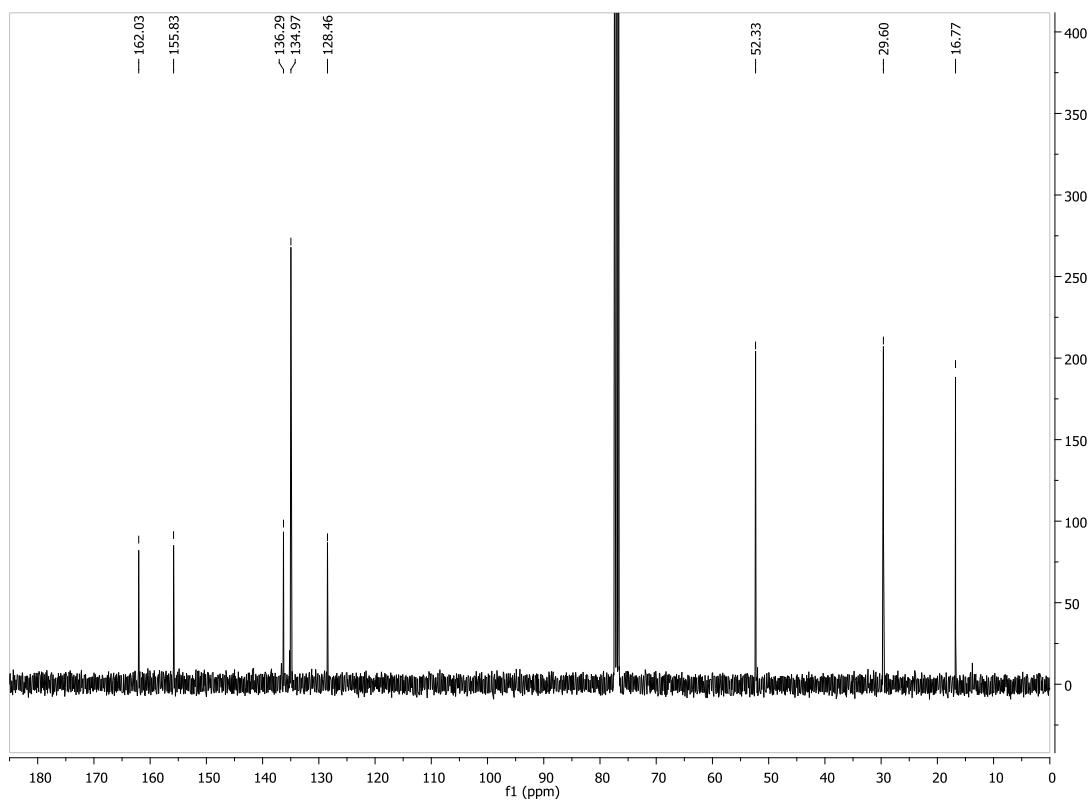
7.4   List of Abbreviations

A	absorption
AICAR	aminoimidazole carboxamide ribonucleotide
Ala	alanine
$AlCl_3$	aluminium chloride
Alloc	allyloxycarbonyl
Alloc-Cl	allyl chloroformate
APCI	atmospheric-pressure chemical ionization
aq.	aqueous
Ar	aryl
ATP	adenosine triphosphate
$B(OMe)_3$	trimethyl borate
BSA	bovine serum albumin
calcd.	calculated
$CDCl_3$	deuterated chloroform
CD_3CN	deuterated acetonitrile
$CHCl_3$	chloroform
CH_2Cl_2	dichloromethane
CHO	Chinese hamster ovary cells
CI	chemical ionization
CuCN	copper(I) cyanide
d	dublet
d	distance
δ	chemical shift
DABCO	1,4-diazabicyclo[2.2.2]octane
DAD	diode array detector
DIPEA	*N,N*-diisopropylethylamine or Hünig's base
DMF	dimethylformamide
DMSO	dimethyl sulfoxide
DTE	1,2-dithienylethene
EI	electron ionization
Elk1	transcription factor in the cell nucleus, which is activated by ERK1/2
ELISA	enzyme-linked immunosorbent assay
ERK	extracellular signal-regulated kinase
ES	electrospray ionization

Et	ethyl
EtOAc	ethyl acetate
EtOH	ethanol
Et$_2$O	diethylether
eq.	equivalents
E. coli	*Escherichia coli*
g	gaseous
g	grams
Fmoc	fluorenylmethyloxycarbonyl
h	hours
HCl	hydrochloric acid
HClO$_4$	perchloric acid
HEK	human embryonic kidney cells
HPLC	high-performance liquid chromatography
HisF	imidazole glycerol phosphate synthase
HOBt	hydroxybenzotriazole
H$_2$O	water
HP(O)(OEt)$_2$	diethyl phosphite
HR	high resolution
Hz	hertz
ImGP	imidazole glycerol phosphate
IR	infrared
J	joule
J	coupling constant
K	kelvin
k_{cat}	apparent unimolecular rate constant
K_i	inhibition constant
K_M	Michaelis constant
KO^{t}Bu	potassium *tert*-butoxide
L	liters
λ	wavelength
LAH	lithium aluminium hydride
LiI	lithium iodide
M	molar
m	meters
m	multiplet

MAPK	mitogen-activated protein kinase
Me	methyl
MeCN	acetonitrile
MD	molecular dynamics
MeOD	deuterated methanol
MeOH	methanol
$MgSO_4$	magnesium sulfate
min	minutes
mol	mole
m.p.	melting point
MS	mass spectrometry
*mt*PriA	phosphoribosyl-isomerase A from *Mycobacterium tuberculosis*
m/z	mass to charge
N	normal
$\tilde{\nu}$	wavenumber
n.a.	not available
NaCl	sodium chloride
Na_2CO_3	sodium dicarbonate
$NaHCO_3$	sodium hydrogen carbonate
NaOH	sodium hydroxide
NBS	*N*-bromosuccinimide
*n*BuLi	*n*-butyl lithium
NEt_3	triethylamine
NH_4OH	aqueous ammonia
NIR	near infrared
NMR	nuclear magnetic resonance
PCR	polymerase chain reaction
PE	petrol ether
PDB	Protein Data Bank
$Pd(OAc)_2$	palladium(II) acetate
$Pd(PPh_3)_2Cl_2$	bis(triphenylphosphine)palladium(II)dichloride
$Pd(PPh_3)_4$	tetrakis(triphenylphosphine)palladium(0)
$POCl_3$	phosphorous(V) oxychloride
PPh_3	triphenylphosphine
ppm	parts per million

PRFAR	N´-[(5´-phosphoribulosyl)-formimino]-5-aminoimidazole-4-carboxamide-ribonucleotide
ProFAR	N′-[(5′-phosphoribosyl)-formimino]-5-aminoimidazole-4-carboxamide ribonucleotide
PS	photostationary state
q	quaternary carbon
R_f	retardation factor
rpm	revolutions per minute
s	seconds
s	singlet
SE	standard error
$SOCl_2$	thionyl chloride
SPPS	solid phase peptide synthesis
r.t.	room temperature
T	temperature
t	triplet
t	time
TBTU	O-(benzotriazol-1-yl)-$N,N,N′,N′$-tetramethyluronium tetrafluoroborate
TICT	twisted intramolecular charge transfer
TFA	trifluoroacetic acid
THF	tetrahydrofuran
TLC	thin layer chromatography
tmHisF	imidazole glycerol phosphate synthase from *Thermotoga maritima*
TMS-Br	bromotrimethylsilane
Tris	tris(hydroxymethyl)aminomethane
TTN	thallium trinitrate
UV	ultraviolet
Vis	visible light
W	watt
Å	Ångström

7.5 Curriculum Vitae

Personal Data

Date of Birth	16th of March 1986
Birthplace	Hof
Nationality	German

Education

11/2010 – 02/2014	**PhD studies, Organic Chemistry,** University of Regensburg Supervisor: Prof. Burkhard König *"Synthesis and Biological Activity of Functionalized Photochromic Dithienylethenes"*
01/2010 – 09/2010	**Master thesis**, Universities of Regensburg/Gothenburg (SE) Supervisors: Prof. Burkhard König, Prof. Morten Grøtli *"Photoswitchable Kinase Inhibitors"*
10/2008 – 09/2010	**Master of Science, Chemistry**, University of Regensburg Studies in Organic Chemistry (mayor), Biochemistry and Inorganic Chemistry
10/2005 – 09/2008	**Bachelor of Science, Chemistry**, University of Regensburg
09/1996 – 07/2005	**Abitur**, Schiller-Gymnasium Hof

Advancement

03/2012 – 02/2014	**Emil Fischer Graduate Program**, Universities of Erlangen/ Regensburg, *"Pharmaceutical Sciences & Molecular Medicine"*

7.6 Publications and Conference Contributions

Publications

"Exploiting Protein Symmetry to Design Light-Controllable Enzyme Inhibitors"

B. Reisinger[+], <u>N. Kuzmanovic</u>[+], P. Löffler, R. Merkl, B. König, R. Sterner, *Angew. Chem.* **2014**, *126*, 606-609; *Angew. Chem. Int. Ed.* **2014**, *53*, 595-598.

"Immobilisation of Photoswitchable Diarylcyclohexenes Synthesised via Cobalt-Mediated Diels-Alder Reaction"

P. Raster, A. Schmidt, M. Rambow, <u>N. Kuzmanovic</u>, B. König, G. Hilt, *Chem. Commun.* **2014**, *50*, 1864-1866.

"Acetylcholinesterase Inhibitors with Photoswitchable Inhibition of β-Amyloid-Aggregation"

X. Chen, S. Wehle, <u>N. Kuzmanovic</u>, B. Merget, U. Holzgrabe, B. König, C. Sotriffer, M. Decker, *ACS Chem. Neurosci.* **2014**, accepted.

Conference Contributions

09/2012	Summer School Medicinal Chemistry, Regensburg *"Photoswitchable Kinase Inhibitors"* (poster and talk)
08/2012	EuCheMS (European Association for Chemical and Molecular Sciences) Congress 2012, Prag (CZ) *"Photoswitchable Kinase Inhibitors"* (poster)
07/2012	Research Day of the Emil Fischer Graduate School *"Photoswitchable Kinase Inhibitors"* (poster and talk)
02/2012	Leibniz Symposium 2012 *"Artwork from bits and pieces: Strategies to build up molecular complexity"*, Hannover *"Photoswitchable Kinase Inhibitors"* (poster)
09/2011	GDCh-Wissenschaftsforum Chemie 2011, Bremen *"Photoswitchable Kinase Inhibitors"* (poster)
07/2011	Drug Discovery and Selection - 47th International Conference on Medicinal Chemistry (RICT 2011), Lyon (F) *"Photoswitchable Kinase Inhibitors"* (poster)

7.7 Danksagung

Allen voran möchte ich meinem Doktorvater Prof. Dr. Burkhard König für die Betreuung meiner Dissertation sehr herzlich danken. Danke für viele hilfreiche Diskussionen und Ratschläge, für die fördernde Unterstützung bei all meinen Vorhaben und für die positive Einstellung, auch wenn das ein oder andere nicht nach Plan gelaufen ist. Ich bin sehr dankbar für die Freiheit und das Vertrauen diverse Projekte und Aufgaben in großen Teilen selbständig verfolgt haben zu dürfen.

Prof. Dr. Kirsten Zeitler danke ich für die Übernahme des Zweitgutachtens und darüber hinaus für ein stets kompetentes und freundliches Feedback, wann immer ich Rat suchte. Weiterhin geht mein Dank an Prof. Dr. Reinhard Sterner für seinen Einsatz als dritter Prüfer und die sehr angenehme und effiziente Zusammenarbeit. Vielen Dank auch an Prof. Dr. Joachim Wegener für das Übernehmen des Vorsitzes meines Promotionskolloquiums.

Ich danke den Mitarbeitern der zentralen Analytik unserer Fakultät für die schnelle und saubere Ausführung der analytischen Messungen. Dr. Rudolf Vasold danke ich für die absolut zuverlässige Durchführung der HPLC-Messungen, insbesondere für diverse Last-Minute-Einsätze.

Ein großer Dank geht an Bernd Reisinger für die erfolgreiche und produktive Kooperation zur Entstehung unserer Veröffentlichung in der Angewandten. I owe my thanks to Prof. Dr. Morten Grøtli and Dr. Nuška Tschammer for their great support in the kinase project. Carolin Falenczyk und Daniel Wutz danke ich für die sehr angenehme Zusammenarbeit auf dem Gebiet der Dithienylmaleimide. Weiterhin danke ich Peter Raster für viele hilfreiche Diskussionen und ein gutes Zusammenwirken in diversen Photoswitch-Projekten.

For lab work support in the course of bachelor theses or research internships I thank Tobias Burger, Anna Fielder, Theresa Fischer, Maria Gockert, Julian Greindl, Florian Hastreiter, Sabine Kerres, Anika Kolb, Christian Lankes, Chen Mengya, Andreas Meyer, Matthias Mickert, Sabine Möhle, Nadja Simeth and Daniel Wutz.

Ich danke den Festangestellten des AK Königs für jegliche Hilfe und Unterstützung rund um den Arbeitsalltag und für die netten Gespräche zwischendurch.

Meinen Korrekturlesern Manuel Bause, Carolin Falenczyk, Dr. Andreas Hohenleutner und Dr. Susanne Kümmel danke ich für ihr konstruktives Feedback und die akribische Suche nach Fehlern.

Außerdem danke ich Manuel Bause für seine allzeit großartige technische Unterstützung und seine Hilfsbereitschaft, die besonders im Endspurt sehr wertvoll war.

My grateful thank goes to the whole past and present König group; especially Andi M., Ani, Cristian, Caro Fischer, Durga, Fliesn, Javier, Malte, Melli, Michl, Mischko, Mouchumi, Qiu, Robbl, Simone, Steffi, Supratim, Troppi, Willi and all the ones I forgot. Thank you for sharing expertise and advice, for helping each other in every aspect of our everyday work and for the great time we had beyond.

I am very thankful for the always enjoyable and friendly atmosphere I had in the lab with Masha, Tanja, Thomas and various short-term labmates.

Anna, Balki, Benno, Flo, Caro Falenczyk, Caro Ruß, Josef, Sanne, Susa und Thea danke ich speziell für die gemeinsame Organisation diverser AK-Veranstaltungen, für viele mehr oder weniger ernsthafte Diskussionen und all die unvergesslichen Erlebnisse während und nach der Arbeit. Ganz besonders bedanken möchte ich mich dabei bei Andi H., der mir über die Jahre ein sehr enger Freund geworden ist. Danke für die unzähligen Gespräche und Ratschläge.

Ich danke all meinen Freunden, die hier namentlich nicht erwähnt sind, die mich während meines Studiums begleitet und mein Leben darüber hinaus geprägt und bereichert haben.

Meiner Familie gebührt ein ganz besonders herzlicher Dank für ihre Fürsorge, ihre Hilfe und jede erdenkliche Unterstützung in allen Lebenslagen, wodurch das Erreichen meiner Ziele überhaupt erst möglich wurde.

Abschließend möchte ich Julia aus tiefstem Herzen für ihre bedingungslose Rückendeckung, ihr Vertrauen und ihre Liebe danken. Danke für all die wunderbaren Momente, die mir trotz der schier unendlichen To-do-Liste eine glückliche und relativ entspannte Zeit des Zusammenschreibens bereitet haben.